Nuclear Waste Technical Review Board

Thermal-Response Evaluation of Yucca Mountain During the Preclosure and Postclosure Phases

July 2008

Executive Summary

The purpose of this white paper is to document a systematic evaluation of the thermal response of the proposed Yucca Mountain repository for various thermal loadings. The U. S. Nuclear Waste Technical Review Board (NWTRB) staff has developed calculation tools that allow performing these calculations rapidly to determine what parameters are important to an acceptable thermal response and to identify the bounding conditions both for emplacement of the waste and for permanent closure of the repository. The methods used in the document have been benchmarked against the U. S. Department of Energy's (DOE) analytical approaches and show good agreement. However, it is important to recognize that these tools represent simplified analyses and models whose primary purpose is to gain insights into the repository thermal response and to help identify key parameters affecting the thermal response.

The Yucca Mountain thermal response is an important input to the Total System Performance Analysis (TSPA) used by DOE to determine the dose rates to the public from the waste disposed of at the proposed Yucca Mountain repository. Until very recently, DOE used an assumption of a single waste stream with a specific power and decay function as the basis for determining the thermal response. DOE is now developing an integrated thermal management strategy using the Total System Model (TSM) and WPLoad models to evaluate several waste acceptance, processing, and emplacement scenarios. In addition, DOE has developed an Estimated Limiting Waste Stream (ELWS) that predicts the potentially hottest commercial waste stream to be received at the repository and is using the actual assembly powers and decay curves as the basis for the analysis rather than a single power and decay rate as has been done in the past. As a result of these efforts, DOE has been able to increase the maximum allowable thermal operating requirements at emplacement from 11.8 kW to 18 kW per waste package and the linear line load from 1.45 kW/meter to 2.0 kW/meter over a seven-package segment. The postclosure thermal response to support the License Application (LA) is based on this ELWS, and DOE has shown that this waste stream can be emplaced and the repository closed within 100 years from the start of waste emplacement.

DOE has made significant advances both in their understanding of the repository thermal response and in the thermal methodology for repository operation. However, the thermal strategy is still based on an estimated limiting waste stream rather than on the amount of thermal energy that the mountain can absorb without exceeding any established thermal limit. Performing more general evaluations, as presented in this document, to determine the maximum thermal energy that can be absorbed by the mountain would provide increased flexibility to control when the repository may be closed by changing the ventilation duration and/or the linear line load, regardless of the waste emplaced. This is especially true during the preclosure phase, where rather arbitrary thermal limits for emplacement have been established on the basis of the predicted waste stream. The current 2.0 kW/meter thermal limit provides approximately 90^{o}C margin to the 200^{o}C drift wall temperature limit for the 30-day loss-of-forced-ventilation event. Increasing the allowable thermal limits at emplacement would allow the majority of waste received at the repository to be emplaced immediately, thus reducing the amount of surface storage.

Specific findings and recommendations based on the NWTRB staff's analyses are as follow:

1. The calculations performed by DOE and the NWTRB staff are in reasonable agreement and suggest that the DOE technical basis is valid.

2. Establishing the thermal limits for emplacement on the basis of the ELWS appears to be overly conservative. DOE should reevaluate the thermal limits for emplacement based on the capacity of the mountain to absorb the thermal energy rather than on the predicted waste stream. This approach would result in higher thermal limits for emplacement and reduce the amount of surface storage required at the repository.

3. Initiating the loss of forced ventilation during the preclosure period at 30 days after emplacement may not be the most limiting case. DOE should reevaluate this event and determine when the loss of forced ventilation results in the shortest time to reach the 200°C drift wall thermal limit.

4. Surface aging of the hotter Commercial Spent Nuclear Fuel (CSNF), as opposed to subsurface aging, has limited benefit on the postclosure thermal response. DOE should reevaluate the need to surface-age the CSNF at the repository.

5. The DOE postclosure thermal response to support the LA is based on an ELWS. However, performing more general evaluations, as presented in this document, to determine the maximum thermal energy that can be absorbed by the mountain would provide increased flexibility to control when the repository may be closed by adjusting the ventilation duration and/or the linear line load, regardless of the waste emplaced.

6. The Board agrees with DOE that if the 96°C mid-pillar temperature limit is required, the requirement determines the maximum allowable thermal loading. However, if the 96°C limit were eliminated, the drift wall's maximum temperature of 200°C would determine the maximum allowable thermal loading, and the preclosure ventilation period could be decreased by approximately 25 years.

7. Thermal conductivity has a significant effect on the peak temperatures. Variations in the thermal conductivity used in the calculations to predict the repository thermal response should be taken into account on the basis of actual thermal conductivity measurements along with appropriate uncertainties and margins.

Preface

This study and report were prepared by Gene W. Rowe and Bruce Kirstein of the U.S. Nuclear Waste Technical Review Board staff in support of the Board's analysis of issues associated with thermal management, an effort lead by Professor Andrew C. Kadak.

Table of Contents

Tables

Figures

Appendix

1. Introduction

1.1. Background

The United States Nuclear Waste Technical Review Board (NWTRB) since its inception has maintained a focus on the issue of thermal management. In the Board's *Fifth Report to Congress*, it characterized thermal management as a pivotal and crosscutting issue, one that requires both an incremental approach and an integrated solution and encompasses the waste management system as a whole. For preclosure, the report recognized the importance of the relationships among waste acceptance, transportation, surface and subsurface facility design, and the concepts of waste handling and waste emplacement. The Board also recognized that the performance of the repository is implicitly tied to the thermal management strategy and that coupled hydrological, mechanical, and chemical processes are all strongly temperature dependent. The Board also concluded that the repository environment would likely produce conditions on the surface of a waste package that could lead to corrosion and to degradation of waste package performance.

The philosophy used by DOE to develop a thermal strategy has evolved over several years and has been influenced by several companies and organizations. The approach has been to predict the waste characteristics and delivery schedule (referred to as the "waste stream") of the waste shipped to Yucca Mountain and to use this information as the basis for determining the thermal response of the mountain, from emplacement of waste through the entire thermal pulse.

Until very recently, DOE used a single waste stream with a single power and decay function as the basis for determining the thermal response. The project recently developed two computer models, the Total System Model (TSM) and WPLoad, to create an integrated thermal management strategy that evaluates several waste acceptance, repackaging, and emplacement scenarios. The TSM evaluates waste acceptance, transportation, and site throughput, and the WPLoad model evaluates the thermal conditions for emplacement. As part of the new strategy, DOE developed an ELWS that predicts the potentially hottest commercial waste stream to be received at the repository and is using the actual assembly powers and decay curves as the basis for the analysis rather than a single power and decay rate as they have done in the past. As a result of these efforts, DOE has been able to increase the maximum allowable thermal operating requirements at emplacement from 11.8 kW to approximately 18 kW per waste package and the linear line load from 1.45 kW/meter to 2.0 kW/meter over a seven-package segment.

This new approach is much more comprehensive than the original approach and provides a better understanding of the thermal response of the repository. However, it is still based on a single predicted waste stream and does not evaluate other potential receipt scenarios or determine the maximum amount of thermal energy that the repository can absorb without exceeding an established thermal limit. The present approach appears to have decreased the amount of surface storage required at Yucca Mountain, but significant surface storage is still required to allow sequencing of the waste package emplacement to maintain the required 2.0 kW/meter linear line load over a seven-package segment.

1.2. Purpose

The purpose of this paper is to document a systematic evaluation of the thermal response of Yucca Mountain for various waste stream scenarios. The Board staff has developed calculation tools that allow performing multiple calculations quickly to determine what parameters are important to the mountain's acceptable thermal response and to identify the bounding conditions both for emplacement of the waste and for permanent closure of the repository.

The purpose of this white paper is not to evaluate or endorse the validity, the technical basis, or the operating requirements for the thermal limits used by DOE as its design basis.

1.3. Approach

1.3.1. General

The thermal response during both the preclosure and the postclosure phases is highly dependent on the initial conditions at the start of each phase. The important factors for establishing these initial conditions appear to be (1) the characteristics of the waste when it is discharged from the reactor (initial enrichment and burnup) and (2) the age since discharge from the reactor of the waste at the start of each phase. Because of the acceptance criteria established by the standard contract, 10CFR961, DOE has very little influence on the characteristics of the waste that it will receive. However, DOE controls the sequence in which the various waste packages will be loaded into the repository. Although sequencing of waste packages has some benefits, controlling the age of the waste at the start of the preclosure period (by aging the waste on the surface before emplacement) and at the start of the postclosure period (by controlling the length of the preclosure ventilation period) has a greater effect on the thermal response. Therefore, the approach taken in this evaluation is to determine the appropriate initial conditions (age of the waste) for both the preclosure period (thermal operating requirements for emplacement) and the postclosure phase (thermal operating requirements for closure) for waste having various characteristics.

DOE has taken a different approach by establishing one set of thermal operating requirements (for emplacement) and assuming a fixed preclosure period to prevent exceeding thermal limits during either the preclosure or the postclosure period. Although not technically incorrect, this approach may be overly conservative, require additional operations during the preclosure phase, and limit the flexibility to close the repository.

1.3.2. Age of Waste

Throughout this document, the term "age" generally refers to the number of years since the assembly was discharged from the reactor. Age is used to refer to three different events:

Age at receipt: The number of years between when the assembly was discharged from the reactor and is received at the repository.

Age at emplacement: The number of years between when the assembly was discharged from the reactor and is emplaced in the repository.

Age at closure: The number of years between when the assembly was discharged from the reactor and the repository is permanently closed.

The term "aging" refers to the act of storing the assembly to allow for radionuclide decay in order to reduce the assembly power. Aging can be done on the surface before emplacement, referred to as "surface aging," or after emplacement but before repository closure, referred to as "subsurface aging" or the "ventilation period".

1.3.3. Temperature Variations Along Drift Wall

The emplacement of waste packages of differing powers will result in varying drift wall temperatures opposite those packages. However, the effect of axial radiant-heat transfer in a drift loaded with varying-power packages is such that the axial drift wall temperature variations are relatively small, as

shown in project document 800-00C-WIS0-00100-000-00B, *Repository Twelve Waste Package Segment Thermal Calculation*. During normal operating conditions, in a segment containing waste packages with initial powers varying between approximately 0.5kW and 11.8kW, the axial variation in peak drift wall temperature is approximately 9°C during preclosure and approximately 6°C during postclosure. For the accident conditions of a loss of forced ventilation during the preclosure period, the variation in drift wall temperature is approximately 28°C but quickly returns to normal after forced ventilation is restored.

Because the maximum drift wall axial temperature variation is small and is much less at longer time frames of a few hundred years, modeling individual packages in a drift is not necessary. An average line load can be used over the distance spanned by a segment of several waste packages. This allows the waste packages in an entire drift to be represented as a series of segments.

This is the approach that is taken throughout this evaluation. Rather than model each individual waste package, an average linear line load for the drift is assumed. The drift can be modeled as a series of segments, each segment contains multiple waste packages, and the average linear line load is applied to each segment. The mountain thermal response is determined by adding the energy contribution from each segment.

1.3.4. Estimation of Assembly Cladding Temperature

DOE has adopted the use of a Transportation/Aging/Disposal canister, referred to as a "TAD", for disposing of all Commercial Spent Nuclear Fuel (CSNF). The internal configuration of the TAD has a major effect on the ability of the waste package to transfer the energy from the assembly to the outside surface of the waste package and therefore the maximum cladding temperature. Because the internal design of the TAD has not been completed, calculating the cladding temperature is not possible at this time. Therefore, calculation of the cladding temperature was not performed as part of this evaluation. The assumption is that the peak cladding temperature will not become a limiting criterion for either the preclosure or the postclosure. However, this assumption will need to be verified after the TAD design has been finalized.

2. Calculation Models

The development and basis for the calculation models used in this evaluation are in Appendix A. They are simplified models and are not intended to be the basis for the actual repository design. However, the NWTRB believes that the models are accurate enough to allow performing the parametric evaluations necessary to understand the thermal response as well as to determine which parameters are important to the thermal response. They also provide an indication of the validity of the calculations and results performed by DOE. Descriptions of the three models used are in Sections 2.2 through 2.4.

2.1. Assembly Power Representation

The power of a decaying radionuclide as a function of time can be represented as a decaying exponential in the form of Equation 1.

$$Q(t) = Q_0 e^{-\lambda t} \qquad \textbf{Equation 1}$$

Because a nuclear fuel assembly is composed of several decaying sources, each with a different decay function, a single exponential term cannot be used. A more accurate representation of assembly decay is

provided as the sum of three decaying exponentials in the form of Equation 2, where the coefficients are watts/meter and the time is years.

$$Q(t) = Q_1 e^{-\lambda_1 t} + Q_2 e^{-\lambda_2 t} + Q_3 e^{-\lambda_3 t} \qquad \textbf{Equation 2}$$

For determining the six constants in Equation 2 for an assembly with a particular burnup, six equations were written based on the data provided in *PWR Source Term Generation and Evaluation*, 000-00C-MGR0-00100-000-00B and *BWR Source Term Generation and Evaluation*, 000-00C-MGR0-00200-000-00A, at six different times, and the constants "Q" and "λ" were determined using MathCad. An example of the calculation is in Appendix B, the results for PWR and BWR assemblies are in Appendix C, and a comparison of the assembly powers in the *PWR Source Term Generation and Evaluation*, 000-00C-MGR0-00100-000-00B, and *BWR Source Term Generation and Evaluation*, 000-00C-MGR0-00200-000-00A tables, and the calculated powers using the methodology in Appendix B is in Appendix D.

Based on DOE Engineering Study 000-00R-G000-01000-000-000, *Total System Model Analysis for Repository Postclosure Thermal Envelope Study, Phase2*, data file WP_Decay_70K22kw_011707.xls, the average PWR and BWR assemblies are as follow:

Table 1 Average PWR and BWR Assembly Characteristics

Assembly Type	Average Loading (MTHM)	Average Burnup (Gwd/ton)	Average Age at Receipt (Years)
PWR	0.413	47.66	17.95
BWR	0.175	45.41	14.25

The assembly powers provided in *PWR Source Term Generation and Evaluation*, 000-00C-MGR0-00100-000-00B, and *BWR Source Term Generation and Evaluation*, 000-00C-MGR0-00200-000-00A, assumed the initial loading of a PWR assembly to be 0.475 Metric Tons Heavy Metal (MTHM)/assembly and of a BWR assembly to be 0.200 MTHM/assembly. These values are relatively high in comparison to the average assembly and result in powers that are unrealistically high. To obtain a more representative assembly power, the power coefficients in Appendix B are corrected by multiplying the power coefficients by the ratio of the actual MTHM/assembly to the base case MTHM/assembly. In all calculations performed as part of this evaluation, the correction factors used are as follow:

PWR assembly 0.413/0.475 = 0.869

BWR assembly 0.175/0.200 = 0.875

2.2. Finite-Length Decaying Line Source Calculation

For the majority of the calculations performed in this evaluation, the thermal response of the mountain was determined using a finite-length decaying line source, as shown in Figure 1.

Figure 1 Representation of Finite-Length Decaying Line Source

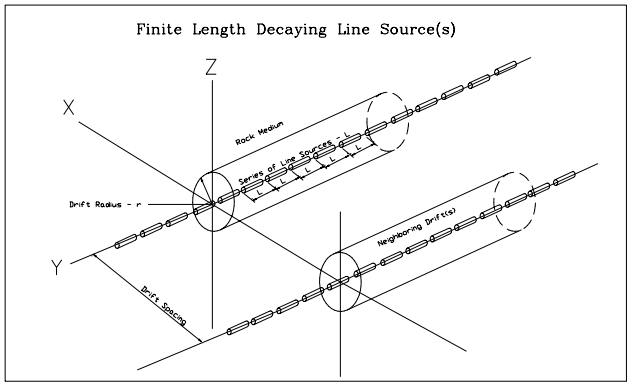

The temperature as a function of time for a finite-length decaying line source can be determined using Equation 3.

$$v(x,y,z,t) = \frac{Qe^{-\lambda t}}{8\pi K}\int_0^t \left\{ erf\left(\frac{z}{2\sqrt{\kappa\theta}}\right) - erf\left(\frac{z-L}{2\sqrt{\kappa\theta}}\right)\right\}\frac{e^{+\lambda\theta}}{\theta}e^{-\frac{(x^2+y^2)}{4\kappa\theta}}d\theta \qquad \textbf{Equation 3}$$

where x and y represent the radial distance from the center of the waste package, z is the location on the segment centerline axis, Q is the lead coefficient in watts/meter that describes the exponential decay of the source with a rate of decay of λ reciprocal time, K is the thermal conductivity, L is the source length, and κ is the thermal diffusivity. For a number of equal length sources, *n*, lined up on the z axis, the temperature is calculated by Equation 4.

$$v(x,z,t) = \sum_{i=1}^{n} v_i(x, z-(i-1)L, t) \qquad \textbf{Equation 4}$$

where y = 0 to represent the centerline plane of the waste package and the subscript *i* is applied to the decaying power as Q_i and λ_i. The temperature contribution from neighboring drifts is calculated by Equation 5, where m equals the number of neighboring drifts.

$$v(x,z,t) = \sum_{i=1}^{m} v_i(m \times Drift\_space - x, z, t) + v_i(m \times Drift\_space + x, z, t) \qquad \textbf{Equation 5}$$

The detailed development of this methodology is presented in Appendix A. Two calculation methods are used; one assuming that the repository is loaded with waste packages that all have the same characteristics, Attachment E, and one assuming an identical seven-package segment that is replicated throughout the repository, Appendix F.

2.2.1. Effects of Host-Rock Thermal Conductivity on Temperature

Variations in host-rock thermal conductivity will affect the peak postclosure temperatures at both the drift wall and the mid-pillar. For determining the magnitude of the temperature variations due to changes in host-rock thermal conductivity, the peak temperatures for the drift wall and the mid-pillar were calculated for a range of host-rock thermal conductivities using the methodology described in Section 2.2. The basis for selecting this range of thermal conductivities comes from DTN: MO0702PASTREAM.001 and is summarized in Table 2.

Table 2 Summary of DTN: MO0702PASTREAM.001 Host-Rock Thermal Conductivities

	Upper Lithophysal (TSW33)		Upper Nonlithophysal (TSW34)		Lower Lithophysal (TSW35)		Lower Nonlithophysal (TSW36)	
	Dry	Wet	Dry	Wet	Dry	Wet	Dry	Wet
Minimum	0.423	1.171	0.613	1.389	0.570	1.326	0.861	1.573
10%	0.949	1.550	1.147	1.827	**1.071**	1.690	1.283	1.944
50%	1.132	1.749	1.389	2.052	1.240	1.863	1.443	2.102
90%	1.369	1.82	1.626	2.302	1.414	**2.055**	1.609	2.274
Maximum	2.057	2.782	2.511	3.199	1.924	2.585	2.117	2.741

Because the majority of the repository will be located in the lower lithophysal rock, the conductivities for this host rock were selected. The 10-percentile dry represents a reasonable lower bound, and the 90-percentile wet represents a reasonable upper bound. Therefore, temperatures were calculated using the method described in Section 2.2 for conductivities between 1.0 W/m-^{o}C and 2.0 W/m-^{o}C at 0.1 W/m-^{o}C intervals for waste packages containing 48 Gwd/t PWR assemblies that were 18 years old at emplacement and were ventilated for 50 and 100 years. The results are shown in Table 3 and Figure 2.

Table 3 Effect of Host-Rock Thermal Conductivity on Peak Temperatures

Thermal Conductivity	50 Years of Ventilation				100 Years of Ventilation			
	Drift Wall Peak Temperature		Mid-Pillar Peak Temperature		Drift Wall Peak Temperature		Mid-Pillar Peak Temperature	
	Temperature (deg-C)	Time of Peak Temperature (Years from Emplacement)	Temperature (deg-C)	Time of Peak Temperature (Years from Emplacement)	Temperature (deg-C)	Time of Peak Temperature (Years from Emplacement)	Temperature (deg-C)	Time of Peak Temperature (Years from Emplacement)
1.00	313	71	150	447	226	140	131	519
1.10	293	70	145	437	211	141	127	510
1.20	275	70	140	429	199	143	123	501
1.30	260	70	136	421	189	145	119	494
1.40	247	70	132	414	180	148	116	487
1.50	235	69	129	407	172	157	113	480
1.60	224	69	126	400	165	155	111	474
1.70	215	69	123	394	159	158	108	468
1.80	207	69	121	388	153	162	106	464
1.90	199	69	118	383	149	191	104	457
2.00	193	70	116	377	144	171	102	452

Figure 2 Effect of Host-Rock Thermal Conductivity on Peak Temperatures

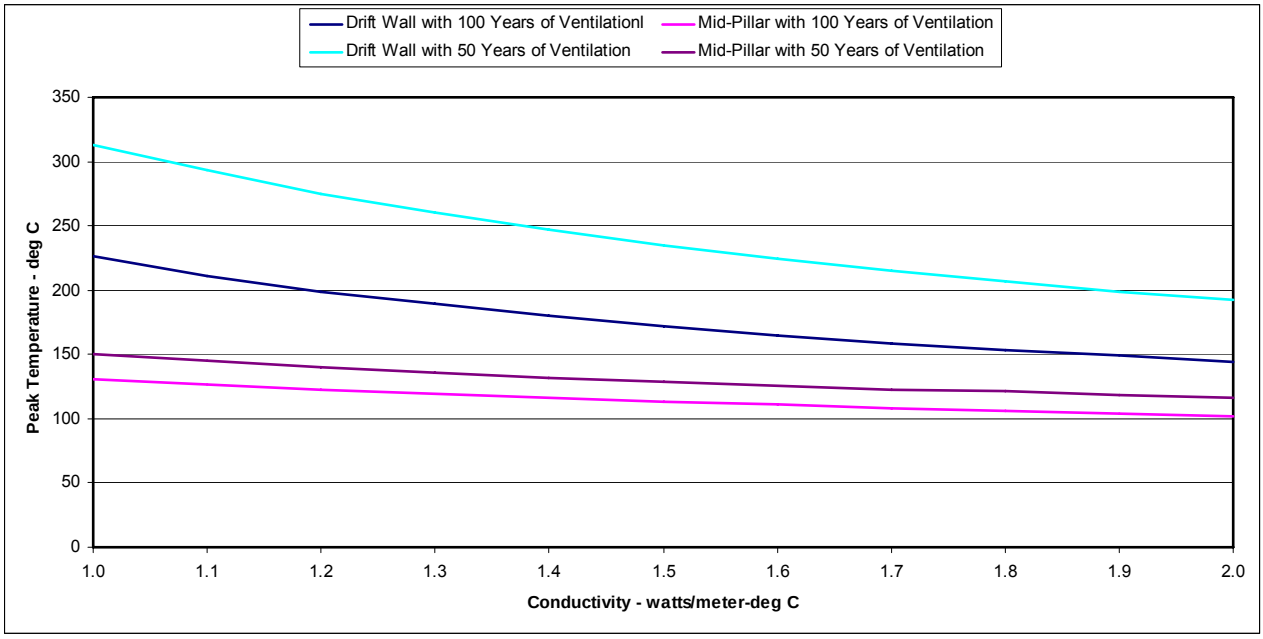

For 50 years of ventilation, a variation of thermal conductivity around a nominal value of 1.8 W/(m-^{o}C) of ±0.1 W/(m-^{o}C) will result in a difference in the peak drift wall temperature of approximately ∓8^{o}C and a difference in the mid-pillar temperature of approximately ∓2.5^{o}C, and for 100 years of ventilation, a difference in the peak drift wall temperature of approximately ∓5^{o}C and a difference in the mid-pillar temperature of approximately ∓2^{o}C. These results suggest that the thermal conductivity has a significant effect on the peak drift wall and to a lesser degree on mid-pillar temperatures and is more pronounced for higher heat sources. This variation must be accounted for either by measuring actual host-rock thermal conductivity and using as-built data in the calculation or by placing sufficient margin on the thermal limits so that a variation in rock conductivity will not cause the actual temperatures to exceed established limits.

2.3. Infinite-Length Cylinder Calculation

As stated in Appendix A, the methodology described in Section 2.2 is valid for drift wall temperatures only after approximately 5 years. For the majority of the calculations performed in this evaluation, this is acceptable because peak postclosure temperatures usually occur much beyond 5 years after emplacement. However, for determining the drift wall temperatures for the shorter preclosure periods, an infinite-length cylinder model as shown in Figure 3 was used.

Figure 3 Representation of Infinite-Length Cylinder

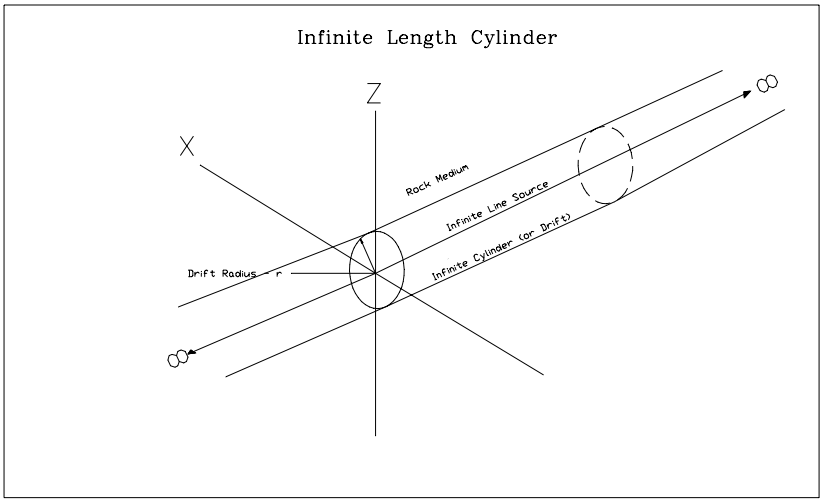

The temperature for the region bounded internally by a cylinder, i.e., a tunnel in the rock, is:

$$v(r) = \frac{2Q}{\pi \rho C_p} \int_0^{\infty} \frac{e^{-\lambda t} - e^{-\kappa u^2 t}}{\lambda - \kappa u^2} \cdot \frac{J_0(ur)Y_1(ua) - Y_0(ur)J_1(ua)}{J_1^2(ua) + Y_1^2(ua)} du \qquad \textbf{Equation 6}$$

where "Q" is the energy wall flux, "a" is the cylinder (tunnel) radius, ρ is the bulk density, Cp is the heat capacity, κ is the thermal diffusivity, $J_\nu(z)$ is the Bessel function of the first kind of order ν, and $Y_\nu(z)$ is the Bessel function of the second kind of order ν. This equation is two dimensional in r and thus represents a drift of infinite length. Equation 7 is applied to account for the heat removed by the ventilation system.

$$v(r,t,i) = \sum_i^n (1 - Vent_{eff}) \times v_i(x,t,i) \qquad \textbf{Equation 7}$$

where $Vent_{eff}$ represents the fraction of heat removed by the ventilation system and the subscript *i* is applied to the decaying power as Q_i and λ_i. The detail development of this methodology is shown in Appendix A, and a sample calculation is shown in Appendix G.

2.3.1. Effects of Host-Rock Thermal Conductivity on Temperature

As shown in Section 2.2.1, variations in rock conductivity have a significant effect on peak postclosure temperatures. Although Equation 6 contains the constant "thermal diffusivity" rather than "thermal conductivity", the temperature difference due to variations in thermal diffusivity can be evaluated by varying the thermal conductivity because the relationship between thermal conductivity and thermal diffusivity is as follows:

$$\kappa = \frac{K_{rock}}{\rho C_p}$$ **Equation 8**

where "κ" is thermal diffusivity in m^2/day, "K_{rock}" is host rock thermal conductivity in watts/meter-^oC, "ρ" is rock density = 2097 kg/$meter^3$, and "C_p" is rock specific heat = 1119 joules/kg-^oC.

Peak drift wall temperatures were calculated using the method described in Section 2.3 for conductivities between 1.0 W/m-^oC and 2.0 W/m-^oC at 0.1 W/m-^oC intervals for waste packages containing 48 Gwd/t PWR assemblies that were 16 years old at emplacement. The results are shown in Table 4 and Figure 4.

Table 4 Effect of Host-Rock Thermal Conductivity on Drift Wall Temperature

Thermal Conductivity	Time of Peak Temperature (Years)	Peak Temperature (deg-C)
1.0	15.26	110
1.1	14.99	103
1.2	14.76	98
1.3	14.55	93
1.4	14.36	89
1.5	14.18	86
1.6	14.02	83
1.7	13.87	80
1.8	13.73	77
1.9	13.60	75
2.0	13.47	73

Figure 4 Effect of Host-Rock Thermal Conductivity on Drift Wall Temperature

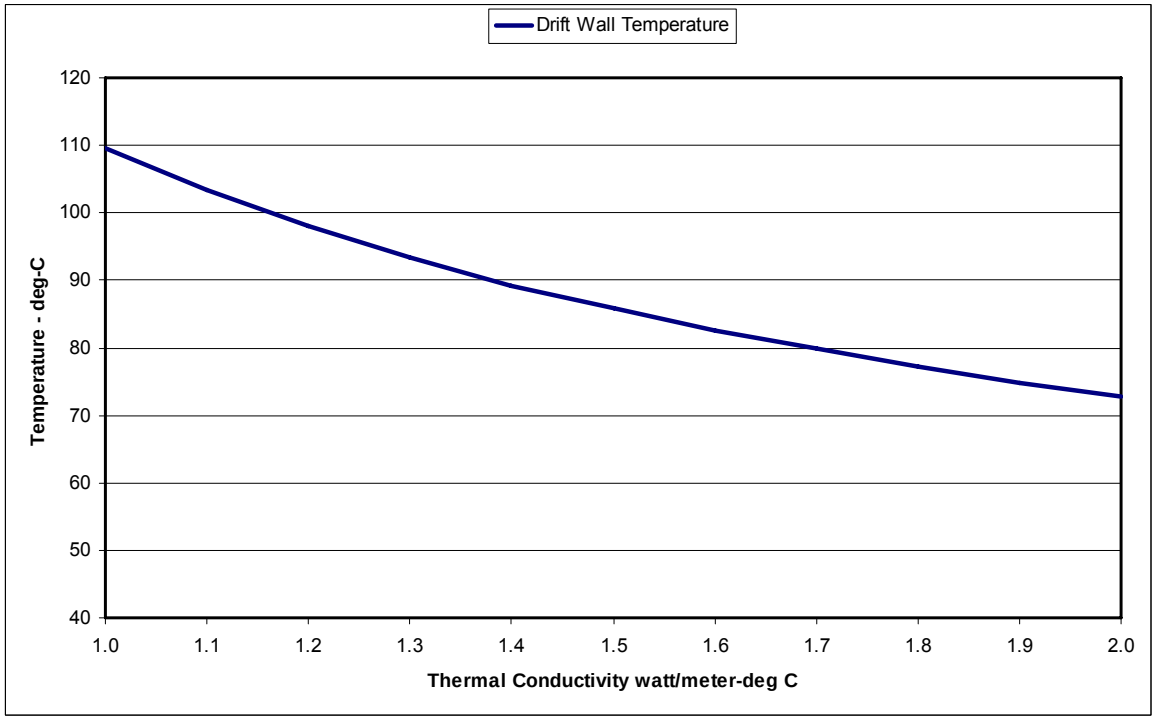

Variation of thermal conductivity around a nominal value of 1.8 W/(m-^{o}C) of ±0.1 W/(m-^{o}C) will result in a difference in the peak drift wall temperature of approximately ∓2.0^{o}C. This suggests that thermal conductivity has less effect on drift wall peak temperature during the preclosure period than during the postclosure period. This is probably because the peak temperatures occur much sooner during preclosure, so the ability for the rock to dissipate heat is not as important.

2.4. Radiant-Heat Transfer Between Two Concentric Cylinders

The waste package surface temperature is calculated from the transfer of radiant heat between two concentric cylinders, as described in the open literature. Natural convection and conduction are not taken into account. The temperature across an annulus due to radiant-heat transfer is shown in Equation 9.

$$Q_{12} = \frac{\sigma\left(T_1^4 - T_2^4\right)}{\left[\frac{1}{A_1 e_1} + \frac{1}{A_2}\left(\frac{1}{e_2} - 1\right)\right]} \qquad \textbf{Equation 9}$$

where $\sigma = 5.67 \times 10^{-8}$ W m^{-2} K^{-4}, Q_{12} is the energy per unit time transported from surface 1 to 2, T_i are the absolute surface temperatures, A_i are the surface areas per unit length, and e_i are the respective emissivities. Given the drift wall temperature and the package power, the package temperature can be calculated. The above equation can be applied to the package and the drip shield and to the drip shield and the drift wall. A sample calculation is in Appendix H.

2.5. Effect of Ventilation

During the preclosure period, forced ventilation through the emplacement drifts removes a large portion of the heat generated by the waste packages. The effect of ventilation as used by DOE in its temperature analyses is the use of a constant ventilation efficiency for all times and locations in a drift. The ventilation efficiency is defined as the energy removed by flowing air divided by the energy of the source for the entire drift length for the entire ventilation duration. Therefore, this ventilation efficiency is called an "integrated efficiency". The details of the ventilation model are described in *Ventilation Model and Analysis Report,* ANL-EBS-MD-000030, REV04. The ventilation model is based on heat transfer from the waste package to the air by convection and to the rock wall by radiation. The air receives energy by convection from the rock wall and the waste package. The bulk rock is heated by the difference in energy received by radiation and lost by conduction into the air. The solution for all of the temperatures is time dependent. Typically, temperatures are calculated on a one-year time step and the drift is divided into 100-meter lengths, where the air exiting one segment is the input to the next segment. This is shown in Figure 5.

Figure 5 Representation of Ventilation Model

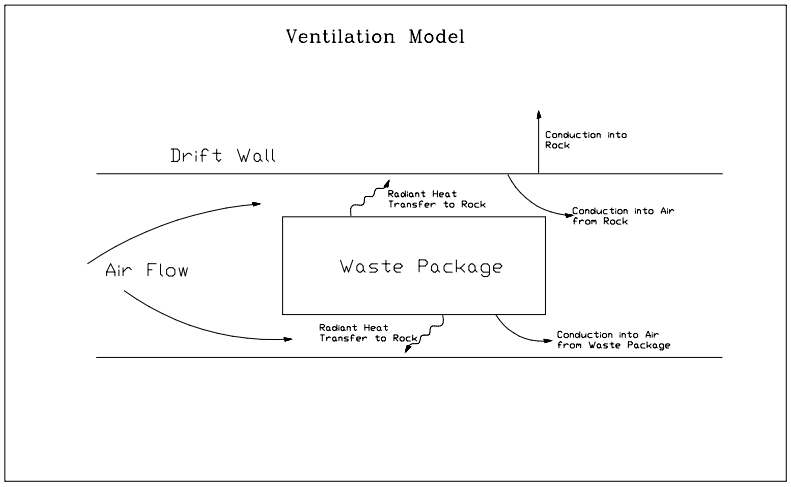

For the purpose of most of the calculations performed as part of this white paper, the assumption was that the ventilation efficiency decreases linearly as the air moves down the drift and is heated. The ventilation efficiency was assumed to be 90 percent at the entrance of the drift and 80 percent at the exit of the drift.

2.6. Thermal Properties

The set of thermal-physical properties used to calculate temperatures are based on the properties of the lower lithophysal unit, which comprises most of the repository footprint. The calculated bulk density is 2097 kg/m3 and takes into account a water saturation of 90 percent of the porosity, which is 0.13. The heat capacity of the bulk rock with water present is calculated as 1119 Joules/(kg-^{o}C). The thermal conductivity of the bulk rock with 90 percent water saturation is a linear interpolation between dry and fully saturated and is calculated as 1.83 W/(m$\cdot$ ^{o}C).

2.7. Benchmarking of Analytical Solutions

The calculated thermal-physical properties in Section 2.6 were used to calculate the peak drift wall and mid-pillar temperatures for comparison with those obtained from the *Multiscale Thermohydrologic Model*, (MSTHM), ANL-EBS-MD-000049, REV03, for the lower lithophysal unit. The MSTHM takes into account water-vapor movement, hydrology, and stratigraphy. The MSTHM peak drift wall temperature for a typical waste package is 136.8°C (refer to MSTHM, Figure 6.3-15a), and the temperature calculated at that location using the methods described in this document is 137.5°C. The MSTHM peak mid-pillar temperatures for two locations are 87.3°C and 89.6°C, and the temperature calculated using the methods described in this document is 87.8°C. These differences in calculated temperatures are considered small, so the methods described in this document are of sufficient accuracy for the thermal strategy analyses presented in this document.

3. Thermal Limits

At the July 31, 2007, fact-finding meeting between DOE and the NWTRB, DOE provided the thermal limits listed below as the basis for design. Not clear is whether these limits consider the accuracy of the calculation methods or any margin to the thermal limits. They are important considerations that DOE needs to include when making its final recommendations for establishing the thermal limits and the thermal operating methodology.

Although these thermal limits are used throughout this evaluation, the use of these limits does not imply acceptance or endorsement of the limits by the NWTRB.

Maximum CSNF cladding temperature:

Before repository closure: 400°C

After repository closure: 350°C

Maximum waste package surface temperature: 300°C

Maximum drift wall temperature: 200°C

Maximum temperature halfway between emplacement drifts ("mid-pillar"): 96°C

4. Thermal Evaluations

4.1. Preclosure

4.1.1. General

During the preclosure phase, a nominal ventilation flow rate of approximately 15m^3/sec is provided through each emplacement drift by a series of fans located external to the drift. The ventilation system removes approximately 85 percent of the waste package heat. This evaluation will calculate the drift wall temperature for a uniform drift loading during both normal and loss-of-ventilation conditions using the methodology described in Section 2.3.

The parameters used for this evaluation are as follow:

WP type – 21 PWR
WP length – 5.85 m
WP spacing – 0.1 m
WP spacing (DOE case) – 0.7 m
Drift length – Infinite

Forced ventilation efficiency – 85%
Natural ventilation efficiency – 0%
Drift spacing – 81 m
No. drifts – 1

Rock density – 2097 kg/m^3
Heat capacity – 1119 Joules/kg-^oC
Rock thermal conductivity – 1.83W/m-^oC
Initial rock temperature – 22.8^oC

4.1.2. Comparison of DOE and NWTRB Evaluations

DOE document 800-00C-WIS0-00600-000-00B, *Temperature in as "As-Loaded" and Thermally-Misloaded Segment*, provides preclosure temperatures for both the normal and loss-of-forced-ventilation conditions. To evaluate these results, the NWTRB calculated the temperatures using the same linear line load of 1.99 kW/meter (waste package spacing was increased to 0.7 meters to achieve the same linear line load as used in the DOE calculation), with a loss of forced ventilation for 30 days, 30 days after emplacement. The results are compared with the DOE results in Table 5.

Table 5 Comparison of DOE and NWTRB Preclosure Temperatures

	Normal Condition		Loss-of-Ventilation Condition	
	DOE Results	NWTRB Results	DOE Results	NWTRB Results
Waste Package Temperature - ºC	111.9	115	162.1	148
Drift Wall Temperature - ºC	?	55	113.9	108

The differences in results could be attributed to the following.

1. Effect of invert — DOE attempts to model the actual properties of the invert; the NWTRB model assumes the invert acts as a fixed insulator for 25 percent of the surface area
2. Thermal conductivity — The NWTRB model assumes a constant 1.83 watts/meter-^{o}C conductivity; the DOE model has a variable conductivity.
3. Geometric model — The NWTRB model assumes two concentric circles to represent the waste package and drift wall; in reality, the center of the waste package is offset from the center of the drift

Despite the differences in the two models, the results indicate reasonable agreement.

4.1.3. Preclosure Thermal Response During Normal Operation

Several calculations were performed for various assembly powers at emplacement using the methodology in Section 2.3. On the basis of these calculations, the determination was that the maximum drift wall temperature was 139^{o}C, or approximately 60^{o}C below the maximum allowable limit of 200^{o}C for all cases with normal ventilation flow. Figure 6 shows the drift wall temperature as a function of time for the most severe case of 5-year-old PWR assemblies with a burnup of 70 Gwd/ton (which corresponds to a linear line load of 6.51 kW/meter at emplacement).

Figure 6 Drift Wall Temperature with Normal Ventilation Flow

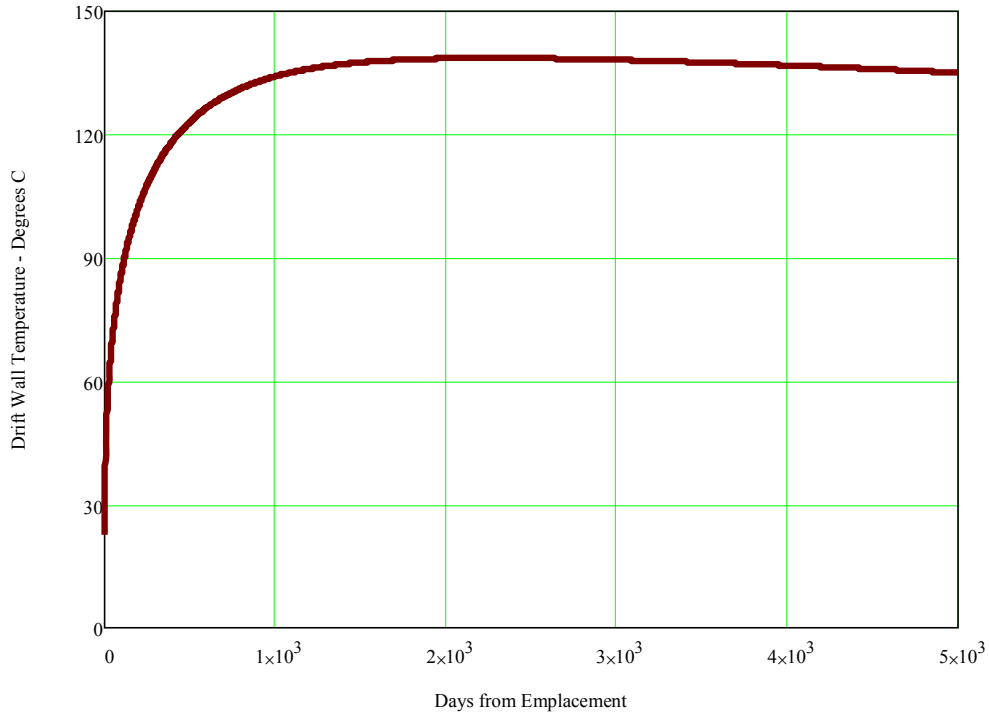

These results suggest that under normal preclosure ventilation conditions, any waste that is received at the repository can be emplaced immediately with no surface aging without exceeding the maximum allowable drift wall temperature of 200°C.

4.1.4. Preclosure Thermal Response for Loss of Forced Ventilation

During the preclosure period, forced ventilation could be lost. DOE considers the loss-of-forced-ventilation event the basis for establishing the thermal conditions for emplacement and has set the maximum linear line load over a seven-waste package segment at emplacement at less than 2.0 kW/meter. The results shown in Table 4 make apparent that establishing the linear line load at 2.0 kW/meter may be overly conservative because there is approximately 60°C of margin to the drift wall maximum temperature of 200°C. For evaluating the loss-of-ventilation event, several calculations were performed using the methodology described in Section 2.3 to determine how long it would take for the drift wall temperature to reach the maximum allowable temperature of 200°C when forced ventilation is lost at various times after emplacement. Figure 7 and Table 6 present an example of the calculation for 5-year-old assemblies with a burnup of 40 Gwd/ton.

Figure 7 Loss-of-Forced-Ventilation Example Graph

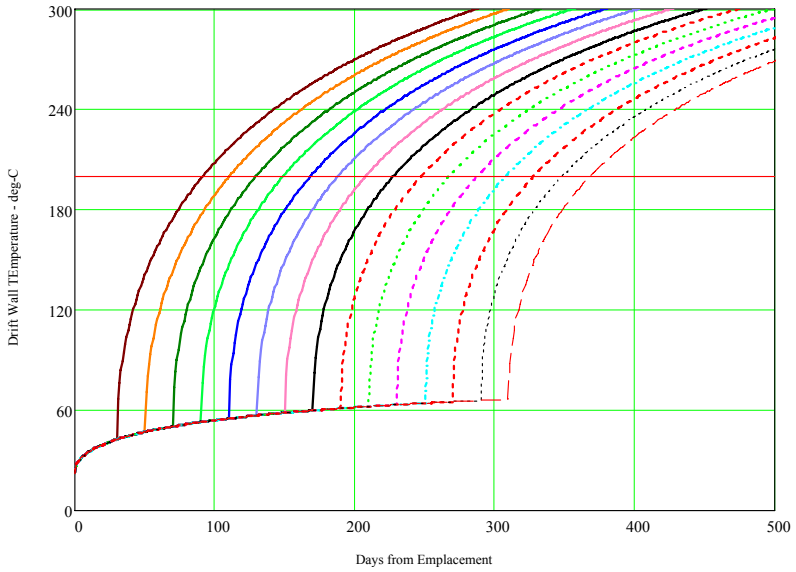

Table 6 Loss- of-Forced-Ventilation Example Results

Time After Emplacement when Forced Ventilation is Lost (Days)	Time Required After Loss of Forced Ventilation Until 200 deg-C Drift Wall Temperature is Reached (Days)
30	62
50	61
70	60
90	59
110	59
130	58
150	58
170	58
190	58
210	58
230	58
250	58
270	58
290	59
310	59

This example shows that the shortest time to reach 200°C after ventilation is lost is 58 days and occurs not at 30 days after emplacement but sometime between 110 and 290 days after emplacement.

For determining the parameters that define the shortest time to reach 200°C 30 days after forced ventilation is lost, several calculations were performed. The calculations were performed for waste packages loaded with PWR assemblies with ages of 5, 10, 15, and 20 years out of reactor at emplacement and burnup between 35 and 70 Gwd/ton. The results are shown in Table 7 and Figure 8.

Table 7 Loss-of-Forced-Ventilation During Preclosure Period

Assembly Burnup	Age at Emplacement	Line Load at Emplacement	Number of Days of Forced Ventilation	Minimum #Days Required to Reach 200 deg-C Drift Wall Temperature
35	5	2.76	80	93
40	5	3.19	130	58
45	5	3.68	180	36
50	5	4.17	280	23
35	10	1.83	140	316
40	10	2.12	360	185
45	10	2.45	550	109
50	10	2.79	600	69
55	10	3.17	750	43
60	10	3.55	850	28
65	10	3.99	1350	17
45	15	2.08	800	175
50	15	2.36	1200	109
55	15	2.67	1050	69
60	15	2.99	1000	46
65	15	3.34	1400	29
70	15	3.70	1650	19
45	20	1.86	650	255
50	20	2.11	1000	159
55	20	2.39	1100	101
60	20	2.66	1250	67
65	20	2.97	1500	44
70	20	3.28	1500	30
45	25	1.69	550	365
50	25	1.92	800	227
55	25	2.16	950	145
60	25	2.40	1150	97
65	25	2.67	1350	65
70	25	2.94	1450	45

Figure 8 Days Required to Reach 200°C Drift Wall Temperature After Loss of Forced Ventilation

These results suggest that an emplacement drift can be loaded to a higher linear line load than is presently assumed by DOE, up to approximately 3.25 kW/meter, without exceeding the 200°C drift wall temperature limit, even with a 30-day loss of forced ventilation and no credit taken for natural ventilation.

4.1.5. Discussion

During the preclosure period, the mid-pillar temperature limit is not important because the peak mid-pillar temperature occurs hundreds of years after repository closure. Therefore, during the preclosure period, the limiting thermal limit appears to be the maximum drift wall temperature of 200°C. According to the above calculations, it appears that during normal operation with forced ventilation, there is no restriction on the power of the waste emplaced. However, if forced ventilation is lost for 30 days, the drift wall temperature can be exceeded. For preventing exceeding drift wall temperature, an operating limit of approximately 3.25 kW/meter linear line load should be maintained. This value is significantly higher than the 2.0 kW/meter criteria assumed by the project and corresponds to an average waste package power of approximately 19.3 kW.

4.2. Postclosure

4.2.1. General

At some point, the forced ventilation system will be shut down and the repository will be closed. This will result in a rise in repository temperatures because none of the heat generated by the waste packages will be removed by the ventilation system. The following evaluation will compare waste package power and mid-pillar temperatures results from DOE evaluations with NWTRB evaluations. In addition, the minimum age of various burnup fuels that result in not exceeding either the maximum mid-pillar temperature of 96°C or the maximum drift wall temperature of 200°C will be calculated. The parameters used for this evaluation are as follow:

Drift length: 583 m	Rock density: 2097 kg/m^3
No. drifts: 11 (5 on each side)	Heat capacity: 1119 Joules/ kg-°C
Drift spacing: 81 m	Rock thermal conductivity: 1.83 W/m-K
No. segments per drift: 15	Initial rock temperature: 22.8°C
No. WP per segment: 7	Initial ventilation efficiency: 90%
WP spacing: 0.1 m	Final ventilation efficiency: 80%

4.2.2. Comparison of DOE and NWTRB Evaluations

DOE Engineering Study 000-00R-G000-01000-000-000, *Total System Model Analysis for Repository Postclosure Thermal Envelope Study, Phase2*, data file WP_Decay_70K22kw_011707.xls, provides the individual average waste package characteristics and the maximum mid-pillar temperature if the entire repository were loaded with waste packages with these characteristics. As a check of these results, several waste packages were selected, and the waste package power at emplacement and peak mid-pillar temperature were calculated. The results are shown in Table 8.

Table 8 Comparison of DOE and NWTRB WP Power and Peak Mid-pillar Temperatures

Waste Package Characteristics										Power at Emplacement (watts)		Peak Post closure Mid-pillar Temperature (deg-C)		Comparison of DOE with NWTRB Results	
WP ID	Shipment ID	WP Length (meters)	Year Created	Total MTHM	Average Burnup (Gwd/ton)	Age at Emplacement (Years OOR)	Age at Closure (Years OOR)	Number of Assemblies per WP	SNF TYPE	DOE Results	NWTRB Results	DOE Results	NWTRB Results	Power Difference (%)	Temperature Difference (%)
130958	201706700	5.85	2018	7.476	40	7	103	44	BWR	11,692.6	11,567.7	79	75	1%	5%
131027	201807206	5.85	2019	7.568	38	10	105	44	BWR	9,514.0	9,421.7	76	72	1%	5%
131028	201807207	5.85	2019	7.568	40	11	106	44	BWR	9,654.3	9,590.3	78	75	1%	4%
135949	202908306	5.85	2030	7.591	42	26	110	44	BWR	7,371.3	7,311.5	80	75	1%	6%
135955	202910202	5.85	2030	7.810	51	6	90	44	BWR	17,229.6	17,572.0	94	92	-2%	2%
135962	202908603	5.85	2030	7.717	55	17	101	44	BWR	12,222.5	12,232.1	93	90	0%	3%
141094	204005612	5.85	2040	7.798	46	31	105	44	BWR	7,542.2	7,568.8	85	81	0%	5%
141112	204005703	5.85	2040	7.811	54	5	79	44	BWR	19,129.0	20,879.0	97	99	-9%	-2%
141113	204005704	5.85	2040	7.814	62	6	80	44	BWR	21,315.9	22,732.2	106	106	-7%	0%
130915	DTF1WP97	5.85	2017	7.675	24	26	123	21	PWR	4,362.6	4,369.4	61	57	0%	7%
130916	DTF1WP98	5.85	2017	5.705	23	44	141	21	PWR	2,277.8	2,254.4	49	46	1%	6%
130954	DTF1WP108	5.85	2018	7.265	50	12	108	21	PWR	12,722.6	12,814.9	100	97	-1%	3%
135852	202909104	5.85	2030	9.135	47	21	105	21	PWR	12,033.4	12,058.4	115	111	0%	3%
135853	202909400	5.85	2030	9.534	52	8	92	21	PWR	19,938.1	21,587.0	130	130	-8%	0%
135854	202909401	5.85	2030	9.534	54	9	93	21	PWR	20,595.5	21,315.0	134	132	-3%	1%
141090	204007302	5.85	2040	9.040	62	14	88	21	PWR	19,748.8	19,945.1	140	140	-1%	0%
141091	204007401	5.85	2040	9.172	54	8	82	21	PWR	21,317.1	21,839.1	134	133	-2%	1%
141092	204007402	5.85	2040	9.172	50	16	90	21	PWR	16,534.3	14,467.0	124	122	13%	2%
	Note:	The "Total MTHM" values for WPs DTF1WP97, DTF1WP98, and DTF1WP108 contained in WP_Decay_70K22kw_011707.xls and BatchInfo.mdb were inconsistant. The value contained in BatchInfo.mdb were used.													

The NWTRB and DOE results are in reasonable agreement. The difference between the "Power at Emplacement" values can be attributed to the following:

- The NWTRB calculation utilized average waste package characteristics, whereas the DOE calculation calculates waste package power on the basis of the individual assembly characteristics.
- The NWTRB calculation rounds assembly burnup values to the nearest integer, whereas the DOE calculation uses actual burnup values
- The NWTRB calculation assumes a constant 4.0 percent BWR and 4.5 percent PWR enrichment, whereas the DOE calculation uses actual assembly enrichment.

The difference in "Peak Postclosure Mid-pillar Temperature" can be attributed to the fact that the NTWRB calculation utilized a finite-length drift model, whereas the DOE model utilized an infinite-length drift model. Therefore, the NWTRB results were consistently lower than the DOE results.

A further check was performed to determine the accuracy of the linear line load and mid-pillar temperature for a seven-package segment. Three random seven-package segments were chosen, one emplaced in 2021, one emplaced in 2031, and one emplaced in 2050; the results are shown in Table 9.

Table 9 Comparison of Linear Line Load and Mid-pillar Temperature over a Seven-Package Segment

WP ID (Note 1)	Shipment ID (Note 1 & 2)	WP Type (Note (1)	SNF Type (Note 1)	Average MTHM (Note 4)	Average Burnup (Gwd/ton) (Note 2)	Emplacement Year (Note 1)	Average Age at Emplacement (Years) (Note 4)	Ventilation Duration (Years) (Note 4)	WP Power at Emplacement (watts/WP)		Lineal Line Load at Emplacement (watt/meter)		Individual Mid-pillar Temperature (deg-C)		Seven Segment Average Mid-pillar Temperature (deg-C)	
									DOE Calculation (Note 1)	NWTRB Calculation (Note 4)	DOE Calculation (Note 1 & 5)	NWTRB Calculation (Note 4)	DOE Calculation (Note 1)	NWTRB Calculation (Note 4)	DOE Calculation (Note 1 &5)	NWTRB Calculation
131463	DTF1WP336	WP	PWR	0.4616	43.4	2021	20	96	12,008.1	11,738.0		2,003	114	107	85	N/A
131543	DTF1WP372	WP	PWR	0.4379	43.7	2021	12	96	13,976.9	13,896.8		2,371	112	107	85	N/A
131642	DTF1WP433	WP	PWR	0.4180	36.3	2021	27	96	7,966.8	7,622.6		1,301	92	85	85	N/A
130987	201806105	WPMPC	BWR	0.1718	11.9	2021	26	96	1,965.4	1,971.3		336	38	35	85	N/A
131351	202004600	WPMPC	BWR	0.1770	52.6	2021	6	96	17,879.3	18,430.6		3,145	93	91	85	N/A
131333	DTF1WP282	WP	BWR	0.0762	17.2	2021	45	96	879.6	876.8		150	35	31	85	N/A
131428	202008205	WPMPC	PWR	0.3507	57.1	2021	9	96	17,405.8	17,680.9		3,017	111	108	85	N/A
						Total			72,082.0	72,216.9	N/A	N/A	N/A		N/A	N/A
						Average			10,297.4	10,316.7	1,735	1,761	85	81	85	82

WP ID (Note 1)	Shipment ID (Note 1 & 2)	WP Type (Note (1)	SNF Type (Note 1)	Average MTHM (Note 4)	Average Burnup (Gwd/ton) (Note 2)	Emplacement Year (Note 1)	Average Age at Emplacement (Years) (Note 4)	Ventilation Duration (Years) (Note 4)	WP Power at Emplacement (watts/WP)		Lineal Line Load at Emplacement (watt/meter)		Individual Mid-pillar Temperature (deg-C)		Seven Segment Average Mid-pillar Temperature (deg-C)	
									DOE Calculation (Note 1)	NWTRB Calculation (Note 4)	DOE Calculation (Note 1 & 5)	NWTRB Calculation (Note 4)	DOE Calculation (Note 1)	NWTRB Calculation (Note 4)	DOE Calculation (Note 1 & 5)	NWTRB Calculation
133759		WP	WPCodisposeL	0.4169		2031	0	86	353.0	407.0		78	24	24	82	N/A
134029	202600601	WPMPC	PWR	0.4618	56.5	2031	16	86	17694.4	18147.0		3097	138	134	82	N/A
134226	202606302	WPMPC	PWR	0.4552	57.1	2031	16	86	17826.4	17887.6		3052	138	133	82	N/A
135834	202908800	WPMPC	PWR	0.4566	53.7	2031	14	86	17795.1	17618.3		3007	133	129	83	N/A
133762		WP	WPCodisposeL	0.4169		2031	0	86	353.0	407.0		78	24	24	83	N/A
135557	202903302	WPMPC	BWR	0.1716	55.1	2031	7	86	16190.7	17313.9		2955	94	93	82	N/A
133765		WP	WPCodisposeL	0.4169		2031	0	86	353.0	407.0		78	24	24	82	N/A
						Total			70,565.6	72,187.8	N/A	N/A	N/A		N/A	N/A
						Average			10,080.8	10,312.5	1,779	1,763	82	80	82	81

WP ID (Note 1)	Shipment ID (Note 1 & 2)	WP Type (Note (1)	SNF Type (Note 1)	Average MTHM (Note 4)	Average Burnup (Gwd/ton) (Note 2)	Emplacement Year (Note 1)	Average Age at Emplacement (Years) (Note 4)	Ventilation Duration (Years) (Note 4)	WP Power at Emplacement (watts/WP)		Lineal Line Load at Emplacement (watt/meter)		Individual Mid-pillar Temperature (deg-C)		Seven Segment Average Mid-pillar Temperature (deg-C)	
									DOE Calculation (Note 1)	NWTRB Calculation (Note 4)	DOE Calculation (Note 1 & 5)	NWTRB Calculation (Note 4)	DOE Calculation (Note 1)	NWTRB Calculation (Note 4)	DOE Calculation (Note 1 & 5)	NWTRB Calculation
141079	DTF1WP3952	WP	PWR	0.4326	26.9	2050	66	67	3256.8	3071.7		516	81	68	81	N/A
141027	204003904	WPMPC	BWR	0.1775	44.2	2050	46	67	5566.6	5537.2		931	81	76	81	N/A
132617	202303001	WPMPC	BWR	0.1726	44.6	2050	43	67	5739.6	5805.6		976	81	76	81	N/A
140808	203910205	WPMPC	BWR	0.1775	44.0	2050	45	67	5627.0	5631.9		947	81	77	81	N/A
137451	203210206	WPMPC	BWR	0.1775	42.7	2050	40	67	5940.0	5988.8		1007	81	77	81	N/A
138191	203405610	WPMPC	BWR	0.1771	42.6	2050	36	67	6319.3	6413.2		1078	81	78	81	N/A
140044	DTF1WP3604	WP	PWR	0.4132	30.9	2050	62	67	3719.2	3635.9		611	81	74	81	N/A
						Total			36,168.6	36,084.3	N/A	N/A	N/A		N/A	N/A
						Average			5,166.9	5,154.9	870	866	81	75	81	75

Notes: 1. Data taken from WP_Empl_Lin_Dana_YFF5_22kw_011707-236_050107a_Mod_R2.xls Sheet Emplaced (85C 4 year 18kw)
2. Data taken from WP_Decay_70k_22kw_011707.xls sheet WP_Decay
3. Data taken from Batch_Info.mdb
4. Calculated value
5. Represents a running average over 7 waste packages

These results are consistent with the results in Table 8. The waste package powers are in reasonable agreement, and the mid-pillar temperatures calculated by the NWTRB are consistently lower because of the use of a finite line source rather than an infinite line source.

DOE also performed an engineering study, and the results were documented in data file WPLOAD_OUPUT_case_3b.TXT. A comparison of these results and the NWTRB calculations is provided in Table 10.

Table 10 Comparison of Mid-pillar Temperatures Calculated by WPLoad

WP ID (Note 2 &)	WP Type (Note 2)	WP Length (Note 1)	Emplacement Year (Note 2 & 4)	Assembly Numbers (Note 3 &)	Batch Number (Note 4 & 7)	Shipping Cask Number (Notes 4 & 7)	Number Assemblies (Note 7)	Total MTU (Note 7)	Average Burnup (Gwd/ton) (Note 7)	Year Discharged (Note 4 & 7)	Average Age at Emplacement (Years) (Note 8)	Ventilation Duration (Years) (Note 8)	WP Power at Emplacement (watts/WP)		Lineal Line Load at Emplacement (watt/meter)		Individual Mid-pillar Temperature (deg-C)	
													DOE Calculation (Note 2)	NWTRB Calculation (Note 8)	DOE Calculation (Note 5)	NWTRB Calculation (Note 8)	DOE Calculation (Note 6)	NWTRB Calculation (Note 8)
2620	21PWRTAD	5.85	2018	1666 - 1686														
				1666 - 1670	2149	58	4	1.7143	28.9	1979	39							
				1670 - 1686	1555	58	17	7.7513	31.5	1978	40							
				Total			21	9.4656										
				Average				0.4507	31.0		40	99	5,804	5,569	1.85	0.98	92	78
2641	21PWRTAD	5.85	2018	2214 -2234														
				2215 - 2221	4342	88	8	3.6568	30.0	1983	35							
				2222 - 2231	3345	88	13	5.9566	29.8	1981	37							
				Total			21	9.6134										
				Average				0.4578	29.9		36	99	5,977	5,832	1.71	0.98	91	78
209	21PWRTAD	5.85	2018	102 - 122														
				102 - 106	24975	3 & 4	5	1.7297	43.7	2009	9							
				107 - 115	24563	4, 5, & 6	9	3.1135	47.6	2008	10							
				116 - 120	24562	6 & 7	5	1.7297	43.7	2008	10							
				121 - 122	24049	7 & 8	2	0.6919	50.6	2006	12							
				Total			21	7.2648										
				Average				0.3459	46.0		10	99	13,011	12,560	1.74	2.11	98	92
2626	44BWRTAD	5.85	2018	1820 - 1863														
				1820 - 1853	26053	62	34	5.8486	50.6	2012	6							
				1854- 1863	26052	62	10	1.7202	47.1	2012	6							
				Total			44	7.5688										
				Average				0.1720	49.8		6	99	17,983	16,582	1.88	2.79	91	86
2621	21PWRTAD	5.85	2018	1687 - 1707														
				1687 - 1707	1554	59	21	9.5730	28.4	1978	40							
				Total			21	9.5730										
				Average				0.4559	28.4		40	99	5,297	5,037	1.73	0.85	87	73
245	21PWRTAD	5.85	2018	123 - 143														
				123 - 125	24049	8	3	1.0379	50.6	2006	12							
				126 - 129	24049	9	4	1.3838	50.6	2006	12							
				130 - 133	24049	10	4	1.3838	50.6	2006	12							
				134 - 135	24049	11	2	0.6919	50.6	2006	12							
				136 - 137	24048	11	2	0.6919	46.8	2006	12							
				138 - 141	16830	12	4	1.5404	12.2	1996	22							
				142	16831	12	1	0.3867	12.5	1996	22							
				143	16821	13	1	0.3852	18.6	1996	22							
				Total			21	7.5016										
				Average				0.3572	39.6		15	99	10,450	9,256	1.69	1.56	86	84
2628	21PWRTAD	5.85	2018	1872 - 1892														
				1872	24976	65	1	0.3459	47.6	2009	9							
				1873 - 1880	24048	65, 66 & 67	8	2.7675	46.8	2006	12							
				1881 - 1884	24047	68	4	1.3839	43.0	2006	12							
				1885 - 1892	23605	69 & 70	8	3.4595	53.2	2005	13							
				Total			21	7.9568										
				Average				0.3789	48.6		12	99	12,996	13,700	1.72	2.30	101	102
											Average		**10,217**	**9,791**	**1.72**	**1.65**	**92**	**85**
											Based on 7 package segment analysis			**9,791**		**1.65**		**85**

Notes:
1. Taken from WPLOAD_OUPUT_case_3b.TXT Section 1
2. Taken from WPLOAD_OUPUT_case_3b.TXT Section 6
3. Taken from WPLOAD_OUPUT_case_3b.TXT Section 8
4. Taken from WPLOAD_OUPUT_case_3b.TXT Section 9
5. Taken from WPLOAD_OUPUT_case_3b.TXT Section 13
6. Taken from WPLOAD_OUPUT_case_3b.TXT Section 14
7. Taken from WASTESTREAM.TXT
8. Calculated

As with the TSM calculations, the NWTRB and DOE results are reasonably consistent and show the same trend; the DOE calculations tend to calculate a higher mid-pillar temperature than the NWTRB calculations.

The result of this evaluation is that the approach and calculation methods used by the DOE appear reasonable and consistent with the completely independent calculations performed by the NWTRB staff. The "Power at Emplacement" results from the DOE model are potentially more accurate than the NWTRB results because the finer detail used in calculating the waste package power and the "Peak Postclosure Mid-pillar Temperature" is potentially more conservative because of the use of an infinite-length drift model.

4.2.3. Mid-pillar Temperature Evaluation

The approach used by DOE to determine the maximum mid-pillar temperature limit was to predict the incoming waste stream and calculate the mid-pillar temperature on the basis of this waste stream. The approach taken by the NWTRB was to determine the age of the waste at closure that would prevent exceeding the 96°C mid-pillar temperature for various assembly burnup, age, and ventilation durations. Each calculation assumed a similar seven-package segment replicated throughout the repository containing one DOE long co-disposal waste package, one DOE short co-disposal waste package, and five PWR waste packages with the same characteristics. Several calculations using the methodology described in Section 2.2 were performed, and the age of the fuel was adjusted until the peak postclosure mid-pillar temperature approached 96°C without exceeding the 96°C limit. In some cases, the minimum age at emplacement of 5 years results in a temperature that does not approach the 96°C limit. The results are shown in Table 11 and Figure 9.

Table 11 Thermal Conditions to Maintain Mid-pillar Temperature Below 96°C

Assembly Burunup (Gwd/ton)	Ventilation Duration (Years)	Age at Emplacement (Years from reactor discharge)	Line Load at Emplacement (kW/meter)	Age at Closure (Years from reactor discharge)	Line Load at Closure (kW/meter)	Time of Peak Drift Wall Temperature (Years from Emplacement)	Peak Drift Wall Temperature (oC)	Time of Peak Mid-pillar Temperature (Years from Emplacement)	Peak Mid-pillar Temperature (oC)
35	25	5	2.2	30	0.93	39	189	302	90
40	25	12	1.58	37	0.96	40	194	331	96
45	25	31	1.25	56	0.82	43	172	360	96
50	25	52	1.01	77	0.7	48	155	372	96
55	25	69	0.89	94	0.64	56	147	365	96
60	25	84	0.81	109	0.6	74	144	356	96
40	50	5	2.53	55	0.71	67	161	392	91
45	50	12	1.82	62	0.74	68	166	383	96
50	50	31	1.4	81	0.65	73	153	394	96
55	50	47	1.2	97	0.6	82	146	386	96
60	50	61	1.07	111	0.58	101	145	378	96
45	75	5	2.9	80	0.58	97	146	420	92
50	75	12	2.05	87	0.6	100	150	412	96
55	75	29	1.62	104	0.55	113	144	406	96
60	75	43	1.41	118	0.53	136	143	397	96
50	100	5	3.28	105	0.49	135	138	440	93
55	100	12	2.32	112	0.52	145	142	422	96
60	100	27	1.86	127	0.49	172	141	422	96

Figure 9 Thermal Conditions at Emplacement to Maintain Mid-pillar Temperature Below 96°C

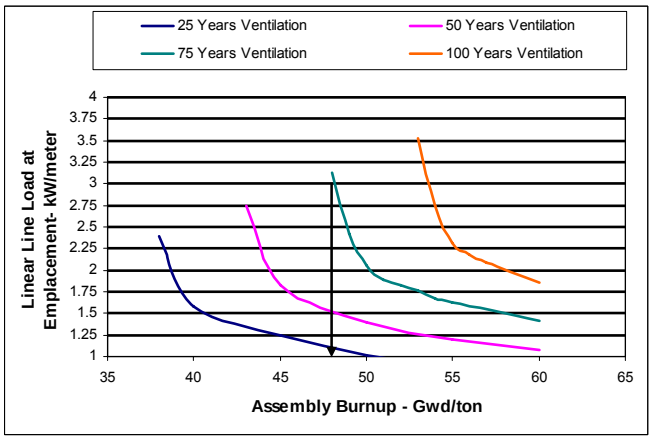

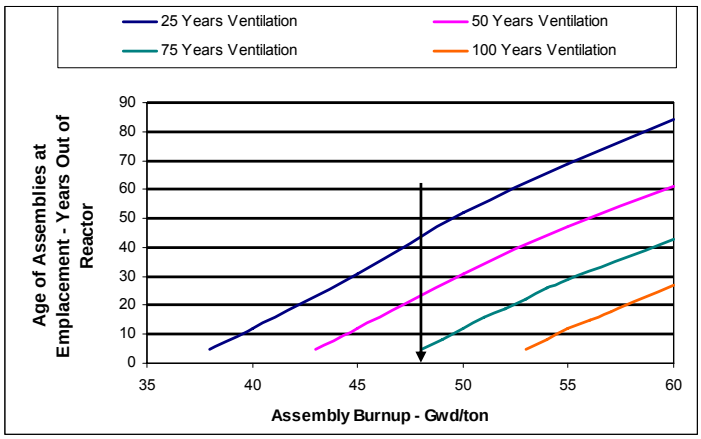

These results indicate that waste with an average burnup of approximately 48 Gwd/ton could be emplaced when it is approximately 5 years old out of reactor (which would correspond to an average linear line of approximately 3.0 kW/meter) and ventilated for 75 years, and the mid-pillar temperature would still be maintained below 96°C. The same data, but plotted in terms of conditions at closure, are presented in Figure 10.

Figure 10 Thermal Conditions at Closure for Maintaining Mid-pillar Temperature Below 96°C

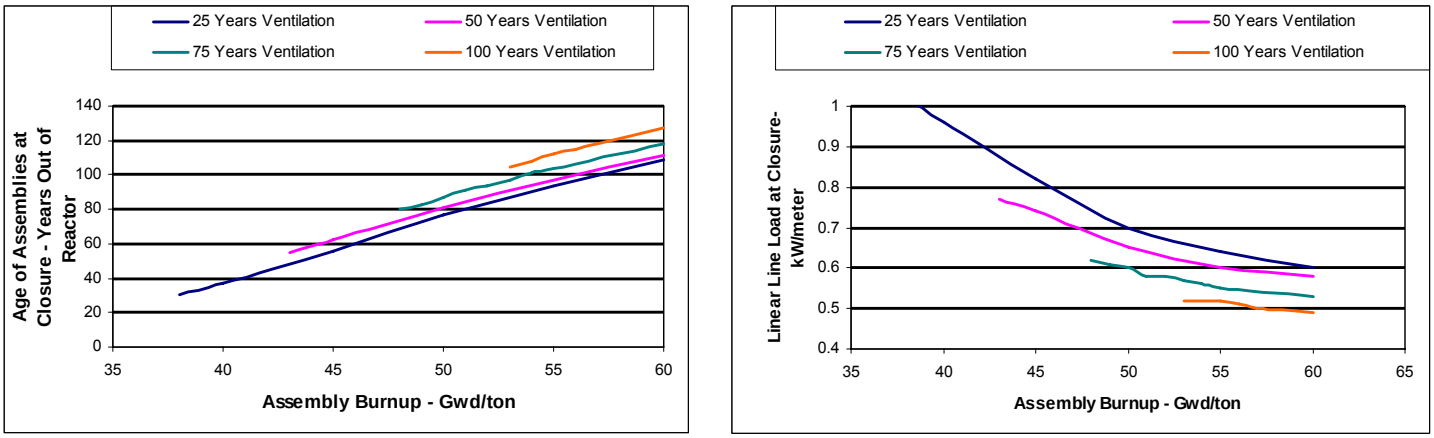

The data indicate that the duration of the preclosure ventilation phase has less influence on the mid-pillar temperature than does the age of the waste at closure. The following can be observed from Table 11:

Table 12 Effects of Ventilation Duration on Age of Assemblies at Closure

Assembly Burnup (Gwd/ton)	Ventilation Duration (Years)	Age of Assemblies Not to Exceed 96°C Mid-pillar Temperature (Years Out of Reactor)
50	50	81
50	75	87

Therefore, for 50 Gwd/ton assemblies, ventilating for an additional 25 years reduces the age at closure by only 6 years.

4.2.4. Drift Wall Temperature Evaluation

The results shown in Table 10 confirm that the mid-pillar thermal limit is reached before the drift wall temperature limit. If the mid-pillar temperature limit were eliminated, the thermal power of the emplaced waste could be increased. To determine how much the thermal power could be increased, the age of the waste at closure was determined that would prevent exceeding the 200°C drift wall temperature for various assembly burnup, age, and ventilation durations. Each calculation assumed a similar seven-package segment replicated throughout the repository containing one DOE long co-disposal waste package, one DOE short co-disposal waste package, and five PWR waste packages with the same characteristics. Several calculations using the method described in Section 2.2 were performed, and the age of the fuel was adjusted until the peak postclosure drift wall temperature approaches 200°C without exceeding the 200°C limit. In some cases, the minimum age at emplacement of 5 years results in

a temperature that does not approach the 200°C limit. The results are provided in Table 12 and Figures 11 and 13.

Table 13 Thermal Condition for Maintaining Drift Wall Temperature Below 200°C

Assembly Burunup (Gwd/ton)	Ventilation Duration (Years)	Age at Emplacement (Years from reactor discharge)	Line Load at Emplacement (kW/meter)	Age at Closure (Years from reactor discharge)	Line Load at Closure (kW/meter)	Time of Peak Drift Wall Temperature (Years from Emplacement)	Peak Drift Wall Temperature (oC)	Time of Peak Mid-pillar Temperature (Years from Emplacement)	Peak Mid-pillar Temperature (oC)
35	25	5	2.20	30	0.93	39	190	302	90
37	25	5	2.33	30	0.99	39	200	296	94
40	25	10	1.71	35	0.99	40	200	322	97
45	25	19	1.54	44	0.98	41	199	330	102
50	25	27	1.50	52	0.97	42	200	334	106
55	25	35	1.46	60	0.96	43	199	328	109
60	25	42	1.43	67	0.95	44	199	322	112
49	50	5	3.20	55	0.89	66	197	352	106
50	50	6	2.93	56	0.90	66	198	352	107
52	50	9	2.46	59	0.90	67	198	349	108
53	50	10	2.39	60	0.90	67	199	347	109
54	50	11	2.35	61	0.91	67	200	345	110
55	50	13	2.25	63	0.90	67	199	346	110
56	50	14	2.24	64	0.90	68	200	344	111
58	50	17	2.17	67	0.90	68	200	343	112
60	50	20	2.12	70	0.89	69	199	342	113
60	75	5	4.11	80	0.78	95	189	364	112

Figure 11 Thermal Condition at Emplacement for Maintaining Drift Wall Temperature Below 200°C

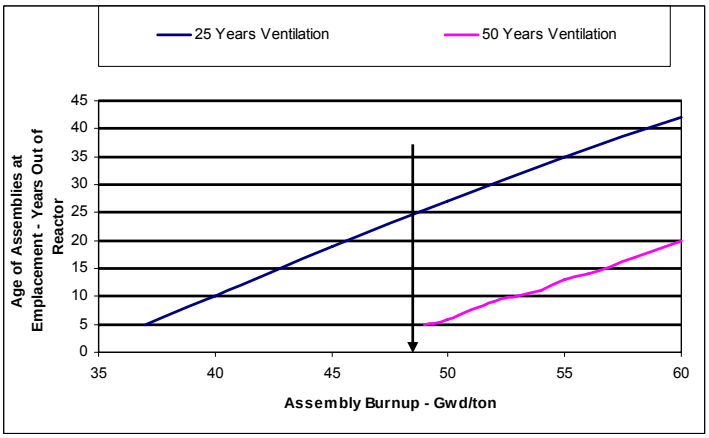

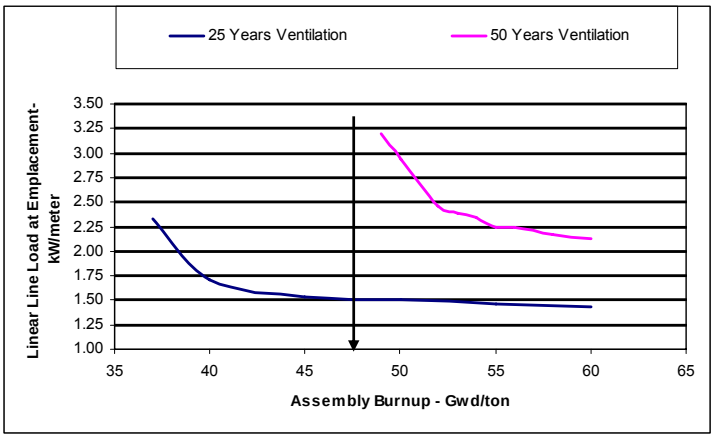

Figure 12 Thermal Condition at Closure for Maintaining Drift Wall Temperature Below 200°C

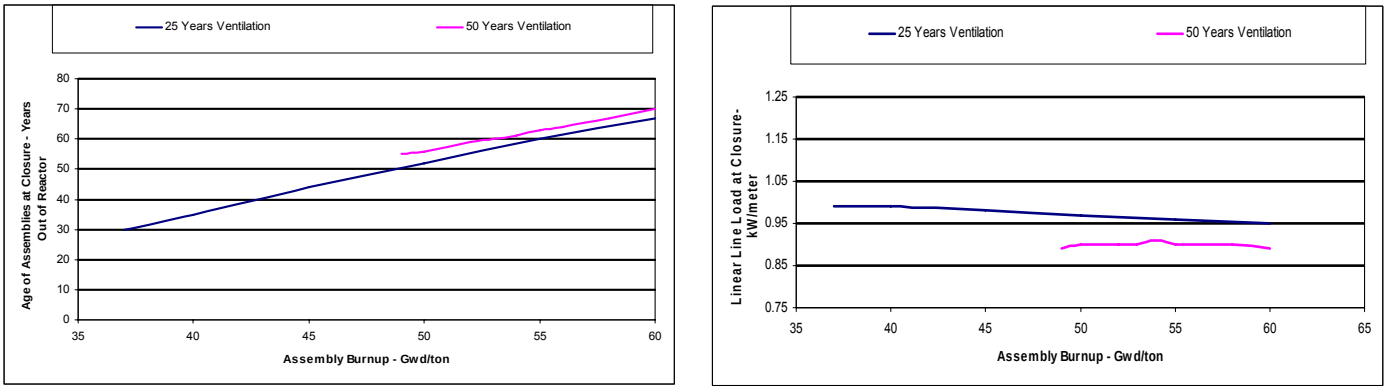

These results indicate that for CSNF with an average burnup of approximately 48 Gwd/ton, the ventilation duration could be reduced from 75 years to approximately 50 years and drift wall temperature would be maintained below 200°C.

4.2.5. Waste Package Surface Temperature

For calculating the waste package surface temperature, the drift wall surface temperatures were first calculated using the method described in Section 2.2. On the basis of the drift wall temperature, the drip shield and waste package surface temperatures were calculated according to the method described in Section 2.4. A plot of drift wall, drip shield, and waste package temperatures is shown in Figure 13 for the case of 50 Gwd/ton assemblies emplaced 27 years out of reactor and ventilated for 25 years.

Figure 13 Waste Package Temperature for 200°C Maximum Drift Wall Temperature

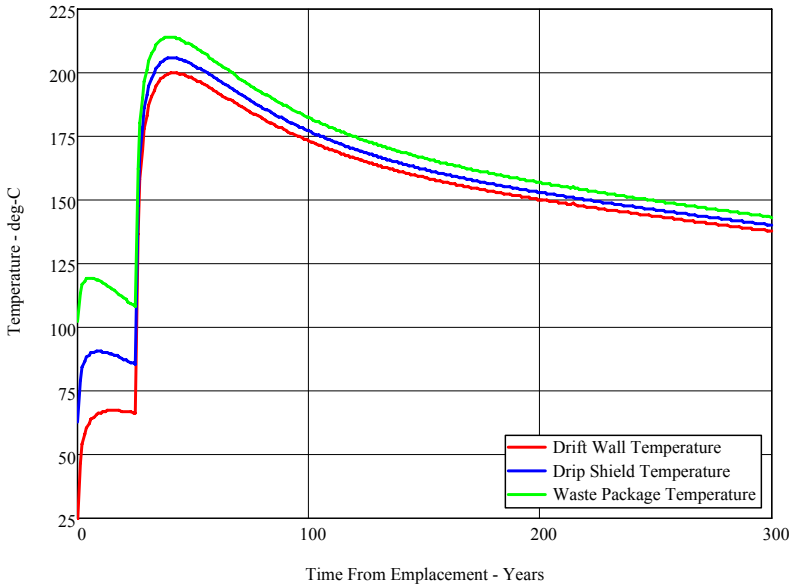

The waste package surface temperature was calculated for the same cases described in Sections 4.2.3 and 4.2.4. The results are presented in Table 14 and Table 15.

Table 14 Peak Temperatures for 96°C Mid-Pillar Temperatures

Assembly Burunup (Gwd/ton)	Ventilation Duration (Years)	Age at Emplacement (Years from reactor discharge)	Line Load at Emplacement (kW/meter)	Age at Closure (Years from reactor discharge)	Line Load at Closure (kW/meter)	Time of Peak Drift Wall Temperature (Years from Emplacement)	Peak Drift Wall Temperature (oC)	Peak Drip Shield Temperature (oC)	Peak Waste Package Temperature (oC)
35	25	5	2.2	30	0.93	39	190	196	204
38	25	5	2.4	30	1.02	39	205	211	219
40	25	12	1.58	37	0.96	40	195	201	209
45	25	31	1.25	56	0.82	43	173	179	187
50	25	52	1.01	77	0.7	48	155	161	168
55	25	69	0.89	94	0.64	56	147	153	160
60	25	84	0.81	109	0.6	74	145	149	156
40	50	5	2.53	55	0.71	66	162	168	175
43	50	5	2.75	55	0.77	66	174	179	187
45	50	12	1.82	62	0.74	68	167	173	180
50	50	31	1.4	81	0.65	73	153	159	166
55	50	47	1.2	97	0.6	81	147	152	159
60	50	61	1.07	111	0.58	96	145	149	156
45	75	5	2.9	80	0.58	96	146	151	158
48	75	5	3.13	80	0.62	96	155	160	167
49	75	8	2.42	83	0.61	97	154	159	166
50	75	12	2.05	87	0.6	99	151	156	163
51	75	16	1.89	91	0.58	101	149	154	160
52	75	19	1.82	94	0.58	102	148	152	159
53	75	22	1.76	97	0.57	104	147	151	158
54	75	26	1.67	101	0.56	107	145	150	156
55	75	29	1.62	104	0.55	110	144	149	155
60	75	43	1.41	118	0.53	128	143	147	153
50	100	5	3.28	105	0.49	135	138	143	149
53	100	5	3.53	105	0.52	132	145	150	156
54	100	8	2.74	108	0.52	135	144	149	155
55	100	12	2.32	112	0.52	140	142	147	153
56	100	15	2.18	115	0.51	144	142	146	152
57	100	18	2.08	118	0.5	148	142	146	152
60	100	27	1.86	127	0.49	161	141	145	150

Table 15 Peak Temperatures for 200°C Drift Wall Temperatures

Assembly Burunup (Gwd/ton)	Ventilation Duration (Years)	Age at Emplacement (Years from reactor discharge)	Line Load at Emplacement (kW/meter)	Age at Closure (Years from reactor discharge)	Line Load at Closure (kW/meter)	Time of Peak Drift Wall Temperature (Years from Emplacement)	Peak Drift Wall Temperature (oC)	Peak Drip Shield Temperature (oC)	Peak Waste Package Temperature (oC)
35	25	5	2.2	30	0.93	39	190	196	204
37	25	5	2.33	30	0.99	39	200	206	214
40	25	10	1.71	35	0.99	40	200	206	214
45	25	19	1.54	44	0.98	41	199	205	213
50	25	27	1.5	52	0.97	42	200	206	214
55	25	35	1.46	60	0.96	43	199	205	212
60	25	42	1.43	67	0.95	44	199	205	213
49	50	5	3.2	55	0.89	66	197	203	210
50	50	6	2.93	56	0.90	66	198	204	211
52	50	9	2.46	59	0.90	67	198	204	211
53	50	10	2.39	60	0.90	67	199	205	212
54	50	11	2.35	61	0.91	67	200	206	214
55	50	13	2.25	63	0.90	67	199	205	212
56	50	14	2.24	64	0.90	68	200	206	213
58	50	17	2.17	67	0.90	68	200	205	213
60	50	20	2.12	70	0.89	69	199	205	212
60	75	5	4.11	80	0.78	95	189	194	201

For all cases in Table 14 and Table 15, the peak waste package temperature is well below the maximum allowable limit of 300°C.

4.2.6. Discussion

The DOE postclosure thermal response to support the LA is based on an estimated limiting waste stream. However, performing more-general evaluations to determine the maximum thermal energy that can be absorbed by the mountain would provide increased flexibility to control when the repository may be closed by adjusting the ventilation duration and/or the linear line load, regardless of the waste emplaced.

This analysis shows that the postclosure thermal response is more a function of the initial conditions at the start of closure than it is of the conditions at waste emplacement. The amount of preheat of the mountain during the preclosure period has some influence on the postclosure thermal response, but the power of the waste at closure has a much greater influence. This is because the ventilation system removes between 80 and 90 percent of the heat during the ventilation phase. Therefore, the use of surface aging of the waste has limited benefit in reducing the postclosure mid-pillar peak temperature.

On the basis of the characteristics of the waste that is expected to be received, the mid-pillar temperature limit of 96°C can be maintained and the repository can be closed in approximately 75 years after completion of waste emplacement. If the mid-pillar temperature limit were eliminated, the drift wall temperature limit would be controlling and the preclosure ventilation duration could be reduced by approximately 25 years. This preclosure period could be decreased further if the linear line load at emplacement is reduced by either de-rating the waste packages or increasing the spacing between waste packages.

5. Conclusions

5.1. General

DOE has made significant advances in both their understanding of the repository thermal response and in the thermal methodology for repository operation. However, their thermal strategy is still based on an estimated limiting waste stream rather than on the amount of thermal energy that the mountain can absorb without exceeding any established thermal limit. Performing more-general evaluations, as presented in this document, to determine the maximum thermal energy that can be absorbed by the mountain would provide increased flexibility to control when the repository may be closed by changing the ventilation duration and/or the linear line load, regardless of the waste emplaced. This is especially true during the preclosure phase, where DOE has established rather arbitrary thermal limits for emplacement that are based on the predicted waste stream. The current 2.0 kW/meter thermal limit provides approximately 90°C margin to the 200°C drift wall temperature limit for the 30 day loss of forced ventilation event. Increasing the allowable thermal limits at emplacement would allow the majority of waste received at the repository to be emplaced immediately, thus reducing the amount of surface storage.

5.2. Comments and Suggestions

As a result of this evaluation and review of DOE calculations, the Board offers the following comments and suggestions.

1. The calculations performed by DOE and the NWTRB staff are in reasonable agreement and suggest that the DOE technical basis is valid.

2. Establishing the thermal limits for emplacement based on the estimated limiting waste stream appears to be overly conservative. DOE should reevaluate the thermal limits for emplacement

according to the capacity of the mountain to absorb the thermal energy rather than according to the predicted waste stream. This would result in higher thermal limits for emplacement and reduce the amount of surface storage required at the repository.

3. Initiating the loss of forced ventilation during the preclosure period at 30 days after emplacement may not be the most limiting case. DOE should reevaluate this event and determine when the loss of forced ventilation results in the shortest time to reach the 200°C drift wall thermal limit.

4. Surface aging of the hotter CSNF, as opposed to subsurface aging, has limited benefit on the postclosure thermal response. DOE should reevaluate the need to surface age the CSNF at the repository.

5. The DOE postclosure thermal response for supporting the license application (LA) is based on an estimated limiting waste stream. However, performing more-general evaluations, as presented in this document, to determine the maximum thermal energy that can be absorbed by the mountain would provide increased flexibility to control when the repository may be closed by adjusting the ventilation duration and/or the linear line load, regardless of the waste emplaced.

6. The Board agrees with DOE that if the 96°C mid-pillar temperature limit is required, this limit determines the maximum allowable thermal loading. However, if the 96°C limit were eliminated, the drift wall maximum temperature of 200°C would determine the maximum allowable thermal loading and the preclosure ventilation period could be decreased by approximately 25 years.

7. Thermal conductivity has a significant effect on the peak temperatures. Variations in the thermal conductivity used in the calculations to predict the repository thermal response should be taken into account on the basis of actual thermal conductivity measurements along with appropriate uncertainties and margins.

Appendix A
Development and Basis for Calculation Models

Analysis of Repository Temperatures Using Analytical Solutions

Introduction: Repository rock temperatures can be calculated using the analytical solution for a finite-length decaying line source. Constant-efficiency ventilation can also be simulated with this line-source solution. Repository rock temperatures include all temperatures from the drift wall out into the rock mass at any position in the repository. The drift wall temperature at the end of a drift where a package is at the end of the drift is an upper-bound approximation. In-drift temperatures are calculated after rock temperatures are determined by working back into the drift from the drift wall temperature. Waste package powers are approximated as a sum of three decaying exponentials for use in the analytical solution. Based on experience any waste package power, or combination of waste package powers, can be adequately approximated as a sum of three decaying exponentials.

The principle of superposition is used to calculate the temperature anywhere in the rock mass by repeated use of the analytical solution for a finite-length decaying line source. Thus for any location in the rock, the temperature is determined from the temperature contribution of all sources, or waste packages, in the same drift and in neighboring drifts. The analytical solution for a finite-length decaying line source is simply "placed" at all locations of interest by shifting the coordinate frame, a temperature calculated for the location of interest, and all the temperatures summed for the final temperature.

The validation, or verification, of the use of the analytical solution for a finite-length decaying line source for temperature predictions has been conducted by comparing predicted temperatures for special cases with those published in Analysis/Model Reports. The implementation of the prediction of repository temperatures using the line-source solution is accomplished with Mathcad. Details follow here for the line-source analytical solution and also discussions of why a single-medium solution can be used instead of taking into account stratigraphy, drift wall temperature variation as a function of waste-package power variation, ventilation, and neighboring drifts.

The Finite-Length Decaying Line Source: The derivation of the temperature due to a finite-length decaying line source proceeds from the solution for a constant point source as described by H.S. Carslaw and J.C. Jaeger, *Conduction of Heat in Solids*, 1959, Section 10.4, Equation (2). This solution for a constant point source is used to derive the solution for a decaying point source through the use of Laplace transforms. This decaying-point-source solution is then integrated over a finite length to obtain the solution for a finite-length decaying line source. The details of this derivation are presented in the Section A-1: *Temperatures Due to Decaying Point and Line Sources*. The temperature due to a finite-length decaying line source is:

$$v(x,y,z,t) = \frac{Qe^{-\lambda t}}{8\pi K}\int_0^t \left\{ erf\left(\frac{z}{2\sqrt{\kappa\theta}}\right) - erf\left(\frac{z-L}{2\sqrt{\kappa\theta}}\right)\right\}\frac{e^{\lambda\theta}}{\theta}e^{-\frac{(x^2+y^2)}{4\kappa\theta}}d\theta \qquad (1)$$

where z is the location on the axis and the source is centered at z = +L/2, Q is the lead coefficient in power/meter that describes the exponential decay of the source with a rate of decay of λ reciprocal time, K is the thermal conductivity, L is the source length, κ is the thermal diffusivity, and x and y are points in the medium. For a number of equal-length sources lined up on the z axis, the temperature is:

$$v(x,y,z,t) = \sum_{i=1}^{n} v_i(x,y,z-(i-1)L,t) \tag{2}$$

where the subscript i now is applied to the decaying power as Q_i and λ_i. When neighboring sources are to be taken into account and the temperature in the plane is of interest, set y = 0 and x equal to the drift spacing, or multiples of the drift spacing, and repeat the above equation.

Decaying Sources: The waste package powers, and for all intents and purposes, can be represented as decaying sources. More specifically, the meaning of the word "decaying" is that of a decaying exponential. The above equations require that the source be represented as:

$$Q = qe^{-\lambda t} \tag{3}$$

The actual use of this representation of a decaying source is implemented as a sum of three such terms as:

$$Q = \sum_{i=1}^{n} q_i e^{-\lambda_i t} \tag{4}$$

This summation for three terms is what works; all of the waste package powers, or assembly powers, can be represented with this three-term summation. This then requires that the equations for temperature above be solved three times and the results added to obtain the final temperature. This is an application of the superposition principle. An example of this three-term summation for a 1.42 kW/meter line load at emplacement is:

$$Q = 101 \cdot e^{-0.33t} + 1052 \cdot e^{-0.022t} + 266 \cdot e^{-0.0014t} \tag{5}$$

where the coefficients are watts/meter and the time is years. This particulate summation describes the line load for Enhanced Design Alternative II (EDA-II) from the *License Application Design Selection* report and is essentially the same power decay used in the Total System Performance Analysis to within a scale factor of 1.021 times the above, which yields 1.45 kW/meter at emplacement (Bechtel SAIC Company 2005a).

Drift Wall Temperature Predictions: Drift wall temperature predictions are obtained by setting x in Equation 1 to the drift radius. Since the line-source solution considers only a homogeneous medium, the drift region is filled with that medium, i.e., rock. In order to demonstrate that this line solution yields the correct temperatures for a drift wall, the solution for the region bounded internally by a cylinder from Carslaw and Jaeger, *Conduction of Heat in Solids*, Section 13.5, Equation 16, is used. This solution is for a constant heat flux applied to the wall and is the basis for deriving the solution for a decaying flux applied to the wall. This decaying flux is the same form as that given above in Equation 4. The solution for the region bounded internally by a cylinder, i.e., a tunnel, is derived in Section A-2: *Decaying Cylindrical Source Derivations*. The temperature for the region bounded internally by a cylinder, i.e., a tunnel in the rock, is:

$$v(r) = \frac{2Q}{\pi\rho C_p} \int_0^{\infty} \frac{e^{-\lambda t} - e^{-\kappa u^2 t}}{\lambda - \kappa u^2} \cdot \frac{J_0(ur)Y_1(ua) - Y_0(ur)J_1(ua)}{J_1^2(ua) + Y_1^2(ua)} du \tag{6}$$

where Q is the energy wall flux, "a" is the cylinder (tunnel) radius, ρ is the bulk density, C_p is the heat capacity, κ is the thermal diffusivity, $J_\nu(z)$ is the Bessel function of the first kind of order ν, and $Y_\nu(z)$ is the Bessel function of the second kind of order ν. This equation is two dimensional in r and θ (or x and y) and thus represents a drift of infinite length. The corresponding equation for a line source of infinite length is obtained by taking the limit in Equation 1 as the source length becomes infinite, and this limit yields:

$$v(r) = \frac{Qe^{-\lambda t}}{4\pi K}\int_0^t \frac{e^{\lambda\theta}}{\theta}\cdot e^{-\frac{r^2}{4\kappa\theta}}d\theta \tag{7}$$

Equation 6 is used to verify that the decaying line-source solution, Equation 7, approximates the drift wall temperature by setting r in both equations to the drift radius. The results of this verification show that the temperatures at the drift wall are essentially the same for times of interest, longer than 5 years, for physical properties pertinent to the medium of interest.

Ventilation Simulation: The removal of energy by ventilation from a power source in a drift is simulated by applying a constant efficiency over the ventilation duration. The ventilation efficiency is defined as the amount of energy removed by ventilation air divided by the source energy during the ventilation duration. The ventilation efficiency is typically around 86 to 88 percent for the parameters of interest (Bechtel SAIC Company 2004). Given that the solution for the temperature of the drift wall, or anywhere in the rock, is available as:

$$v = f(t) \tag{8}$$

where f(t) is given by equation (1) or (2), then the drift wall temperature due to a constant ventilation efficiency, ε, for duration t_v is:

$$v = (1-\varepsilon)f(t) \qquad for\ \ t \le t_v \tag{9}$$

At $t = t_v$, the ventilation ceases and all the source power is delivered to the rock. At this time, the fraction of the source power applied as an addition is ε, and the effect of this additional power is to be added to the (1-ε) solution. However, the contribution to the drift wall temperature from the application of the ε fraction begins at $t = t_v$, and thus the ε fraction solution must have its t = 0 begin at $t = t_v$. As a result, the drift wall temperature, or rock temperature, for $t > t_v$ is written as:

$$v = (1-\varepsilon)f(t) + \varepsilon f(t-t_v) \qquad for\ \ t \ge t_v \tag{10}$$

The solutions f(t) and $f(t-t_v)$ are additive because these heat-transfer solutions are linear.

It is important to recognize that the solution that "starts" at $t-t_v$ have its source power also begin with t = 0 at $t = t_v$. Each solution above must have its own time scale. To illustrate, suppose that the source power is written as equation (3). Equation (3) applies at the start of the problem, applies for all t, and the solution is multiplied by (1-ε) as indicated in equation (10). At the end of ventilation the additional power that applies is:

$$Q = qe^{-\lambda t_v}e^{-\lambda(t-t_v)} \quad for\ \ t > t_v \tag{11}$$

Thus the time argument of the exponential begins at zero when $t = t_v$. The temperature solution for this source is multiplied by ε and added to the (1-ε) solution. Note that the lead coefficient of this power is "decayed."

Stratigraphy, Hydrology and Dryout: Equations (1), (6) and (7) for temperature predictions as presented above are based on an infinite homogeneous medium that is described by one set of physical properties. These equations are generally referred to as "conduction only" equations. Therefore, there is no stratigraphy, no water flow or movement, no latent heat effects due to the vaporization of water, and only a single effective thermal conductivity. The purpose of this section is to show that these phenomena are not important for predicting temperatures for the situations of interest and that heat transfer by "conduction only" is sufficient.

The recognition that conduction-only predictions are adequate is documented in the *Ventilation Model and Analysis Report* (Bechtel SAIC Company 2004, Section 6.4.1.3). This document states that conduction heat transfer dominates other heat-transfer mechanisms (i.e., convection in fractures and lithophysae, and latent heat) in the host rock. This statement originates from Sass et al. 1988 (page 35). This statement is supported by conclusions of data and modeling of the Drift Scale Test (Birkholzer and Tsang, 2000, page 1439). The *Ventilation Model and Analysis Report* concludes that for the level of confidence required for the ventilation model, the assertion that conduction dominates the heat transfer in the host rock is consistent with the validity of the conceptual model (for the ventilation model).

The assertion that "conduction only" is consistent and sufficient for the objective of predicting temperatures in Yucca Mountain can be verified by comparing conduction-only temperature predictions with thermohyology-based predictions. This has been done for a drift of infinite length as described by equations (6) and (7) and results from the Multiscale Thermohydrologic Model (MSTHM) (Bechtel SAIC Company 2005b). The locations chosen from the MSTHM are in the middle of the repository so that there is little or no edge cooling effect. These MSTHM predictions are obtained from the two-dimension line-averaged-heat-source, drift-scale, thermohydrologic (2-D LDTH) model for the mean thermal conductivity and mean infiltration rate for a BWR package that is very close to the line average power of 1.45 kW/meter. The 2-D LDTH peak drift wall temperature prediction is 136.8°C. The analytical solution prediction using equation (7) for the peak drift wall temperature is 137.5°C. This temperature difference is considered acceptable. The 2-D LDTH peak mid-pillar temperatures at two locations in the middle of the repository are 87.3 and 89.6°C. The analytical solution prediction using equation (7) for the peak mid-pillar temperature is 87.8°C. Likewise, these temperatures are considered acceptable. These analytical results are based on the calculated thermal-physical properties of thermal conductivity at 1.83 W/(m K), heat capacity at 1119 Joules/(kg C) and bulk rock density at 2097 kg/m^3. The reason these are calculated properties is that they take into account 90 percent saturation of the rock.

The comparison of peak drift wall and peak mid-pillar temperatures from the two prediction techniques, analytical conduction only and thermohydrologic, shows that the temperatures agree to within a few degrees. Thus, stratigraphy, hydrology and rock dryout as described in the MSTHM do not have a significant effect on temperature predictions.

The effect of infiltration on temperature can be investigated by considering the following simplified problem. Consider a slab 600-meters thick with the temperature at each face fixed and a heated plane at the 300-meter location. This plane is heated so that the steady-state temperature is about 88°C, i.e., 88°C above ambient. Water flows from top to bottom through this slab at a specified rate. Solve for the temperature profile as a function of water-flow rate, and compare the temperature profile with the no-flow profile. This problem is described by J. Bear in *Dynamics of Fluids in Porous Media* (1988, page 653). This problem was solved with parameters pertinent to Yucca Mountain and water-flow rates of 0, 4 and 10-mm/year. The zero water-flow-

rate temperature of the heat source is 88°C, the 4-mm/year water-flow-rate temperature is 87.9°C, and the 10-mm/year water-flow-rate temperature is 87.6°C. Thus, for the anticipated percolation flux at, or through, Yucca Mountain, the effect on temperature at the heated plane, and elsewhere, is too small to consider.

Drift Wall Temperature Variation: The emplacement of waste packages of differing powers will result in varying drift wall temperatures opposite the packages. However, the effect of axial radiant-heat transfer in a drift loaded with varying-power packages is such that the axial drift wall temperature varies by about ±1.5°C at the time of occurrence of peak drift wall temperatures. At times greater than the occurrence of peak drift wall temperatures the variation is much less and scales approximately according the power relative to the peak power. This statement that the drift wall temperature variation is about ±1.5°C was determined by analyzing a simplified radiant-heat transfer problem. This simplified problem is based on a coaxial cylindrical heat source inside a cylinder (tunnel). The cylindrical heat source is represented as a string of adjacent one-meter-wide rings where the power of each ring can be specified. Five such one-meter-wide rings represent a waste package. The drift wall is likewise represented as a string of adjacent one-meter-wide rings but is not a power source. Because waste packages in a long drift will not "see" the ends of the drift, external heat loss from the outer rings is included. For all intents and purposes, all the source heat from the inner cylinder is transported through the outer rings to the adjacent rock medium. The details of the definition of this problem, the derivation, and the solution for parameters of interest are presented in Section A-3: *Radiant Heat Transfer in a Coaxial Cylindrical System.*

Because the maximum drift wall axial temperature variation is about 3°C, and much lower at longer time frames of a few hundred years, it is not necessary to simulate individual packages in a drift. An average line load can be used over the distance spanned by a segment of about seven waste packages, as illustrated in Section A-3. This allows the waste packages in an entire drift to be represented as a series of segments if desired, or the entire drift can be represented with a single line load. Given that the waste packages are about 5.8 meters in length, a seven-package segment is about 40 meters in length. Thus a 600-meter-long drift will contain about 15 segments, each of which can be represented with equation (1) above. A reason for not using one line load for the entire drift is that it may be worthwhile to load segments at the ends of the drift with more power to take advantage of the edge-cooling effect. An advantage of using 15 segments, rather than individual packages, is that there are only 15 segments to keep track of rather than 105 packages.

References:

Bear, J., 1988, *Dynamics of Fluids in Porous Media*, Dover Publications.

Bechtel SAIC Company, 2004, *Ventilation Model and Analysis Report*, ANL-EBS-MD-000030 REV04, Las Vegas, Nevada: Bechtel SAIC Company.

Bechtel SAIC Company, 2005a, *IED Waste Package Decay Heat Generation [Sheet 1 of 1]*, 800-IED-WIS0-00701-000-00A, Las Vegas, Nevada: Bechtel SAIC Company.

Bechtel SAIC Company, 2005b, *Multiscale Thermohydrologic Model*, ANL-EBS-MD-000049 REV03, Las Vegas, Nevada: Bechtel SAIC Company.

Birkholzer, J.T. and Y.W. Tsang, 2000, *Modeling the Thermal-Hydrologic Processes in a Large-Scale Underground Heater Test in Partially Saturated Fractured Tuff*. Water Resources Research, 36, (6), 1431-1447. Washington, D.C.: American Geophysical Union.

Carslaw, H.S., and J.C. Jaeger, 1959, *Conduction of Heat in Solids*, Oxford University Press.

Sass, J.H., A.H. Lachenbruch, W.W. Dudley, Jr., S.S. Priest, and R.J. Munroe, 1988, *Temperature, Thermal Conductivity, and Heat Flow Near Yucca Mountain, Nevada: Some Tectonic and Hydrologic Implications.* Open-File Report 87-649. Denver, Colorado: U.S. Geological Survey.

Section A-1: Temperature Due to Decaying Point and Line Sources

Introduction: The derivation for the temperature due to a decaying line source proceeds from the solution for the temperature due to a constant point or line source. For the case for a decaying infinite-length line source, the starting point is the constant infinite-length line source as given by H.S. Carslaw and J.C. Jaeger, *Conduction of Heat in Solids*, Section 10.4, page 261, equation (5). For the case for a decaying finite-length line source, the starting point is the constant point source as given by Carslaw and Jaeger, Section 10.4, page 261, equation (2). The solution for the constant point source is used as the starting point to derive the temperature for a decaying point source, and then this decaying point source is integrated over a finite length to yield the solution for a decaying finite-length line source. A decaying source is defined as an exponential decay, such as that which describes radioactive decay. The derivations presented here in order are the decaying infinite-length line source, the result of which is given in equation (A-1.15); the decaying point source, the result of which is given in equation (A-1.26); and the decaying finite-length line source, the result of which is given in equation (A-1.55). The Laplace transform is used in these derivations by recognizing that the transform solution due to a decaying source is obtained by replacing the transform parameter (denoted as p) with the transform parameter plus the rate of decay in the transform for a constant source, as explained below. The resulting Laplace transforms are then inverted as described in Carslaw and Jaeger, Chapter XII.

Decaying Infinite-Length Line Source: The derivation of the temperature due to a decaying line source proceeds from the solution for the temperature due to a constant line source. The energy per unit time per unit length is defined by a decaying exponential, thus the name "decaying," as:

$$Q = Q_o e^{-\lambda t} \tag{A-1.1}$$

The temperature due to constant infinite-length line source is give by Carslaw and Jaeger, Section 10.4, page 261, equation (5), as:

$$v = \frac{Q_\ell}{4\pi\kappa}\int_{r^2/4\kappa t}^{\infty}\frac{e^{-u}}{u}du = -\frac{Q_\ell}{4\pi\kappa}Ei\left(-\frac{r^2}{4\kappa t}\right) \tag{A-1.2}$$

where the usual notation applies. Heat is liberated at the rate of $\rho C Q_\ell$ per unit time per unit length so that given a linear power as Q watts/meter, $Q_\ell = Q/\rho C$, and Q_ℓ has units of (m^2 °C)/sec.

Now consider the Laplace transform of v in equation (A-1.2) by using transform pair (26) in Carslaw and Jaeger, Appendix V, page 495. This transform pair is:

$$p^{\frac{1}{2}\upsilon-1}K_\upsilon\left(x\sqrt{p}\right) \Leftrightarrow x^{-\upsilon}2^{\upsilon-1}\int_{x^2/4t}^{\infty}e^{-u}u^{\upsilon-1}du \tag{A-1.3}$$

Set $\upsilon = 0$ to obtain:

$$\frac{K_0\left(x\sqrt{p}\right)}{p} \Leftrightarrow \frac{1}{2}\int_{x^2/4t}^{\infty}\frac{e^{-u}}{u}du \tag{A-1.4}$$

The right side above is in the same form as equation (A-1.2). To continue, use the following change of variables:

$$x^2 \equiv \frac{r^2}{\kappa} \tag{A-1.5}$$

so that the transform pair in equation (A-1.4) becomes:

$$\frac{K_0(rq)}{p} \Leftrightarrow \frac{1}{2}\int_{r^2/4\kappa t}^{\infty} \frac{e^{-u}}{u}du \tag{A-1.6}$$

where $q^2 \equiv p/\kappa$ as defined in Carslaw and Jaeger, Section 12.4, page 304, equation (2). The Laplace transform for a decaying line source becomes:

$$\overline{v} = \frac{Q_\ell}{2\pi\kappa}\frac{K_0(rq)}{p+\lambda} \tag{A-1.7}$$

The reason $(p + \lambda)$ replaces p in equation (A-1.7) is because the Laplace transform of a constant (boundary condition) is $1/p$ while the Laplace transform of $e^{-\lambda t}$ is $1/(p + \lambda)$. Therefore, rearrange the above as:

$$\overline{v}(p+\lambda) = p\overline{v} + \lambda\overline{v} = \frac{Q_\ell}{2\pi\kappa}K_0(rq) \tag{A-1.8}$$

Term-by-term inversion of the above equation is accomplished using Carslaw and Jaeger, Section 12.2, equation (2), page 299, and transform pair (23), Appendix V, page 495. Transform pair (23) written exactly as it appears is:

$$K_0(qx) \Leftrightarrow \frac{1}{2t}e^{-x^2/4\kappa t} \tag{A-1.9}$$

Now let x = r and rewrite the above as:

$$K_0(qr) \Leftrightarrow \frac{1}{2t}e^{-r^2/4\kappa t} \tag{A-1.10}$$

and now invert equation (A-1.8) term by term to obtain:

$$\frac{dv}{dt} + \lambda v = \frac{Q_\ell}{4\pi\kappa t}e^{-r^2/4\kappa t} \tag{A-1.11}$$

The integrating factor for this differential equation is $e^{+\lambda t}$:

$$\frac{d\left(ve^{\lambda t}\right)}{dt} = \frac{Q_\ell e^{+\lambda t}}{4\pi\kappa t} e^{-r^2/4\kappa t} \tag{A-1.12}$$

Integrating between 0 and t yields:

$$ve^{\lambda t} = \frac{Q_\ell}{4\pi\kappa} \int_0^t \frac{e^{+\lambda\theta}}{\theta} e^{-r^2/4\kappa\theta} d\theta \tag{A-1.13}$$

Clearing the exponential on the left side yields:

$$v = \frac{Q_\ell e^{-\lambda t}}{4\pi\kappa} \int_0^t \frac{e^{+\lambda\theta}}{\theta} e^{-r^2/4\kappa\theta} d\theta \tag{A-1.14}$$

Now eliminate Q_ℓ and put in terms of Q_o from equation (A-1.1) to obtain the final form of the temperature due to a decaying infinite-length decaying line source:

$$v = \frac{Q_o e^{-\lambda t}}{4\pi K} \int_0^t \frac{e^{+\lambda\theta}}{\theta} e^{-r^2/4\kappa\theta} d\theta \tag{A-1.15}$$

Decaying Point Source: The derivation of the temperature due to a decaying point source proceeds from the solution for the temperature due to a constant point source. The Laplace transform is used again as described in the preceding section by replacing p with $(p + \lambda)$ for the case of a decaying source as defined in equation (A-1.1).

The temperature due to a constant point source is given by Carslaw and Jaeger, Section 10.4, page 261, equation (2) as:

$$v = \frac{Q_p}{4\pi\kappa r} erfc\left(\frac{r}{\sqrt{4\kappa t}}\right) \tag{A-1.16}$$

Heat is liberated at a rate $Q_p\rho C$. Now consider the Laplace transform of v above by using the transform pair (8) in Carslaw and Jaeger, Appendix V, page 494. This transform pair is:

$$\frac{e^{-qx}}{p} \Leftrightarrow erfc\left(\frac{x}{2\sqrt{\kappa t}}\right) \tag{A-1.17}$$

Using this transform pair yields the Laplace transform of v in equation (A-1.16) as:

$$\overline{v} = \frac{Q_p}{4\pi\kappa r}\frac{e^{-qr}}{p} \tag{A-1.18}$$

where $q^2 \equiv p/\kappa$ as defined in Carslaw and Jaeger, Section 12.4, page 304, equation (2). The Laplace transform for a decaying source is written by replacing p with $(p + \lambda)$ to obtain:

$$\overline{v} = \frac{Q_p}{4\pi\kappa r}\frac{e^{-qr}}{p+\lambda} \tag{A-1.19}$$

To invert this equation, rewrite as:

$$\overline{v}\left(p+\lambda\right) = p\overline{v} + \lambda\overline{v} = \frac{Q_p}{4\pi\kappa r}e^{-qr} \tag{A-1.20}$$

Term-by-term inversion of this equation is accomplished using Carslaw and Jaeger, Section 12.2, equation (2), page 299, and transform pair (6), Appendix V, page 494. Transform pair (6) is:

$$e^{-qx} \Leftrightarrow \frac{x}{2\sqrt{\pi\kappa t^3}}e^{-\frac{x^2}{4\kappa t}} \tag{A-1.21}$$

Using this information to invert equation (A-1.20) yields:

$$\frac{dv}{dt} + \lambda v = \frac{Q_p}{4\pi\kappa r}\frac{r}{2\sqrt{\pi\kappa t^3}}e^{-\frac{r^2}{4\kappa t}} = \frac{Q_p}{8\left(\pi\kappa t\right)^{3/2}}e^{-\frac{r^2}{4\kappa t}} \tag{A-1.22}$$

The integrating factor for this differential equation is $e^{+\lambda t}$, using this yields:

$$\frac{d\left(ve^{\lambda t}\right)}{dt} = \frac{Q_p e^{\lambda t}}{8\left(\pi\kappa t\right)^{3/2}}e^{-\frac{r^2}{4\kappa t}} \tag{A-1.23}$$

Now integrate between 0 and t to obtain:

$$ve^{\lambda t} = \frac{Q_p}{8\left(\pi\kappa\right)^{3/2}}\int_0^t \frac{e^{\lambda t}}{\theta^{3/2}}e^{-\frac{r^2}{4\kappa\theta}}d\theta \tag{A-1.24}$$

or:

$$v = \frac{Q_p e^{-\lambda t}}{8(\pi\kappa)^{3/2}} \int_0^t \frac{e^{\lambda\theta}}{\theta^{3/2}} e^{-\frac{r^2}{4\kappa\theta}} d\theta \tag{A-1.25}$$

Now eliminate Q_p and put in terms of Q_o using the information following equation (A-1.16) to obtain the temperature due to a decaying point source:

$$v = \frac{Q_o e^{-\lambda t}}{8\rho C(\pi\kappa)^{3/2}} \int_0^t \frac{e^{\lambda\theta}}{\theta^{3/2}} e^{-\frac{r^2}{4\kappa\theta}} d\theta \tag{A-1.26}$$

Decaying Finite-Length Line Source: The derivation of the temperature due to a decaying finite-length line source proceeds from the temperature due to a decaying point source. Equation (A-1.25) is chosen for the starting point, and the meaning of the "power" coefficient, Q_p, will be presented later. Rewrite the "r" term in equation (A-1.25) as:

$$r^2 = (x - x_o)^2 + (y - y_o)^2 + (z - z_o)^2 \tag{A-1.27}$$

and rewrite equation (A-1.25) with this expression for r as:

$$v = \frac{Q_p e^{-\lambda t}}{8(\pi\kappa)^{3/2}} \int_0^t \frac{e^{\lambda t}}{\theta^{3/2}} e^{\frac{-\left\{(x-x_o)^2+(y-y_o)^2+(z-z_o)^2\right\}}{4\kappa\theta}} d\theta \tag{A-1.28}$$

Now integrate with respect to dz_o from z_1 to z_2 parallel to the z axis:

$$v = \frac{Q_p e^{-\lambda t}}{8(\pi\kappa)^{3/2}} \int_{z_1}^{z_2} \int_0^t \frac{e^{-\lambda\theta}}{\theta^{3/2}} e^{\frac{-(z-z_o)^2}{4\kappa\theta}} e^{\frac{-\left\{(x-x_o)^2+(y-y_o)^2\right\}}{4\kappa\theta}} d\theta dz_o \tag{A-1.29}$$

and rearrange to:

$$v = \frac{Q_p e^{-\lambda t}}{8(\pi\kappa)^{3/2}} \int_0^t \left\{ \int_{z_1}^{z_2} e^{\frac{-(z-z_o)^2}{4\kappa\theta}} dz_o \right\} \frac{e^{\lambda\theta}}{\theta^{3/2}} e^{\frac{-\left\{(x-x_o)^2+(y-y_o)^2\right\}}{4\kappa\theta}} d\theta \tag{A-1.30}$$

Now change variables according to:

$$u = \frac{(z - z_o)}{2\sqrt{\kappa\theta}} \tag{A-1.31}$$

$$du = -\frac{dz_o}{2\sqrt{\kappa\theta}} \tag{A-1.32}$$

$$dz_o = -2\sqrt{\kappa\theta}\,du \tag{A-1.33}$$

and substitute accordingly so that equation (A-1.30) becomes:

$$v = \frac{Q_p e^{-\lambda t}}{8(\pi\kappa)^{3/2}} \int_0^t \left\{ \int_{z_o=z_1}^{z_o=z_2} e^{-u^2} \left(-2\sqrt{\kappa\theta}\right) du \right\} \frac{e^{\lambda\theta}}{\theta^{3/2}} e^{\frac{-\left\{(x-x_o)^2+(y-y_o)^2\right\}}{4\kappa\theta}} d\theta \tag{A-1.34}$$

Simplifying some algebra:

$$v = \frac{Q_p e^{-\lambda t}}{8\pi^{3/2}\kappa} \int_0^t \left\{ \int_{(z-z_1)/2\sqrt{\kappa\theta}}^{(z-z_2)/2\sqrt{\kappa\theta}} e^{-u^2} (-2)\, du \right\} \frac{e^{\lambda\theta}}{\theta} e^{\frac{-\left\{(x-x_o)^2+(y-y_o)^2\right\}}{4\kappa\theta}} d\theta \tag{A-1.35}$$

Convert the du integral in the above equation to an error function. Let $z_1 = -L/2$ and $z_2 = +L/2$ centered on the origin so that the du integral becomes:

$$\int_{(z+L/2)/2\sqrt{\kappa\theta}}^{(z-L/2)/2\sqrt{\kappa\theta}} e^{-u^2} du = \int_{(z+L/2)/2\sqrt{\kappa\theta}}^{0} e^{-u^2} du + \int_{0}^{(z-L/2)/2\sqrt{\kappa\theta}} e^{-u^2} du \tag{A-1.36}$$

or:

$$\int_{(z+L/2)/2\sqrt{\kappa\theta}}^{(z-L/2)/2\sqrt{\kappa\theta}} e^{-u^2} du = -\int_{0}^{(z+L/2)/2\sqrt{\kappa\theta}} e^{-u^2} du + \int_{0}^{(z-L/2)/2\sqrt{\kappa\theta}} e^{-u^2} du \tag{A-1.37}$$

Now use the definition of the error function from Carslaw and Jaeger, Appendix II, page 482, equation (1), which is:

$$erf(x) \equiv \frac{2}{\sqrt{\pi}} \int_0^x e^{-\xi^2} d\xi \tag{A-1.38}$$

or:

$$\frac{\sqrt{\pi}}{2} erf(x) = \int_0^x e^{-\xi^2} d\xi \tag{A-1.39}$$

and the du integrals in equation (A-1.37) become:

$$\int_{(z+L/2)/2\sqrt{\kappa\theta}}^{(z-L/2)/2\sqrt{\kappa\theta}} e^{-u^2}\,du = -\frac{\sqrt{\pi}}{2}\left\{erf\left[\frac{(z+L/2)}{2\sqrt{\kappa\theta}}\right] - erf\left[\frac{(z-L/2)}{2\sqrt{\kappa\theta}}\right]\right\} \tag{A-1.40}$$

Now substitute this result into equation (A-1.35), noting that the (-2) cancels and the square root of π from the erf yields π in the denominator leading the integral, and obtain the temperature due to a decaying finite-length line source:

$$v(x,y,z,t) = \frac{Q_p e^{-\lambda t}}{8\pi\kappa}\int_0^t \left\{erf\left[\frac{(z+L/2)}{2\sqrt{\kappa\theta}}\right] - erf\left[\frac{(z-L/2)}{2\sqrt{\kappa\theta}}\right]\right\}\frac{e^{\lambda\theta}}{\theta}e^{\frac{-\left(x^2+y^2\right)}{4\kappa\theta}}\,d\theta \tag{A-1.41}$$

where x_0 and y_o have been set to the origin. When the integration in equation (A-1.29) was set up, the heat release per unit length became $\rho C Q_p$. To verify that this is true, consider taking the limit of the above equation as $L \to \infty$ to obtain the temperature due to a decaying infinite-length line source, which is equation (A-1.15), and then deriving the energy in the rock per unit length at time t. The limits as $L \to \infty$ for the error functions are $erf(\infty) = 1$, and $erf(-\infty) = -1$, refer to Carslaw and Jaeger, Appendix II, page 482. Substituting these limits into the above yields:

$$v(x,y,t) = \frac{Q_p e^{-\lambda t}}{8\pi\kappa}\int_0^2 \{2\}\frac{e^{\lambda\theta}}{\theta}e^{\frac{-\left(x^2+y^2\right)}{4\kappa\theta}}\,d\theta \tag{A-1.42}$$

So, there is no z dependence, only x and y (and t), and this becomes:

$$v(x,y,t) = \frac{Q_p e^{-\lambda t}}{4\pi\kappa}\int_0^t \frac{e^{\lambda\theta}}{\theta}e^{\frac{-\left(x^2+y^2\right)}{4\kappa\theta}}\,d\theta \tag{A-1.43}$$

This is not quite the same form as equation (A-1.15), because of the way Q_p was defined for a point source. Proceed now to calculate the energy in the medium (rock) per unit length at time t by integrating over all space $\rho Cv(x,y,t)$:

$$E = \int_V \rho Cv(x,y,t)\,dV = \frac{\rho C Q_p e^{-\lambda t}}{4\pi\kappa}\int_V\int_0^t \frac{e^{\lambda\theta}}{\theta}e^{\frac{-r^2}{4\kappa\theta}}\,d\theta\,dV \tag{A-1.44}$$

Use $dV = r\,dr\,d\xi$ for integrating over all space where $d\xi$ is the angle that ranges from 0 to 2π. Integrating $d\xi$ yields 2π so that the above integral becomes:

$$E = \frac{\rho C Q_p e^{-\lambda t}}{4\pi\kappa}(2\pi)\int_0^t \frac{e^{\lambda\theta}}{\theta} d\theta \int_0^\infty e^{\frac{-r^2}{4\kappa\theta}} r dr \tag{A-1.45}$$

Consider now the dr integral, change variables as:

$$u^2 = r^2 / 4\kappa\theta \qquad 2\text{udu} = 2\text{rdr}/4\kappa\theta \tag{A-1.46}$$

which yields:

$$\int_0^\infty e^{\frac{-r^2}{4\kappa\theta}} r dr = \int_0^\infty e^{-u^2} (4\kappa\theta) u du = 4\kappa\theta \int_0^\infty e^{-u^2} u du \tag{A-1.47}$$

Now let:

$$z = u^2 \qquad dz = 2udu \tag{A-1.48}$$

and the left integral in equation (A-1.47) becomes:

$$4\kappa\theta \int_0^\infty e^{-u^2} u du = 2\kappa\theta \int_0^\infty e^{-z} dz = 2\kappa\theta \left[-e^{-z} \right]_0^\infty = 2\kappa\theta \tag{A-1.49}$$

Therefore, equation (A-1.45) becomes:

$$E = \frac{\rho C Q_p e^{-\lambda t}}{2\kappa} \int_0^t \frac{e^{\lambda\theta}}{\theta} (2\kappa\theta) d\theta = \rho C Q_p e^{-\lambda t} \int_0^t e^{\lambda\theta} d\theta \tag{A-1.50}$$

Continuing:

$$E = \rho C Q_p e^{-\lambda t} \frac{1}{\lambda} \left[e^{\lambda\theta} \right]_0^t = \frac{\rho C Q_p e^{-\lambda t}}{\lambda} \left(e^{\lambda t} - 1 \right) \tag{A-1.51}$$

or multiplying through the first exponential yields:

$$E = \frac{\rho C Q_p}{\lambda} \left(1 - e^{-\lambda t} \right) \tag{A-1.52}$$

which is the desired result, i.e., heat is liberated at ρCQ_p per unit time per unit length. When $\lambda = 0$ the result is:

$$E = \rho C Q_p t \tag{A-1.53}$$

Now suppose that equation (A-1.1) describes the heat release per unit time per unit length, which yields $Q_o = \rho C Q_p$, so eliminate Q_p in equation (A-1.41) to obtain the final result for the temperature due to a decaying finite-length line source of length L centered at the origin:

$$v(x,y,z,t) = \frac{Q_o e^{-\lambda t}}{8\pi K}\int_0^t \left\{ erf\left[\frac{(z+L/2)}{2\sqrt{\kappa\theta}}\right] - erf\left[\frac{(z-L/2)}{2\sqrt{\kappa\theta}}\right]\right\}\frac{e^{\lambda\theta}}{\theta} e^{\frac{-(x^2+y^2)}{4\kappa\theta}}\, d\theta \qquad \text{(A-1.54)}$$

This is the solution for the temperature due to a decaying finite-length line source of length L centered at z = 0. This location with the center at the origin is sometimes not convenient, and it is more convenient to have the left edge of the source at the origin. Therefore, consider shifting this solution by +L/2 to the right. To do this, subtract L/2 from the independent variable z. This subtraction shifts the center to z = +L/2. To see this, suppose that it is necessary to calculate the temperature due to this decaying finite-length line source at the left end of the source at some distance away, and the left end is to be at z = 0. This temperature is the same as that calculated from equation (A-1.54) with z = –L/2. Thus subtract L/2 from the independent variable to accomplish this shift. In general, to shift by a distant of +L, subtract L from the independent variable. The temperature due to a decaying finite-length line source of length L centered at z = +L/2 is:

$$v(x,y,z,t) = \frac{Q_o e^{-\lambda t}}{8\pi K}\int_0^t \left\{ erf\left[\frac{z}{2\sqrt{\kappa\theta}}\right] - erf\left[\frac{(z-L)}{2\sqrt{\kappa\theta}}\right]\right\}\frac{e^{\lambda\theta}}{\theta} e^{\frac{-(x^2+y^2)}{4\kappa\theta}}\, d\theta \qquad \text{(A-1.55)}$$

Now consider how to calculate the temperature due to series of end-to-end decaying finite-length line sources. Do not shift the first source, shift the second source by L, the third source by 2L, and so on. Furthermore, suppose that each source has a different decay representation. Then the temperature due to a series of these decaying finite-length sources is written as:

$$v(x,y,z,t,n) = v_1(x,y,z,t) + v_2(x,y,z-L,t) + v_3(x,y,z-2L,t) + \qquad \text{(A-1.56)}$$

or in general:

$$v(x,y,z,t,n) = \sum_{i=1}^{n} v_i(x,y,z-(i-1)L,t) \qquad \text{(A-1.57)}$$

References:

Carslaw, H.S., and J. C. Jaeger, 1959, *Conduction of Heat in Solids*, Oxford University Press.

Section A-2: Decaying Cylindrical Source Derivations

Introduction: The temperature due to a decaying flux applied to the inside wall of a cylinder in an infinite medium describes the physical situation of a tunnel in a mountain heated by nuclear-decay heat. The solution to this problem is given in this section as equation (A-2.20). The derivation for a decaying cylindrical source in an infinite medium proceeds from the solution for a constant-flux cylindrical source. The solution for a constant flux applied to the inside wall of a cylinder in an infinite medium is given by H.S. Carslaw and J.C. Jaeger, *Conduction of Heat in Solids*, Second Edition, 1959, Section 13.5, equation (16). In order to fix notation and use results from Carslaw and Jaeger, the problem is defined here beginning with the energy balance partial differential equation and an exponentially decaying boundary condition.

Consider a region bounded internally by a cylinder heat with an exponentially decaying heat source. The partial differential equation that describes the temperature, v, in the region is:

$$\frac{\partial^2 v}{\partial r^2}+\frac{1}{r}\frac{\partial v}{\partial r}-\frac{1}{\kappa}\frac{\partial v}{\partial t}=0 \qquad \text{(A-2.1)}$$

where the thermal diffusivity, κ, is defined as:

$$\kappa \equiv \frac{K}{\rho C} \qquad \text{(A-2.2)}$$

and the usual notation applies. The boundary condition at the inside surface of the cylinder is:

$$-K\frac{dv}{dr}=Q_o e^{-\xi t} \qquad at\ \ r=a \qquad \text{(A-2.3)}$$

The temperature, v, is to remain finite as $r \to \infty$. The initial condition is taken to be 0, i.e., v(r,0) = 0.

The Laplace transform of the above is:

$$\frac{d^2\overline{v}}{dr^2}+\frac{1}{r}\frac{d\overline{v}}{dr}-q^2\overline{v}=0 \qquad \text{(A-2.4)}$$

where the bar above v is the Laplace transform of v, and:

$$-K\frac{d\overline{v}}{dr}=\frac{Q_o}{p+\xi} \qquad at\ \ r=a \qquad \text{(A-2.5)}$$

where the transform variable is p, and q is defined as:

$$q \equiv \sqrt{\frac{p}{\kappa}} \tag{A-2.6}$$

The solution in transform space is:

$$\overline{v}(p) = \frac{Q_o K_o(qr)}{Kq(p+\xi)K_1(qa)} \tag{A-2.7}$$

where $K_\nu(z)$ is the modified Bessel function of the second kind of order ν.

The above can be inverted using the same technique used to invert the transform solution for the constant-flux boundary condition problem described by equation (16), Section 13.5, in Carslaw and Jaeger. To illustrate this technique, proceed with equation (16) as noted:

$$\overline{v} = \frac{QK_o(qr)}{KpqK_1(qa)} \tag{A-2.8}$$

This equation is inverted by using the fundamental property:

$$L\left\{\frac{\partial v}{\partial t}\right\} = p\overline{v} - v_o \tag{A-2.9}$$

where L denotes the Laplace transform operator, and $v_0 = 0$ (the initial condition).

Therefore, the inversion of equation (A-2.8) is conducted by inverting for the derivative of v with respect to time and then the result integrated with respect to time between 0 and some arbitrary time, t. Since the Laplace transform of v(r,t) for the problem with an exponentially decaying power source results in replacing p with p + ξ, compare equation (A-2.7) and (A-2.8), consider the following:

$$(p+\xi)\overline{v} = p\overline{v} + \xi\overline{v} = L\left\{\frac{\partial v}{\partial t}\right\} + \xi L\{v\} \tag{A-2.10}$$

Use Theorem I, Section 12.2, from Carslaw and Jaeger to write:

$$L\left\{\frac{\partial v}{\partial t}\right\} + \xi L\{v\} = L\left\{\frac{\partial v}{\partial t} + \xi v\right\} \tag{A-2.11}$$

Thus, obtain the inverse of equation (A-2.7) by using the inverse of equation (A-2.8), which is equation (17), Section 13.5, Carslaw and Jaeger. This is done as follows, start with equation (17) as noted, which is:

$$v_c = -\frac{2Q}{\pi\kappa}\int_0^\infty (1-e^{-\kappa u^2 t}) f(r)\frac{du}{u^2} \tag{A-2.12}$$

where the subscript c on v denotes the constant flux boundary condition. The function f(r) is defined as:

$$f(r) \equiv \frac{J_0(ur)Y_1(ua) - Y_0(ur)J_1(ua)}{J_1^2(ua) + Y_1^2(ua)} \tag{A-2.13}$$

where $J_\nu(z)$ is the Bessel function of the first kind of order ν, and $Y_\nu(z)$ is the Bessel function of the second kind of order ν. Take the partial derivative of equation (A-2.12) to obtain:

$$\frac{\partial v_c}{\partial t} = -\frac{2Q}{\pi K}\int_0^\infty \kappa u^2 e^{-\kappa u^2} f(r)\frac{du}{u^2} \tag{A-2.14}$$

Simplifying yields:

$$\frac{\partial v_c}{\partial t} = -\frac{2Q}{\pi\rho C}\int_0^\infty e^{-\kappa u^2 t} f(r)du \tag{A-2.15}$$

Now use Theorem I as noted above to write the inverse solution for equation (A-2.8) above as:

$$L^{-1}\left[L\left\{\frac{\partial v}{\partial t}\right\} + \xi\overline{v}\right] = -\frac{2Q_0}{\pi\rho C}\int_0^\infty e^{-\kappa u^2 t} f(r)du \tag{A-2.16}$$

Conducting the operations indicated on the left side yields:

$$\frac{\partial v}{\partial t} + \xi v = -\frac{2Q_0}{\pi\rho C}\int_0^\infty e^{-\kappa u^2 t} f(r)du \tag{A-2.17}$$

The integrating factor is $e^{\xi t}$ so that:

$$\frac{\partial}{\partial t}\left[e^{\xi t} v\right] = -\frac{2Q_0}{\pi\rho C}\int_0^\infty e^{\left(\xi-\kappa u^2\right)t} f(r)du \tag{A-2.18}$$

Integrate by changing t to θ as the integration variable on the right side and integrate between the limits of θ = 0 and θ = t to obtain:

$$e^{\xi t}v = -\frac{2Q_0}{\pi\rho C}\left[\int_0^{\infty}\frac{1}{\left(\xi-\kappa u^2\right)}e^{\left(\xi-\kappa u^2\right)\theta}f(r)du\right]_0^t \tag{A-2.19}$$

Evaluating the limits and clearing $e^{\xi t}$ yields (with f(r) from the definition used) the temperature in the region bounded internally by a cylinder with a decaying flux applied at the cylinder wall as:

$$v = \frac{2Q_0}{\pi\rho C}\int_0^{\infty}\frac{e^{-\xi t}-e^{-\kappa u^2 t}}{\left(\xi-\kappa u^2\right)}\frac{J_0(ur)Y_1(ua)-Y_0(ur)J_1(ua)}{J_1^2(ua)+Y_1^2(ua)}du \tag{A-2.20}$$

Note that the integration variable u ranges from zero to infinity and thus the quantity $(\xi - \kappa u^2)$ in the denominator can be zero, which implies that there is a singularity. However, this is not the case and can be shown by the use of ℓ'Hospital's rule or a series expansion of the fraction containing the exponentials and this quantity. Proceeding to demonstrate that there is no singularity using a series expansion, examine:

$$f(\xi,\kappa,u) = \lim_{\xi\to\kappa u^2}\left[\frac{e^{-\xi t}-e^{-\kappa u^2 t}}{\xi-\kappa u^2}\right] \tag{A-2.21}$$

Expand the exponentials as follows:

$$e^{-\xi t} = 1-\xi t+\frac{\left(-\xi t\right)^2}{2!}+\frac{\left(-\xi t\right)^3}{3!}\ldots \tag{A-2.22}$$

Bring the negative signs out of the ( ) to obtain:

$$e^{-\xi t} = 1-\xi t+\frac{\left(\xi t\right)^2}{2!}-\frac{\left(\xi t\right)^3}{3!}\ldots \tag{A-2.23}$$

Do likewise for the second exponential above to obtain:

$$e^{-\kappa u^2 t} = 1-\kappa u^2 t+\frac{\left(\kappa u^2 t\right)^2}{2!}-\frac{\left(\kappa u^2 t\right)^3}{3!}\ldots \tag{A-2.24}$$

Now form the difference of these exponentials and group like powers of t to obtain:

$$e^{-\xi t}-e^{-\kappa u^2 t} = -\left(\xi-\kappa u^2\right)t+\left(\xi^2-\left(\kappa u^2\right)^2\right)\frac{t^2}{2!}\ldots+(-1)^n\left(\xi^n-\left(\kappa u^2\right)^n\right)\frac{t^n}{n!}\ldots \tag{A-2.25}$$

Clearly, dividing each right-hand term by (ξ - κu^2) yields the lead term as t, but what about the other terms? To proceed, note that the difference of two like powers can be factored as:

$$a^n - b^n = \left(a-b\right)\left(a^{n-1} + a^{n-2}b\,.\,.\, + ab^{n-2} + b^{n-1}\right) \tag{A-2.26}$$

from S.M. Selby, *Standard Mathematical Tables*, 23-th edition, 1975, page 101. Therefore, each term above factors and yields a coefficient of t^n. The n-th coefficient of t^n is of the form:

$$\frac{\left(-1\right)^n}{n!}\left(a^{n-1} + a^{n-2}b\,.\,.\,. + \mathrm{b}^{\mathrm{n\text{-}1}}\right) \tag{A-2.27}$$

where there are n terms in the ( ). Now examine $\xi \rightarrow \kappa u^2$ (or $\kappa u^2 \rightarrow \xi$), or a $\rightarrow$ b, which yields:

$$\frac{\left(-1\right)^n}{n!}\lim_{a\rightarrow b}\left(a^{n-1} + a^{n-2}b + .\,.\, + b^{n-1}\right) = \frac{\left(-1\right)^n}{n!}na^{n-1} = \frac{\left(-1\right)^n}{\left(n-1\right)!}a^{n-1} \tag{A-2.28}$$

Factoring each term in equation (A-2.25), canceling the denominator, and using the results of equation (A-2.28) yields:

$$\lim_{\xi\rightarrow\kappa u^2}\left[\frac{e^{-\xi t} - e^{\kappa u^2 t}}{\xi - \kappa u^2}\right] = \sum_{n=1}\left(-1\right)^n t^n \frac{\xi^{n-1}}{\left(n-1\right)!} \tag{A-2.29}$$

Continuing with some algebra on the right side:

$$= t\sum_{n=1}\left(-1\right)^n \frac{\left(\xi t\right)^{n-1}}{\left(n-1\right)!} \tag{A-2.30}$$

$$= -t\sum_{n=1}\left(-1\right)^{n-1} \frac{\left(\xi t\right)^{n-1}}{\left(n-1\right)!} \tag{A-2.31}$$

$$= -t\sum_{n=1}\frac{\left(-\xi t\right)^{n-1}}{\left(n-1\right)!} \tag{A-2.32}$$

But note that:

$$e^{-x} = 1 - x + \frac{x^2}{2!} - \frac{x^3}{3!} + . . = \sum_{n=0}\left(-1\right)^n \frac{x^n}{n!} = \sum_{n=1}\frac{\left(-x\right)^{n-1}}{\left(n-1\right)!} \tag{A-2.33}$$

so that using equation (A-2.33), equation (A-2.29) becomes:

$$\lim_{\xi \to \kappa u^2} \left[\frac{e^{-\xi t} - e^{-\kappa u^2 t}}{\xi - \kappa u^2} \right] = -t \sum_{n=1} \frac{(-\xi t)^{n-1}}{(n-1)!} = -te^{-\xi t} \qquad \text{(A-2.34)}$$

and this limit proves that the above fraction does not yield a singularity in equation (A-2.20).

References:

Carslaw, H.S., and J.C. Jaeger, 1959, *Conduction of Heat in Solids*, Oxford University Press.

Selby, S.M., 1975, *Standard Mathematical Tables*, 23rd edition, CRC Press, Inc.

Section A-3: Radiant Heat Transfer in a Coaxial Cylindrical System

Introduction: The purpose of this appendix is to demonstrate that it is reasonable to calculate drift wall temperatures using a single linear power in an entire drift rather than using individual package powers. This demonstration is conducted by analyzing the drift wall temperature due to individual packages within a drift where only axial radiant heat transfer occurs. The conclusion derived in this appendix is that the drift wall temperature variation due to varying powers is small for the parameters of interest, on the order of 3°C, and a variation such as this is not consider large enough to justify the computation of temperatures to an accuracy better than this.

Radiant-heat transfer is known to spread, or smear, energy transport. Consequently, maintaining large temperature variations over short distances without power sources is difficult, if not impossible. In the Yucca Mountain Project's analysis for predicting in-drift natural convection and condensation, package-to-package power variation was not used to calculate drift wall temperatures; instead, a single linear power for the entire drift was used (Bechtel SAIC Company 2004, Section 6.3.5.1.1). By virtue of using a single linear power and not the actual package-to-package power variation, the resulting drift wall temperature is smooth with respect to variation over the distance scale of a package length. Thus, the implicit assumption was that the package-to-package power variation would not have a significant effect on the drift wall temperature opposite these packages. This implicit assumption can be tested by analyzing a simplified problem as described here that considers only axial radiant heat transfer in the drift between packages of varying power and the drift wall. The simplified radiant-heat-transfer-only problem analyzed here calculates the drift wall temperature variation opposite a seven-package segment with appropriate individual package powers that approximates that used by the Project (Bechtel SAIC Company 2005a, Figure 6.2-2). This particular package segment embeds low-power packages between high-power packages. The package powers use for the source powers for the problem analyzed here are the powers at approximately the time of peak postclosure temperature, about 75 years after emplacement, and are derived from Bechtel SAIC Company 2005b.

Consider several heat-generating cylinders, axially positioned end to end, with the entire group emplaced coaxially within a single, larger, outer cylinder, with ends open to the environment. Radiant-heat transfer is the only mode of heat transfer within the system. If the thermal power of each heat-generating cylinder varies from one to the next, an axial temperature variation will be imparted on the outer cylinder. In some applications, such as an underground nuclear waste repository, this axial temperature variation on the outer cylinder can be important. This appendix analyzes the axial temperature variation on the outer cylinder.

The problem can be simplified by replacing the smaller heat-generating cylinders with a single heat-generating cylinder, equal in length to the outer cylinder. The reason the heat-generating center cylinder runs the entire length of the outer cylinder is because of the tedium involved in calculating the outer cylinder view factors with a finite-length center cylinder present. Typical dimensions to be considered are 5.5 meters for the outer-cylinder diameter and 2.5 meters for the inner-cylinder diameter. The cylinder length of interest is 100 meters.

The effects of individual heat-generating cylinders are accounted for by subdividing the inner cylinder into 100 equal sections along its length (one meter wide each), with each section capable of having a different thermal power. The power emitted by the inner cylinder is specified for a unit length; for example, 100 watts/meter. Every unit length shall have a specified power, and the entire length of the inner cylinder emits power.

In order to solve a realistic problem, a convective boundary condition is used to transfer energy from the outer cylinder to the outside medium (rock). The reason for doing this is because it is not possible to transport all the

source power out the ends of the cylinder, the cylinder of interest is too long, and the view factors from virtually any position to the ends are very small. The temperature of the outside medium is specified along with the temperature of the environment at each end of this cylindrical system. Because the outside medium (rock) temperature in the situation of interest changes very slowly, energy transfer within the system is quasi-steady-state. The derivation of the heat-transfer equations and solution technique follow.

Derivation: A cylindrical source is placed coaxially in a larger, open-ended cylinder. The outer cylinder wall is divided into a number of equal-width constant-temperature rings, as is the cylindrical source. The inner and outer rings are the same width and are aligned (i.e., an outer ring above an inner ring).

For each outer ring, j, the energy balance for this system is written as:

$$\sum_{\substack{i=1 \\ i \neq j}}^{n} Q_{ij} - \left(E_{j,left} + E_{j,right}\right)\left(T_j - T_e\right) + \sum_{k=1}^{n} P_{kj} - hA_j\left(T_j - T_r\right) = 0 \qquad \text{(A-3.1)}$$

In equation (A-3.1), the first term is the energy transported between outer rings. The second term is the energy transported from the outer rings to the ends, where, the E_j terms are the end loss terms from outer ring, j, T_j is the temperature of outer ring, j, and T_e is the temperature at the ends. The third term is the energy transported from the inner rings to the outer rings. The fourth term is the energy transported out to the rock, where A_j is the area of outer ring, j, h is a heat transfer coefficient, and T_r is the temperature of the rock.

In the first term in equation (A-3.1), Q_{ij} is expressed as the radiant-heat transfer from the outer ring, i, to outer ring, j, with an emissivity of unity for all rings (R.B. Bird, W.E. Stewart, and E.N. Lightfoot, equation 14.4-9, page 440):

$$Q_{ij} = \sigma A_i F_{ij}(T_i^4 - T_j^4) \qquad \text{(A-3.2)}$$

Equation (A-3.2) can be written in linearized form as:

$$Q_{ij} = B_{ij}(T_i - T_j) \qquad \text{(A-3.3)}$$

where:

$$B_{ij} \equiv \sigma A_i F_{ij}(T_i^3 + T_i^2 T_j + T_i T_j^2 + T_j^3) \qquad \text{(A-3.4)}$$

and F_{ij} is the view factor from outer ring, i to outer ring, j.

In the second term in equation (A-3.1), each end-loss term (E_j) for outer ring, j, is linearized, typically, as:

$$E_j \equiv \sigma A_j F_{je}(T_j^3 + T_j^2 T_e + T_j T_e^2 + T_e^3) \qquad \text{(A-3.5)}$$

where F_{je} is the view factor from outer ring, j, to the end.

In the third term in equation (A-3.1), P_{kj} is expressed as the radiant-heat transfer from inner ring, k, to outer ring, j, with an emissivity of unity for all rings:

$$P_{kj} = \sigma A_k F_{kj} (V_k^4 - T_j^4) \tag{A-3.6}$$

where V_k is the temperature of the inner ring, k. Equation (A-3.6) can be written in linearized form as:

$$P_{kj} = C_{kj} (V_k - T_j) \tag{A-3.7}$$

where:

$$C_{kj} \equiv \sigma A_k F_{kj} (V_k^3 + V_k^2 T_j + V_k T_j^2 + T_j^3) \tag{A-3.8}$$

F_{kj} is the view factor from inner ring, k, to outer ring, j.

The temperature of inner ring, k, is not specified. However, the source energy (power) for each inner ring, k, is. An energy balance for each inner ring, k, relates the source energy and the end losses for inner ring, k, and the temperature of inner ring, k, to each outer ring, i:

$$\sum_{i=1}^{n} C_{ki} (V_k - T_i) = Q_k - (E_{k,left} + E_{k,right})(V_k - T_e) \tag{A-3.9}$$

where Q_k is the specified source energy for inner ring, k, and the E_k terms are the end losses from inner ring, k, which also are linearized, typically, as:

$$E_k \equiv \sigma A_k F_{ke} (V_k^3 + V_k^2 T_e + V_k T_e^2 + T_e^3) \tag{A-3.10}$$

where F_{ke} is the view factor from inner ring, k, to the end.

Solving equation (A-3.9) for V_k yields:

$$V_k = \frac{Q_k + (E_{k,left} + E_{k,right}) T_e + \sum_{i=1}^{n} C_{ki} T_i}{(E_{k,left} + E_{k,right}) + \sum_{i=1}^{n} C_{ki}} \tag{A-3.11}$$

Thus, the temperature of inner-ring, k, depends on the temperatures of all the outer rings, i, and the open-end temperature. For convenience, the sum in the denominator is rewritten as:

$$\sum_{i=1}^{n} C_{ki} = \sum_{m=1}^{n} C_{km} \tag{A-3.12}$$

With this notational change, equation (A-3.11) can be condensed to:

$$V_k = \alpha_k + \sum_{i=1}^{n} \beta_{ki} T_i \tag{A-3.13}$$

so that α_k and β_{ki} are defined as:

$$\alpha_k \equiv \frac{Q_k + (E_{k,left} + E_{k,right}) T_e}{(E_{k,left} + E_{k,right}) + \sum_{m=1}^{n} C_{km}} \tag{A-3.14}$$

and:

$$\beta_{ki} \equiv \frac{C_{ki}}{(E_{k,left} + E_{k,right}) + \sum_{m=1}^{n} C_{km}} \tag{A-3.15}$$

Substitution of equation (A-3.13) into equation (A-3.7), followed by substitution of equation (A-3.7) into equation (A-3.1), as well as substitution of equation (A-3.3) into equation (A-3.1), and collecting the coefficients of T_i yields:

$$\sum_{\substack{i=1 \\ i \neq j}}^{n} B_{ij}(T_i - T_j) + \sum_{k=1}^{n} C_{kj} \left\{ \alpha_k + \sum_{i=1}^{n} \beta_{ki} T_i - T_j \right\} - (E_{j,left} + E_{j,right})(T_j - T_e) - hA_j(T_j - T_r) = 0 \tag{A-3.16}$$

Note that:

$$\sum_{k=1}^{n} C_{kj} \sum_{i=1}^{n} \beta_{ki} T_i = \sum_{i=1}^{n} T_i \sum_{k=1}^{n} C_{kj} \beta_{ki} \tag{A-3.17}$$

Rearranging equation (A-3.16), collecting the T_j, yields:

$$\begin{aligned} \sum_{\substack{i=1 \\ i \neq j}}^{n} B_{ij} T_i + \sum_{i=1}^{n} T_i \sum_{k=1}^{n} C_{kj} \beta_{ki} - \left\{ \sum_{\substack{i=1 \\ i \neq j}}^{n} B_{ij} + \sum_{k=1}^{n} C_{kj} + (E_{j,left} + E_{j,right}) + hA_j \right\} T_j \\ = - \sum_{k=1}^{n} C_{kj} \alpha_k - (E_{j,left} + E_{j,right}) T_e - hA_j T_r \end{aligned} \tag{A-3.18}$$

T_j appears once in the double sum in equation (A-3.18) above. Placing this occurrence of T_j with the $\{\} T_j$ term, and regrouping the T_i yields:

$$\begin{aligned} \sum_{\substack{i=1 \\ i \neq j}}^{n} \left\{ B_{ij} + \sum_{k=1}^{n} C_{kj} \beta_{ki} \right\} T_i - \left\{ \sum_{\substack{i=1 \\ i \neq j}}^{n} B_{ij} + \sum_{k=1}^{n} C_{kj} - \sum_{k=1}^{n} C_{kj} \beta_{ki} + (E_{j,left} + E_{j,right}) + hA_j \right\} T_j \\ = - \sum_{k=1}^{n} C_{kj} \alpha_k - (E_{j,left} + E_{j,right}) T_e - hA_j T_r \end{aligned} \tag{A-3.19}$$

This is the working equation for T_j and is the j-th row in the matrix equation,

$$[[A]] \cdot [T] = [B] \tag{A-3.20}$$

with the index j running from 1 to n outer-ring temperatures.

View Factors: The view factors used in the calculation are defined according to the following equation (R.B. Bird, W.E. Stewart, and E.N. Lightfoot; 1960, *Transport Phenomena,* page 440):

$$F_{12} = \frac{1}{\pi A_1} \int\int \frac{\cos\theta_1 \cos\theta_2}{r_{12}^2} dA_1\, dA_2 \tag{A-3.21}$$

where r_{12} is the distance between surfaces 1 and 2, A_1 is the area of surface 1, A_2 is the area of surface 2, θ_1 is the angle between r_{12} and the normal of surface 1, and θ_2 is the angle between r_{12} and the normal of surface 2.

In equation (A-3.4), F_{ij} is the view factor from outer ring, i, to an outer ring, j, with an obscuring, coaxial cylinder present, and is:

$$F_{ij} = \frac{8\Delta y}{\pi r_2} \int_0^{2\cos^{-1}(r_1/r_2)} \frac{\cos^4\left(\frac{\theta}{2}\right)}{\left[\frac{L^2}{r_2^2} + 4\cos^2\left(\frac{\theta}{2}\right)\right]^2} d\theta \tag{A-3.22}$$

where L is the i-to-j separation.

In equation (A-3.8), F_{kj} is the view factor from inner ring, k, to outer ring, j, and is:

$$F_{kj} = \frac{2 r_2 x}{\pi} \int_{\xi_o}^{\pi/2} \frac{\cos\theta_1 \cos\theta_2}{R^2} d\xi \tag{A-3.23}$$

where r_1 = radius of the inner cylinder, r_2 = radius of the outer cylinder, L = k-to-j ring separation, x = ring width, and:

$$\xi_0 = \sin^{-1}\left(\frac{r_1}{r_2}\right) \tag{A-3.24}$$

$$R^2 = \left[r_2^2 + r_1^2 - 2 r_1 r_2 \cos(\pi/2 - \xi)\right] + L^2 \tag{A-3.25}$$

$$R\cos\theta_1 = \left[r_2^2 + r_1^2 - 2 r_1 r_2 \cos(\pi/2 - \xi)\right]^{1/2} \tag{A-3.26}$$

$$\cos\theta_2 = \frac{R^2 + r_2^2 - L^2 - r_1^2}{2Rr_2} \tag{A-3.27}$$

In equation (A-3.5), F_{je} is the view factor from outer ring, *j*, to an end plate with an obscuring coaxial cylinder present, and is:

$$F_{je} = \frac{2}{\pi} \int_{\theta_{\max}}^{0} \left\{ \int_{r_{\min}}^{r_2} \frac{\cos\theta_f \cos\theta_b}{R^2} r\, dr \right\} d\theta \tag{A-3.28}$$

where *S* is the separation of the ring from the end, and:

$$R^2 = r^2 + r_2^2 - 2rr_2\cos\theta + S^2 \tag{A-3.29}$$

$$\theta_{\max} = 2\alpha = 2\cos^{-1}(r_1 / r_2) \tag{A-3.30}$$

For $\theta_{\max} < \theta < \alpha$, the minimum value of *r* is obtained from $\beta = \theta - \alpha$, and:

$$r_{\min} = \frac{r_1}{\cos\beta} \tag{A-3.31}$$

and for $\alpha < \theta < 0$:

$$r_{\min} = r_1 \tag{A-3.32}$$

In equation (A-3.10), F_{ke} is the view factor from inner ring, *k*, to an end plate, and is:

$$F_{ke} = \frac{2}{\pi} \int_{\alpha}^{0} \left\{ \int_{r_{\min}}^{r_2} \frac{\cos\theta_a \cos\theta_b}{R^2} r\, dr \right\} d\theta \tag{A-3.33}$$

where *S* is the separation of the ring from the end, and:

$$r_{\min} = \frac{r_1}{\cos\theta} \tag{A-3.34}$$

$$\alpha = \cos^{-1}\left(\frac{r_1}{r_2}\right) \tag{A-3.35}$$

$$\cos\theta_1 = \frac{r\cos\theta - r_1}{R} \tag{A-3.36}$$

$$\cos\theta_2 = \cos\theta_b = \frac{S}{R} \tag{A-3.37}$$

The view factors given in equations (A-3.22), (A-3.23), (A-3.28), and (A-3.33) were compared with the open literature (i.e., W. M. Rohsenow, J. P. Hartnett, and Y. I. Cho, 1998, *Handbook of Heat Transfer*, and John R. Howell, 1982, *A Catalog of Radiation Configuration Factors*) and found to be satisfactory.

Solution Technique: The view factors given in equations (A-3.22), (A-3.23), (A-3.28), and (A-3.33) were integrated numerically using a Simpson's integration scheme. The cubic temperature functions written in equations (A-3.4), (A-3.5), (A-3.8) and (A-3.10) are the result of the linearization of radiant-heat transfer and thus require an iterative solution technique. The solution proceeds from an initial temperature guess (e.g., the environment temperature beyond the ends of the cylinder) and then solving equation (A-3.20) for all the outer-ring temperatures. These calculated temperatures are then substituted into the cubic temperature functions, and the solution repeated.

At each outer-ring temperature iteration equation (A-3.20) is solved using Gaussian elimination with back substitution. The inner-ring temperatures are then calculated from equation (A-3.13). The iteration proceeds until the temperature for each outer ring from iteration to iteration changes very little. The temperature-convergence criterion used is the sum of the absolute values of each temperature difference from iteration to iteration. Convergence is considered obtained when this sum is less than 0.01. When the solution converges, the energy balance, or power balance, for each ring (inner and outer) and a total energy balance for the system are calculated using the solution temperatures and the classical T^4 difference. In any such iterative calculation for temperature, the energy balances are the objective functions on which to base the conclusion that the convergence criterion is acceptable. The energy balances should always "close" to within a few tenths of a percent. The words "energy balance" and "power balance" are used interchangeably here, and the use of "energy balance" pertains to a specific unit of time, say one second, so that watts becomes joules.

As stated earlier, in order to solve a realistic problem, a convective boundary condition is used to transfer energy from the outer cylinder to the outside medium (rock). The boundary conditions are as follows: The temperature of the outside medium (rock) behind the outer cylinder was set to 140°C, which is about the bulk rock temperature based on a similar transient calculation. The heat-transfer coefficient used for the outside medium was 4 W/m^2-K. The temperature of the environment at the open ends of the cylindrical system was maintained at 140°C. The power output of the inner cylinder was specified as shown in Table A-3.1, and the values used here represent the base-case package powers at the time of peak postclosure temperature at 75 years after emplacement with 50 years of ventilation. Each package is five meters in length and thus the ring power over five-meter segments is the same.

Table A-3.1. Thermal Power of Each Inner Cylinder One-Meter-Wide Ring, these powers are based on the base-case package powers (1.45 kW/meter) at the time of peak postclosure temperature

Ring # (meters)	Power (W)	Ring	Power (W)	Ring	Power (W)	Ring	Power (W)
1	1	26	1	51	440	76	1
2	1	27	1	52	440	77	1
3	1	28	1	53	440	78	1
4	1	29	1	54	448	79	1
5	1	30	1	55	448	80	1
6	1	31	1	56	448	81	1
7	1	32	1	57	448	82	1
8	1	33	1	58	448	83	1
9	1	34	720	59	104.4	84	1
10	1	35	720	60	104.4	85	1
11	1	36	720	61	104.4	86	1
12	1	37	720	62	104.4	87	1
13	1	38	720	63	104.4	88	1
14	1	39	33.8	64	720	89	1
15	1	40	33.8	65	720	90	1
16	1	41	33.8	66	720	91	1
17	1	42	33.8	67	720	92	1
18	1	43	33.8	68	720	93	1
19	1	44	736	69	440	94	1
20	1	45	736	70	440	95	1
21	1	46	736	71	440	96	1
22	1	47	736	72	440	97	1
23	1	48	736	73	440	98	1
24	1	49	440	74	1	99	1
25	1	50	440	75	1	100	1

Results and Conclusions: The energy (or power for one second) transported out of the system calculated from the temperatures determined from the defining equations above is given in Table A.3-2.

Table A.3-2. Calculated Power Losses

Power radiated out both ends from the outer rings (W)	5.820E+01
Power radiated out both ends from the inner rings (W)	1.192E+01
Power transferred through the outer-ring walls (W)	1.820E+04
Total power transported out of the system (W)	1.827E+04

The total inner-ring specified source power (calculated as the sum of values in Table A.3-1) is 1.827E+04 W. Comparing this value with the total power transported out (Table A.3-2) yields a power-balance error of -0.02%. Thus, the total energy balance is satisfied, and the convergence criterion specified earlier is appropriate.

The temperature distribution along the outer cylinder, e.g., the drift wall, is presented in Figure A.3-1. There is a package every five meters at the locations specified in Table A-3.1, and the no-package region runs from 0 meters to 33 meters, and from 74 meters to 100 meters. The solution yields a temperature variation along the drift wall of approximately 3°C, from about 144.5°C (at about 40 meters) to slightly less than 147°C (at about 47 meters), opposite the packages in the region of 34 meters to 73 meters. Because of the end effects, the

temperatures at each end of the package segment are not used here (in reality, there will be more than 100 packages in a drift).

Figure A-3.1 Temperature Distribution Along the Drift Wall (outer cylinder wall)

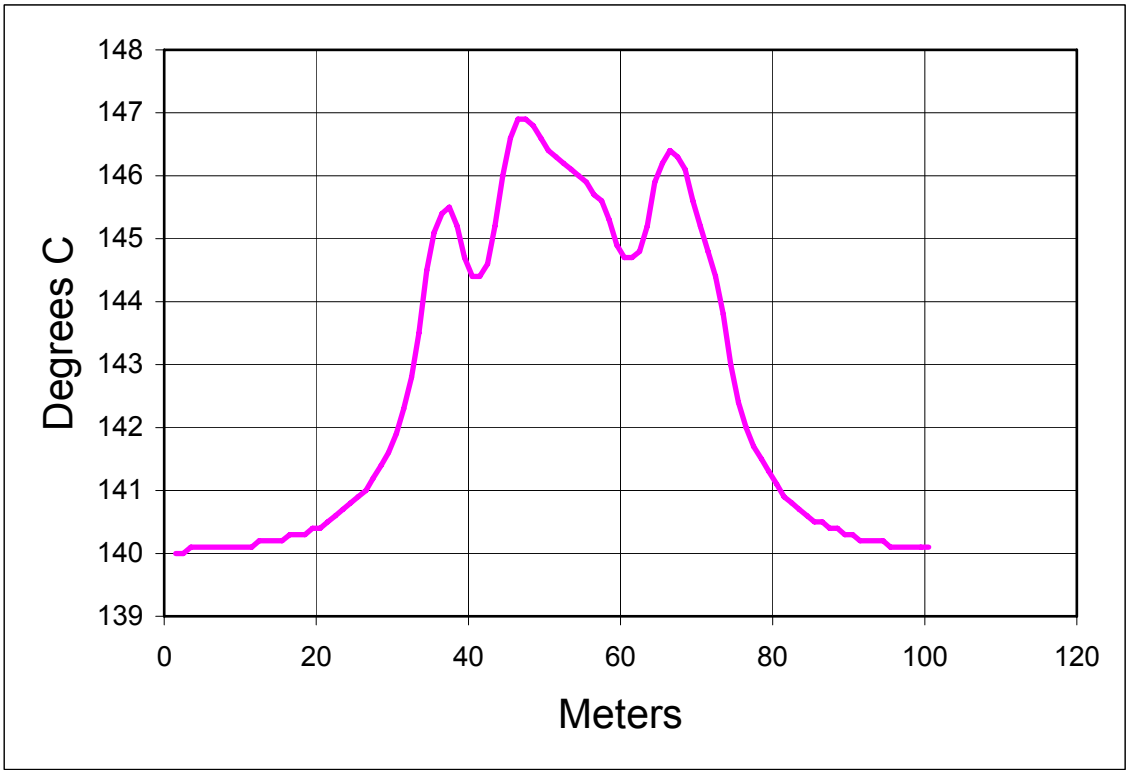

These results indicate that the drift wall temperature variation opposite packages of varying power is not large at the time of peak postclosure temperature, less than 3°C. Thus, conclude that it is justified to use a linear power for the entire drift to calculate drift wall temperatures. Since the problem analyzed here does not consider any axial conduction or natural convection, these results are bounding; the actual drift wall temperature variation will be less. The implicit assumption of a smooth drift wall temperature that does not feel package power variation in the in-drift natural convection and condensation analysis cited earlier is justified.

At the times of interest in the in-drift natural convection and condensation analyses at 300 years and longer, the drift wall temperature variation will be much less. The expectation can be that the drift wall temperature variation will be decreased approximately by the decrease in package powers, which between 75 and 300 years will be a factor of 0.36. Thus the drift wall temperature variation at 300 years will be approximately 1°C, and at other times of interest longer than 1,000 years, the temperature variation will be a small fraction of a degree.

The analyses presented here are based on an emissivity of unity. Clearly, this will not be the case in a repository environment, but the emissivities of the surfaces in a repository environment will be close to unity due to metal oxidation and the presence of dust on the metal surfaces. This dust will most likely determine the emissivities, and thus the emissivities are expected to be in the range of 0.9 and greater. Emissivities in this range will not significantly change the results presented here.

References:

Bechtel SAIC Company, 2004, *In-Drift Natural Convection and Condensation*, MDL-EBS-MD-000001 REV00, Las Vegas, Nevada: Bechtel SAIC Company.

Bechtel SAIC Company, 2005a, *Multiscale Thermohydrologic Model*, ANL-EBS-MD-000049 REV03, Las Vegas, Nevada: Bechtel SAIC Company.

Bechtel SAIC Company, 2005b, *IED Waste Package Decay Heat Generation [Sheet 1 of 1]*, 800-IED-WIS0-00701-000-00A, Las Vegas, Nevada: Bechtel SAIC Company.

Bird, R.B.; W.E. Stewart; and E.N. Lightfoot, 1960, *Transport Phenomena*, New York, New York: John Wiley & Sons.

Howell, John R., 1982, *A Catalog of Radiation Configuration Factors*, New York, New York: McGraw-Hill.

Rohsenow, W.M.; J. P. Hartnett; and Y. I. Cho, 1998, *Handbook of Heat Transfer, Third Edition*, New York, New York: McGraw-Hill.

Appendix B
Assembly Power Constant Calculation

4% Enriched BWR Assemblies

The following assembly powers were taken from the tables generated with Origin.

	Low_BU := 60	High_BU:= 70
5 years OOR	Low_5 := 1714.0800	High_5:= 2120.4600
10 years OOR	Low_10 := 1156.7100	High_10:= 1440.6400
25 years OOR	Low_25 := 783.5390	High_25:= 959.3630
50 years OOR	Low_50 := 500.2433	High_50:= 598.2805
100 years OOR	Low_100 := 259.6294	High_100:= 300.4353
300 years OOR	Low_300 := 100.6072	High_300:= 109.8012

Most of the Origan tables provide data at 10 Gwd/ton intervals. The following equations perform a linear interpulation to calculate the assembly powers at 1 Gwd/ton intervals. The variable Cal_BU is the desired burnup value for the calculation

Calc_BU := 61 Burnup value for calculation

Interperlation for assembly burnup Cal_BU between assembly burnups Low_BU and High_BU.

Assembly Power for burnup Calc_BU at age 5, 10, 25, 50, 100, and 300 yrs OOR.

$$Cal\_5 := Low\_5 + (High\_5 - Low\_5)\cdot\frac{Calc\_BU - Low\_BU}{High\_BU - Low\_BU} \qquad Cal\_5 = 1754.718000$$

$$Cal\_10 := Low\_10 + (High\_10 - Low\_10)\cdot\frac{Calc\_BU - Low\_BU}{High\_BU - Low\_BU} \qquad Cal\_10 = 1185.103000$$

$$Cal\_25 := Low\_25 + (High\_25 - Low\_25)\cdot\frac{Calc\_BU - Low\_BU}{High\_BU - Low\_BU} \qquad Cal\_25 = 801.121400$$

$$Cal\_50 := Low\_50 + (High\_50 - Low\_50)\cdot\frac{Calc\_BU - Low\_BU}{High\_BU - Low\_BU} \qquad Cal\_50 = 510.047020$$

$$Cal\_100 := Low\_100 + (High\_100 - Low\_100)\cdot\frac{Calc\_BU - Low\_BU}{High\_BU - Low\_BU} \qquad Cal\_100 = 263.709990$$

$$Cal\_300 := Low\_300 + (High\_300 - Low\_300)\cdot\frac{Calc\_BU - Low\_BU}{High\_BU - Low\_BU} \qquad Cal\_300 = 101.526600$$

The following six "Guess values" are required by MathCad to solve the six equations in six unknowns provided below. These six equations represent the assembly power as the summation of three expedentional terms at assambly ages of 5, 10, 25, 50, 100, and 300 years out of reactor..

$P1 := 1600 \quad P2 := 130 \quad P3 := 15 \quad \lambda1 := .5 \quad \lambda2 := .02 \quad \lambda3 := .0011$

Given

$$P1 \cdot e^{-5 \cdot \lambda1} + P2 \cdot e^{-5 \cdot \lambda2} + P3 \cdot e^{-5 \cdot \lambda3} = Cal\_5$$

$$P1 \cdot e^{-10 \cdot \lambda1} + P2 \cdot e^{-10 \cdot \lambda2} + P3 \cdot e^{-10 \cdot \lambda3} = Cal\_10$$

$$P1 \cdot e^{-25 \cdot \lambda1} + P2 \cdot e^{-25 \cdot \lambda2} + P3 \cdot e^{-25 \cdot \lambda3} = Cal\_25$$

$$P1 \cdot e^{-50 \cdot \lambda1} + P2 \cdot e^{-50 \cdot \lambda2} + P3 \cdot e^{-50 \cdot \lambda3} = Cal\_50$$

$$P1 \cdot e^{-100 \cdot \lambda1} + P2 \cdot e^{-100 \cdot \lambda2} + P3 \cdot e^{-100 \cdot \lambda3} = Cal\_100$$

$$P1 \cdot e^{-300 \cdot \lambda1} + P2 \cdot e^{-300 \cdot \lambda2} + P3 \cdot e^{-300 \cdot \lambda3} = Cal\_300$$

$$\begin{pmatrix} P1\_Value \\ P2\_Value \\ P3\_Value \\ \lambda1\_Value \\ \lambda2\_Value \\ \lambda3\_Value \end{pmatrix} := Find(P1, P2, P3, \lambda1, \lambda2, \lambda3)$$

MathCad calculated the following values for the six constants:

Calc_BU = 61	P1_Value = 3002.31	λ1_Value = 0.340099
	P2_Value = 1098.44	λ2_Value = 0.026099
	P3_Value = 246.08	λ3_Value = 0.002966

Which results in the following half lives:

$Half\_Life1 := \frac{.693}{\lambda1\_Value}$	$Half\_Life2 := \frac{.693}{\lambda2\_Value}$	$Half\_Life3 := \frac{.693}{\lambda3\_Value}$
Half_Life1= 2.04	Half_Life2= 26.55	Half_Life3= 233.69

Appendix C
PWR and BWR Decay Constants

PWR Decay Constants

4.5 % Enriched

Burnup	Decay 1	Decay 2	Decay 3	Power 1	Power 2	Power 3	Half Life 1	Half Life 2	Half Life 3
10	0.406173	0.024076	0.001286	616.78	171.11	15.47	1.71	28.78	538.88
11	0.404778	0.024028	0.001380	672.46	186.22	18.96	1.71	28.84	502.17
12	0.403622	0.023988	0.001447	728.21	201.32	22.47	1.72	28.89	478.92
13	0.402648	0.023954	0.001498	784.00	216.43	25.97	1.72	28.93	462.62
14	0.401815	0.023925	0.001537	839.83	231.53	29.48	1.72	28.97	450.88
15	0.401096	0.023899	0.001568	895.68	246.63	32.99	1.73	29.00	441.96
16	0.400468	0.023877	0.001593	951.56	261.73	36.51	1.73	29.02	435.03
17	0.399914	0.023857	0.001615	1007.45	276.82	40.02	1.73	29.05	429.10
18	0.399423	0.023839	0.001633	1063.36	291.92	43.53	1.74	29.07	424.37
19	0.398985	0.023823	0.001648	1119.28	307.02	47.05	1.74	29.09	420.51
20	0.398590	0.023808	0.001662	1175.21	322.12	50.56	1.74	29.11	416.97
21	0.394035	0.023725	0.001680	1213.11	337.02	54.46	1.76	29.21	412.50
22	0.390021	0.023650	0.001696	1252.10	351.92	58.35	1.78	29.30	408.61
23	0.386458	0.023580	0.001710	1291.97	366.83	62.23	1.79	29.39	405.26
24	0.383273	0.023515	0.001722	1332.57	381.74	66.12	1.81	29.47	402.44
25	0.380409	0.023456	0.001732	1373.76	396.65	70.00	1.82	29.54	400.12
26	0.377818	0.023400	0.001741	1415.45	411.57	73.87	1.83	29.62	398.05
27	0.375464	0.023348	0.001750	1457.56	426.48	77.75	1.85	29.68	396.00
28	0.373314	0.023300	0.001757	1500.03	441.41	81.62	1.86	29.74	394.42
29	0.371345	0.023255	0.001764	1542.81	456.33	85.49	1.87	29.80	392.86
30	0.369533	0.023213	0.001770	1585.87	471.25	89.35	1.88	29.85	391.53
31	0.368735	0.023316	0.001826	1636.24	487.72	94.21	1.88	29.72	379.52
32	0.367997	0.023413	0.001878	1686.69	504.18	99.08	1.88	29.60	369.01
33	0.367314	0.023505	0.001926	1737.20	520.65	103.94	1.89	29.48	359.81
34	0.366678	0.023591	0.001970	1787.77	537.11	108.81	1.89	29.38	351.78
35	0.366087	0.023672	0.002011	1838.38	553.58	113.68	1.89	29.28	344.60
36	0.365534	0.023749	0.002049	1889.05	570.04	118.55	1.90	29.18	338.21
37	0.365017	0.023822	0.002084	1939.75	586.51	123.43	1.90	29.09	332.53
38	0.364531	0.023891	0.002118	1990.49	602.97	128.31	1.90	29.01	327.20
39	0.364075	0.023957	0.002149	2041.26	619.44	133.18	1.90	28.93	322.48
40	0.363646	0.024019	0.002178	2092.06	635.91	138.06	1.91	28.85	318.18
41	0.361731	0.024100	0.002222	2133.48	655.36	143.00	1.92	28.76	311.88
42	0.359940	0.024177	0.002263	2175.26	674.82	147.94	1.93	28.66	306.23
43	0.358262	0.024249	0.002303	2217.38	694.27	152.88	1.93	28.58	300.91
44	0.356688	0.024318	0.002340	2259.79	713.72	157.83	1.94	28.50	296.15
45	0.355205	0.024383	0.002376	2302.47	733.17	162.78	1.95	28.42	291.67
46	0.353809	0.024445	0.002410	2345.39	752.61	167.74	1.96	28.35	287.55
47	0.352490	0.024505	0.002442	2388.53	772.06	172.70	1.97	28.28	283.78
48	0.351243	0.024561	0.002473	2431.86	791.50	177.66	1.97	28.22	280.23
49	0.350062	0.024615	0.002502	2475.38	810.93	182.63	1.98	28.15	276.98
50	0.348941	0.024667	0.002531	2519.06	830.37	187.60	1.99	28.09	273.80
51	0.347982	0.024829	0.002579	2562.38	854.18	193.04	1.99	27.91	268.71
52	0.347075	0.024983	0.002626	2605.86	878.01	198.46	2.00	27.74	263.90
53	0.346217	0.025129	0.002670	2649.50	901.88	203.86	2.00	27.58	259.55
54	0.345403	0.025268	0.002712	2693.27	925.78	209.24	2.01	27.43	255.53
55	0.344631	0.025401	0.002752	2737.18	949.70	214.62	2.01	27.28	251.82
56	0.343897	0.025527	0.002791	2781.20	973.64	219.98	2.02	27.15	248.30
57	0.343199	0.025647	0.002828	2825.33	997.61	225.33	2.02	27.02	245.05
58	0.342533	0.025763	0.002864	2869.57	1021.59	230.67	2.02	26.90	241.97
59	0.341898	0.025873	0.002898	2913.90	1045.59	236.00	2.03	26.78	239.13
60	0.341292	0.025978	0.002931	2958.31	1069.60	241.32	2.03	26.68	236.44
61	0.340099	0.026099	0.002966	3002.31	1098.44	246.08	2.04	26.55	233.65
62	0.338965	0.026214	0.002999	3046.54	1127.30	250.83	2.04	26.44	231.08
63	0.337885	0.026324	0.003031	3090.99	1156.19	255.56	2.05	26.33	228.64
64	0.336855	0.026429	0.003063	3135.63	1185.08	260.29	2.06	26.22	226.25
65	0.335872	0.026529	0.003093	3180.46	1214.00	265.01	2.06	26.12	224.05
66	0.334933	0.026624	0.003123	3225.45	1242.93	269.72	2.07	26.03	221.90
67	0.334034	0.026715	0.003151	3270.59	1271.87	274.43	2.07	25.94	219.93
68	0.333174	0.026803	0.003179	3315.88	1300.82	279.13	2.08	25.86	217.99
69	0.332350	0.026886	0.003206	3361.30	1329.78	283.82	2.09	25.78	216.16
70	0.331559	0.026967	0.003233	3406.86	1358.76	288.52	2.09	25.70	214.35

BWR Decay Constants

4% Enriched

Burnup	Decay 1	Decay 2	Decay 3	Power 1	Power 2	Power 3	Half Life 1	Half Life 2	Half Life 3
10	0.443891	0.023654	0.001124	240.96	69.33	5.84	1.56	29.30	616.55
11	0.438826	0.023609	0.001222	254.28	75.49	7.01	1.58	29.35	567.10
12	0.434581	0.023571	0.001294	267.89	81.64	8.19	1.59	29.40	535.55
13	0.430966	0.023539	0.001350	281.69	87.80	9.36	1.61	29.44	513.33
14	0.427852	0.023511	0.001395	295.65	93.95	10.54	1.62	29.48	496.77
15	0.425141	0.023487	0.001431	309.74	100.10	11.72	1.63	29.51	484.28
16	0.422759	0.023465	0.001461	323.93	106.25	12.90	1.64	29.53	474.33
17	0.420650	0.023447	0.001486	338.20	112.40	14.08	1.65	29.56	466.35
18	0.418768	0.023430	0.001507	352.53	118.55	15.26	1.65	29.58	459.85
19	0.417079	0.023414	0.001526	366.93	124.70	16.44	1.66	29.60	454.13
20	0.415555	0.023401	0.001542	381.36	130.85	17.62	1.67	29.61	449.42
21	0.412691	0.023427	0.001597	394.24	136.98	19.06	1.68	29.58	433.94
22	0.410117	0.023452	0.001646	407.27	143.11	20.50	1.69	29.55	421.02
23	0.407790	0.023475	0.001689	420.41	149.23	21.94	1.70	29.52	410.30
24	0.405677	0.023497	0.001727	433.67	155.36	23.39	1.71	29.49	401.27
25	0.403749	0.023516	0.001762	447.00	161.48	24.84	1.72	29.47	393.30
26	0.401982	0.023535	0.001793	460.42	167.60	26.29	1.72	29.45	386.50
27	0.400358	0.023552	0.001821	473.90	173.73	27.74	1.73	29.42	380.56
28	0.398859	0.023569	0.001847	487.44	179.85	29.19	1.74	29.40	375.20
29	0.397471	0.023584	0.001871	501.03	185.96	30.64	1.74	29.38	370.39
30	0.396182	0.023598	0.001892	514.66	192.08	32.10	1.75	29.37	366.28
31	0.393343	0.023633	0.001936	526.51	198.54	33.58	1.76	29.32	357.95
32	0.390741	0.023665	0.001977	538.56	205.00	35.06	1.77	29.28	350.53
33	0.388341	0.023695	0.002016	550.77	211.45	36.55	1.78	29.25	343.75
34	0.386124	0.023724	0.002052	563.13	217.90	38.04	1.79	29.21	337.72
35	0.384069	0.023752	0.002085	575.61	224.35	39.53	1.80	29.18	332.37
36	0.382159	0.023778	0.002117	588.21	230.79	41.02	1.81	29.14	327.35
37	0.380379	0.023802	0.002147	600.90	237.24	42.52	1.82	29.12	322.78
38	0.378716	0.023826	0.002175	613.68	243.68	44.01	1.83	29.09	318.62
39	0.377159	0.023848	0.002202	626.54	250.12	45.51	1.84	29.06	314.71
40	0.375698	0.023870	0.002227	639.48	256.56	47.01	1.84	29.03	311.18
41	0.372588	0.023975	0.002276	648.60	264.20	48.59	1.86	28.91	304.48
42	0.369701	0.024074	0.002323	658.02	271.84	50.16	1.87	28.79	298.32
43	0.367013	0.024168	0.002368	667.69	279.49	51.74	1.89	28.67	292.65
44	0.364505	0.024258	0.002410	677.60	287.13	53.32	1.90	28.57	287.55
45	0.362158	0.024343	0.002450	687.70	294.78	54.89	1.91	28.47	282.86
46	0.359957	0.024424	0.002489	697.98	302.42	56.47	1.93	28.37	278.43
47	0.357888	0.024501	0.002526	708.43	310.07	58.05	1.94	28.28	274.35
48	0.355941	0.024574	0.002561	719.02	317.72	59.62	1.95	28.20	270.60
49	0.354104	0.024644	0.002595	729.73	325.36	61.20	1.96	28.12	267.05
50	0.352369	0.024712	0.002628	740.57	333.01	62.78	1.97	28.04	263.70
51	0.352843	0.024955	0.002702	758.20	342.49	64.89	1.96	27.77	256.48
52	0.353326	0.025187	0.002772	775.91	352.00	66.98	1.96	27.51	250.00
53	0.353816	0.025407	0.002838	793.68	361.54	69.06	1.96	27.28	244.19
54	0.354310	0.025617	0.002901	811.52	371.11	71.12	1.96	27.05	238.88
55	0.354807	0.025817	0.002961	829.41	380.70	73.16	1.95	26.84	234.04
56	0.355307	0.026008	0.003019	847.37	390.32	75.19	1.95	26.65	229.55
57	0.355807	0.026190	0.003073	865.37	399.95	77.21	1.95	26.46	225.51
58	0.356306	0.026365	0.003126	883.43	409.61	79.22	1.94	26.28	221.69
59	0.356805	0.026532	0.003176	901.55	419.28	81.21	1.94	26.12	218.20
60	0.357302	0.026692	0.003224	919.71	428.97	83.20	1.94	25.96	214.95
61	0.352606	0.026709	0.003228	921.16	440.21	83.90	1.97	25.95	214.68
62	0.348225	0.026726	0.003233	923.53	451.45	84.59	1.99	25.93	214.35
63	0.344126	0.026742	0.003237	926.68	462.68	85.28	2.01	25.91	214.09
64	0.340282	0.026756	0.003241	930.52	473.91	85.97	2.04	25.90	213.82
65	0.336670	0.026770	0.003245	934.98	485.14	86.66	2.06	25.89	213.56
66	0.333267	0.026783	0.003249	939.98	496.37	87.35	2.08	25.87	213.30
67	0.330056	0.026795	0.003253	945.47	507.59	88.04	2.10	25.86	213.03
68	0.327020	0.026806	0.003257	951.39	518.82	88.72	2.12	25.85	212.77
69	0.324145	0.026816	0.003261	957.70	530.04	89.40	2.14	25.84	212.51
70	0.321418	0.026826	0.003264	964.36	541.26	90.08	2.16	25.83	212.32

Appendix D
Comparison of Assembly Power in Project Documents with Calculated Power

Comparison of Project and NWTRB Assembly Powers

Decay 1		0.396182		0.375698		0.352369		0.369533		0.363646		0.348941
Decay 2		0.023598		0.02387		0.024712		0.023213		0.024019		0.024667
Decay 3		0.001892		0.002227		0.002628		0.00177		0.002178		0.002531
Power 1		514.66		639.48		740.57		1585.87		2092.06		2519.06
Power 2		192.08		256.56		333.01		471.25		635.91		830.37
Power 3		32.1		47.01		62.78		89.35		138.06		187.6
Time from			BWR Assembly						PWR Assembly			
Discharge	30 Gwd/t 4%		40 Gwd/t 4%		50 Gwd/t 4%		30 Gwd/t 4.5%		40 Gwd/t 4.5%		50 Gwd/t 4.5%	
(years)	Origan Power	Calculated Power	Origan Power	Calculated Power	Origan Power	Calculated Power	Origan Power	Calculated Power	Origan Power	Calculated Power	Origan Power	Calculated Power
5	273.5	273.5	371.9	371.9	483.4	483.4	758.1	758.1	1040.1	1040.1	1359.3	1359.3
6	242.0	246.2	331.8	335.8	433.0	438.3	655.5	671.1	904.4	922.9	1191.2	1211.3
7	222.6	226.7	306.0	309.5	399.1	404.6	593.4	608.2	820.7	837.6	1081.0	1102.0
8	210.4	212.3	287.2	289.8	375.2	378.9	551.8	562.0	763.6	774.5	1006.8	1020.0
9	200.2	201.4	273.5	274.8	357.6	359.0	522.7	527.3	723.2	727.0	951.4	957.4
10	193.0	193.0	263.0	263.0	343.1	343.1	500.8	500.8	690.3	690.3	908.6	908.6
11	186.9	186.2	254.5	253.4	330.7	330.1	482.4	479.9	663.9	661.4	873.5	869.7
12	180.9	180.5	247.0	245.5	320.4	319.2	467.1	463.0	642.0	637.8	843.8	837.9
13	175.7	175.6	239.7	238.6	311.1	309.8	453.1	448.8	623.4	618.1	817.7	811.1
14	171.7	171.3	234.3	232.6	302.9	301.5	441.2	436.6	606.1	601.1	794.8	788.0
15	167.8	167.4	227.9	227.1	295.8	294.0	430.5	425.9	591.1	586.1	773.4	767.6
16	163.7	163.7	222.7	222.0	288.8	287.1	420.0	416.2	577.4	572.6	755.3	749.2
17	160.7	160.3	218.4	217.3	281.8	280.7	410.6	407.3	563.9	560.1	737.4	732.3
18	156.8	157.0	213.2	212.9	275.9	274.6	401.2	398.9	551.5	548.5	720.7	716.6
19	153.8	153.9	209.0	208.6	269.0	268.9	393.0	391.0	540.4	537.5	705.3	701.8
20	150.9	150.9	204.7	204.5	264.2	263.4	384.8	383.4	528.3	527.0	690.0	687.7
21	147.9	148.0	200.5	200.5	258.4	258.1	377.6	376.2	518.4	516.9	674.9	674.2
22	145.0	145.2	196.3	196.7	252.6	252.9	370.5	369.2	507.6	507.2	661.9	661.2
23	142.0	142.4	193.2	192.9	247.9	248.0	362.5	362.4	497.9	497.8	649.1	648.7
24	139.0	139.7	189.0	189.3	243.1	243.1	356.4	355.8	488.3	488.7	636.3	636.5
25	137.1	137.1	185.8	185.8	238.4	238.4	349.4	349.4	479.8	479.8	624.7	624.7
26	134.2	134.6	181.6	182.3	233.8	233.9	342.5	343.2	470.3	471.2	612.1	613.2
27	132.1	132.1	178.4	179.0	229.1	229.4	336.4	337.1	461.9	462.8	600.6	602.0
28	129.3	129.7	175.3	175.7	224.5	225.1	330.5	331.1	453.6	454.5	589.2	591.1
29	126.9	127.3	172.1	172.5	219.9	220.8	324.5	325.3	446.3	446.5	578.8	580.5
30	124.7	125.0	169.0	169.3	216.3	216.7	318.6	319.6	438.0	438.7	568.4	570.1
31	122.3	122.7	165.8	166.3	211.7	212.7	313.6	314.1	430.7	431.1	558.1	560.0
32	120.2	120.5	162.7	163.3	208.1	208.7	307.7	308.6	423.5	423.6	547.9	550.1
33	118.0	118.3	160.6	160.4	204.6	204.9	302.7	303.4	415.3	416.3	538.7	540.5
34	116.0	116.2	157.4	157.5	201.1	201.2	297.8	298.2	408.2	409.2	529.5	531.1
35	114.0	114.1	154.2	154.8	196.5	197.5	291.8	293.1	402.0	402.3	520.3	521.9
36	111.9	112.1	152.1	152.0	193.0	193.9	287.8	288.2	394.9	395.5	510.1	512.9
37	109.9	110.2	149.0	149.4	189.5	190.4	282.8	283.3	387.8	388.9	502.0	504.2
38	108.0	108.2	146.5	146.8	187.1	187.0	277.8	278.6	381.7	382.4	492.9	495.6
39	106.2	106.3	144.0	144.2	183.5	183.7	272.9	274.0	375.6	376.0	484.8	487.3
40	104.4	104.5	141.6	141.8	180.1	180.4	268.8	269.5	369.6	369.8	476.7	479.1
41	102.6	102.7	139.1	139.3	176.6	177.3	263.9	265.0	363.5	363.8	469.6	471.1
42	100.9	100.9	136.9	137.0	174.2	174.2	259.8	260.7	357.4	357.9	461.5	463.4
43	99.1	99.2	134.5	134.6	170.7	171.1	255.8	256.5	352.4	352.1	454.5	455.7
44	97.5	97.5	132.3	132.4	168.3	168.2	251.8	252.4	346.3	346.5	446.4	448.3
45	95.8	95.9	130.1	130.2	165.1	165.3	247.7	248.3	340.3	340.9	439.4	441.1
46	94.2	94.3	128.0	128.0	162.4	162.5	243.7	244.4	336.3	335.5	432.3	434.0
47	92.7	92.7	125.8	125.9	159.6	159.7	239.7	240.5	331.2	330.3	425.3	427.0
48	91.1	91.2	123.8	123.8	156.9	157.0	236.6	236.7	325.2	325.1	419.3	420.3
49	89.7	89.7	121.7	121.8	154.3	154.4	232.5	233.0	320.2	320.1	412.2	413.7
50	88.2	88.2	119.8	119.8	151.8	151.8	229.4	229.4	315.2	315.2	407.2	407.2
51	86.9	86.8	117.9	117.9	149.3	149.3	225.3	225.9	311.1	310.4	400.2	400.9
52	85.4	85.4	116.0	116.0	146.8	146.9	222.3	222.4	306.1	305.7	394.2	394.7
53	84.1	84.0	114.2	114.2	144.4	144.5	219.2	219.1	301.1	301.1	388.1	388.7
54	82.7	82.7	112.4	112.4	142.2	142.2	215.1	215.7	297.1	296.6	382.1	382.8
55	81.5	81.4	110.6	110.6	139.9	139.9	212.0	212.5	293.1	292.2	377.1	377.1
56	80.1	80.1	109.0	108.9	137.7	137.6	208.9	209.4	288.1	287.9	371.1	371.4
57	78.9	78.9	107.3	107.2	135.5	135.5	205.8	206.3	284.1	283.7	365.1	365.9
58	77.8	77.6	105.7	105.6	133.4	133.3	203.7	203.2	281.1	279.6	360.1	360.6
59	76.5	76.4	104.0	104.0	131.4	131.3	200.5	200.3	276.1	275.6	356.1	355.3
60	75.4	75.3	102.5	102.4	129.4	129.2	197.3	197.4	273.1	271.6	350.1	350.2
61	74.2	74.1	101.0	100.9	127.4	127.2	194.2	194.6	268.1	267.8	345.1	345.2
62	73.1	73.0	99.5	99.4	125.5	125.3	192.1	191.8	265.1	264.1	340.1	340.3
63	72.1	71.9	98.0	97.9	123.6	123.4	188.9	189.1	262.0	260.4	335.1	335.5
64	71.0	70.9	96.6	96.4	121.8	121.5	186.8	186.5	257.0	256.8	330.1	330.8
65	70.0	69.8	95.2	95.0	120.0	119.7	183.7	183.9	254.0	253.3	327.1	326.2
66	68.9	68.8	93.8	93.7	118.2	118.0	181.3	181.3	251.0	249.9	322.0	321.8
67	68.0	67.8	92.5	92.3	116.5	116.2	178.9	178.9	247.0	246.5	317.0	317.4
68	67.0	66.8	91.2	91.0	114.8	114.5	176.4	176.4	244.0	243.2	313.0	313.1
69	66.0	65.9	89.9	89.7	113.2	112.9	174.1	174.1	241.0	240.0	309.0	308.9
70	65.1	64.9	88.7	88.5	111.6	111.3	171.8	171.7	238.0	236.9	305.0	304.8
71	64.1	64.0	87.4	87.2	110.0	109.7	169.5	169.5	235.0	233.8	301.0	300.8
72	63.3	63.1	86.2	86.0	108.4	108.2	167.3	167.3	231.0	230.8	297.0	296.9
73	62.4	62.3	85.1	84.9	106.9	106.6	165.1	165.1	229.0	227.9	294.0	293.1
74	61.5	61.4	83.9	83.7	105.4	105.2	163.1	163.0	226.0	225.0	290.0	289.4
75	60.7	60.6	82.8	82.6	104.0	103.7	161.0	160.9	223.0	222.2	286.0	285.7
76	59.9	59.8	81.6	81.5	102.6	102.3	158.9	158.8	220.6	219.5	283.0	282.2
77	59.0	59.0	80.6	80.4	101.2	100.9	156.9	156.9	217.3	216.8	279.0	278.7
78	58.3	58.2	79.5	79.4	99.9	99.6	155.0	154.9	215.0	214.2	275.0	275.2
79	57.5	57.4	78.5	78.4	98.5	98.3	153.1	153.0	212.8	211.6	272.0	271.9
80	56.7	56.7	77.5	77.3	97.3	97.0	151.2	151.1	209.6	209.1	269.0	268.6
81	56.1	55.9	76.5	76.4	96.0	95.7	149.4	149.3	207.5	206.6	265.0	265.4
82	55.3	55.2	75.5	75.4	94.8	94.5	147.6	147.5	205.4	204.2	262.0	262.3
83	54.6	54.5	74.6	74.5	93.5	93.3	145.8	145.8	202.4	201.8	260.0	259.2
84	54.0	53.8	73.6	73.5	92.4	92.1	144.1	144.1	200.4	199.5	256.2	256.2
85	53.2	53.2	72.8	72.6	91.2	91.0	142.5	142.4	198.5	197.3	253.9	253.3
86	52.7	52.5	71.8	71.8	90.1	89.8	140.8	140.7	195.6	195.1	250.6	250.4
87	52.0	51.9	71.0	70.9	88.9	88.7	139.2	139.1	193.8	192.9	247.4	247.6
88	51.3	51.3	70.2	70.0	87.8	87.7	137.6	137.6	191.0	190.8	245.3	244.9
89	50.8	50.6	69.3	69.2	86.8	86.6	136.0	136.0	189.3	188.7	242.2	242.2
90	50.1	50.0	68.5	68.4	85.8	85.6	134.6	134.5	187.6	186.7	239.1	239.6
91	49.5	49.5	67.7	67.6	84.7	84.6	133.1	133.1	184.9	184.7	237.1	237.0
92	49.0	48.9	67.0	66.8	83.7	83.6	131.6	131.6	183.3	182.8	234.1	234.5
93	48.4	48.3	66.1	66.1	82.8	82.6	130.2	130.2	181.7	180.9	232.2	232.0
94	47.8	47.8	65.4	65.3	81.8	81.7	128.8	128.8	179.2	179.0	229.4	229.6
95	47.3	47.2	64.7	64.6	80.9	80.7	127.5	127.5	177.6	177.2	226.5	227.2
96	46.7	46.7	63.9	63.9	79.9	79.8	126.2	126.1	176.2	175.4	224.8	224.9
97	46.2	46.2	63.2	63.2	79.0	79.0	124.8	124.8	173.7	173.6	222.0	222.6
98	45.7	45.7	62.6	62.5	78.1	78.1	123.5	123.6	172.3	171.9	220.3	220.4
99	45.2	45.2	61.9	61.9	77.3	77.2	122.3	122.3	170.9	170.3	217.7	218.2
100	44.7	44.7	61.2	61.2	76.4	76.4	121.1	121.1	168.6	168.6	216.1	216.1
110	40.3	40.4	55.3	55.4	68.9	69.0	110.1	110.2	153.8	153.9	195.9	197.1
120	36.8	36.9	50.4	50.6	62.6	63.0	101.1	101.3	141.5	141.9	180.7	181.5
130	33.9	34.0	46.4	46.7	57.5	58.0	93.7	94.0	131.2	132.0	166.8	168.6
140	31.5	31.7	43.1	43.5	53.3	53.9	87.6	88.0	122.5	123.8	155.9	157.9
150	29.4	29.7	40.4	40.8	49.8	50.5	82.6	83.0	115.6	116.9	146.4	148.9
160	27.8	28.1	38.1	38.5	46.8	47.6	78.3	78.8	109.6	111.1	138.1	141.2
170	26.4	26.7	36.1	36.6	44.3	45.1	74.7	75.2	104.4	106.1	131.7	134.5
180	25.2	25.6	34.4	35.0	42.1	43.0	71.7	72.2	100.0	101.7	126.0	128.7
190	24.3	24.6	32.9	33.5	40.1	41.1	69.0	69.6	96.2	97.9	120.9	123.6
200	23.3	23.7	31.7	32.3	38.5	39.5	66.7	67.3	92.8	94.5	116.3	119.1
250	20.3	20.5	27.2	27.6	32.6	33.2	58.4	58.8	80.4	81.7	99.3	101.4
300	18.4	18.4	24.3	24.3	28.7	28.7	53.0	53.0	72.3	72.3	88.3	88.3
350	16.9	16.6	22.2	21.6	26.0	25.1	48.8	48.2	66.1	64.6	80.0	77.5
400	15.7	15.1	20.4	19.3	23.7	22.0	45.3	44.1	61.0	57.8	73.4	68.2
450	14.7	13.7	19.0	17.3	22.0	19.2	42.4	40.3	56.6	51.8	67.8	60.1
500	13.8	12.5	17.7	15.4	20.4	16.9	39.7	36.9	52.8	46.5	63.0	52.9
550	13.0	11.3	16.6	13.8	19.1	14.8	37.4	33.8	49.5	41.7	58.9	46.6
600	12.2	10.3	15.7	12.4	17.9	13.0	35.2	30.9	46.5	37.4	55.2	41.1
650	11.6	9.4	14.8	11.1	16.9	11.4	33.3	28.3	43.8	33.5	51.9	36.2
700	11.0	8.5	14.0	9.9	16.0	10.0	31.5	25.9	41.3	30.1	48.9	31.9
750	10.4	7.8	13.2	8.8	15.1	8.7	29.9	23.7	39.1	27.0	46.2	28.1
800	9.9	7.1	12.6	7.9	14.3	7.7	28.4	21.7	37.0	24.2	43.7	24.8
850	9.5	6.4	12.0	7.1	13.6	6.7	27.0	19.8	35.2	21.7	41.4	21.8
900	9.0	5.8	11.4	6.3	13.0	5.9	25.7	18.2	33.4	19.4	39.3	19.2
950	8.6	5.3	10.9	5.7	12.4	5.2	24.5	16.6	31.8	17.4	37.4	16.9
1000	8.3	4.8	10.4	5.1	11.8	4.5	23.5	15.2	30.3	15.6	35.7	14.9

Comparison of PWR Origin Power with Calculated Power

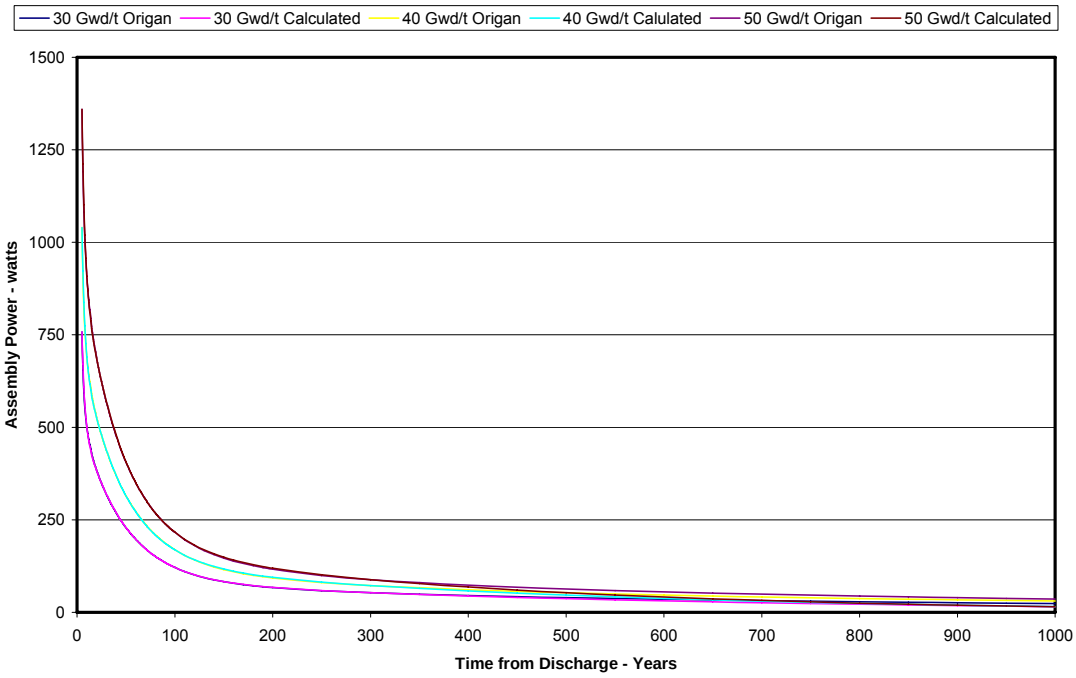

Comparison of BWR Origin Power to Calculated Power

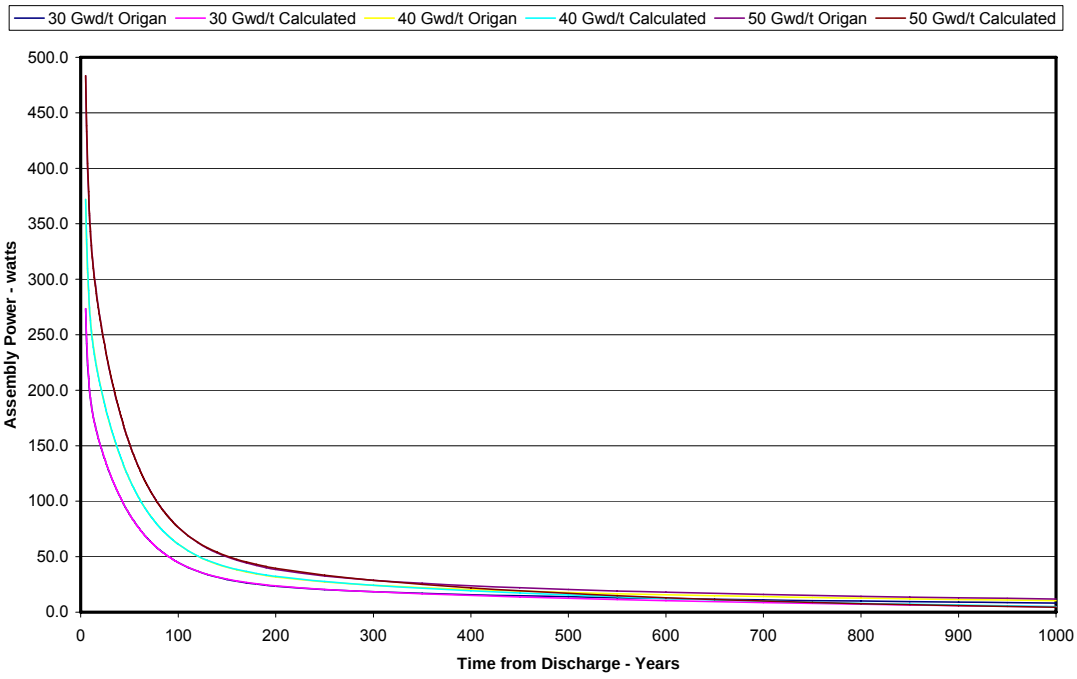

Appendix E
Sample Calculation Using
Finite-Length Decaying Line Source Single Waste Package

Finite Length Decaying Line Source, Single Package

This file calculates temperatures at locations in the repository plane based on a fixed number of neighboring drifts. Each drift is similar and contains a series of end-to-end finite-length decaying line sources, called segments. Each segment consists of the same number of WPs and each WP has the same length and power characteristics. The WP power is determined from the assembly burnup and age out of reactor and is represented by an equation with three decaying exponential terms. During the preclosure phase, forced ventilation provides heat removal with the ventilation efficiency decreasing linearly as the flow moves down the drift.

Independent Variables

The following variables define the conditions for the calculation. The burnup should be an integer between 10 and 70 Gwd/ton.

Initial Rock Temperature $tzero := 22.8$ °C

Ventilation Efficiency at Start of Drift $Eff\_1 := 0.90$ %

Ventilation Efficiency at End of Drift $Eff\_2 := 0.80$ %

Age at Emplacement $A1 := 5$ Years Out of Reactor

Ventilation Duration $Vent := 75$ Years

Age at Closure $A2 := A1 + Vent$ $A2 = 80$ Years Out of Reactor

$Est\_Drift\_Length := 600$ meters

$Drift\_Space := 81$ meters

$WP\_Length := 5.85$ meters

$WP\_Spacing := .1$ meters

$WP\_Per\_Seg := 12$ WP/segment

$Burnup := 45$ Gwd/ton

Number of Neighboring Drifts $nbors := 5$ Drifts

Constants

The following constants are required for the calculation.

$Krock := 1.83$ watt/meter - °C $\qquad \rho := 2097$ kg/meter^3 $\qquad Cp := 1119.0$ joules/kg - °C

$$\kappa := \frac{Krock \cdot 3600\,24 \cdot 365}{\rho \cdot Cp} \quad \text{meter}^2\text{/year}$$

Dependent Variables

The following calculation determines the exact length of the drift and the number of waste packages per drift based on the assumptions provided above.

$$No\_WP\_Est := \text{round}\left(\frac{Est\_Drift\_Length}{WP\_Length + WP\_Spacing}\right) \qquad No\_Seg := \text{round}\left(\frac{No\_WP\_Est}{WP\_Per\_Seg}\right)$$

$$No\_WP := No\_Seg \cdot WP\_Per\_Seg \qquad Drift\_Length := No\_WP \cdot (WP\_Spacing + WP\_Length) - WP\_Spacing$$

$$Seg\_L := \frac{Drift\_Length}{No\_Seg}$$

Actual Drift Length $Drift\_Length = 571.10$ meters Number of WP per Drift $No\_WP = 96$ WP per Drift

Number of Segments per Drift $No\_Seg = 8$ Segments Segment Length $Seg\_L = 71.4$ meters

Decay Variables Calculation

The following files contain the six constants that define the assembly power and decay as a function of burnup for BWR and PWR assemblies. The power values are calculated based on a PWR assembly with an initial loading of 0.475 MTHM/Assembly and a BWR assembly with an initial loading of 0.200 MTHM/Assembly.

BWR := PWR :=

The six constants are selected from the above files based on the burnup defined above and whether BWR or PWR assemblies are loaded into the waste package. To select the type of assembly, change the first term inside the () below to either "BWR" or "PWR" and define the number of assemblies contained in the WP, normally 44 for BWR WPs and 21 for PWR WP's in the "No_Ass" variable. In addition, a correction for the initial assembly MTHM contained in each assembly needs to be performed by defining the base loading, 0.475 for PWR assemblies and 0.200 for BWR assemblies in the "MTHM_Base" variable, and the actual assembly MTHM in the "MTHM_Actual" variable.

$MTHM\_Base := 0.4750$ $No\_Ass := 21$ $MTHM\_Act := .4130$

$Decay := submatrix(PWR, Burnup - 1, Burnup - 1, 1, 3)$ $Power\_Base := submatrix(PWR, Burnup - 1, Burnup - 1, 4, 6)$

$Power\_Base = (2302.47\ \ 733.17\ \ 162.78)$

$Decay = (0.355206\ \ 0.024383\ \ 0.002376)$

$Power\_Correction := \frac{MTHM\_Act}{MTHM\_Base}$

$Half\_Life := \frac{.693}{Decay}$

$Power := Power\_Correction \cdot Power\_Base$

$Half\_Life = (2.0\ \ 28.4\ \ 291.7)$ Years

$Power = (2001.94\ \ 637.47\ \ 141.53)$ watts

Arrays

The following arrays are necessary in order to perform the linear line load and temperature calculations.

$\lambda :=$ for $j \in 0..2$: $\lambda_j \leftarrow Decay_{0,j}$; return λ

$t := 0..1000$

$Q :=$ for $j \in 0..2$: $Q_j \leftarrow Power_{0,j} \cdot No\_Ass \cdot \frac{WP\_Per\_Seg}{Seg\_L}$; return Q watts/meter

$Eff :=$ for $i \in 0..No\_Seg - 1$: $x \leftarrow \frac{Seg\_L}{2} + i \cdot Seg\_L$; $Eff_i \leftarrow \frac{(Eff\_2 - Eff\_1)}{Drift\_Length} \cdot x + Eff\_1$; return Eff

$Line\_Load :=$ for $t \in 0..A2$: $Line\_Load_t \leftarrow 0$; for $j \in 0..2$: $Line\_Load_t \leftarrow Line\_Load_t + Q_j \frac{e^{-\lambda_j \cdot t}}{1000}$; return $Line\_Load$ kW/meter

$WP\_Power :=$ for $t \in 0..A2$: $WP\_Power_t \leftarrow 0$; for $j \in 0..2$: $WP\_Power_t \leftarrow WP\_Power_t + Power_{0,j} \cdot No\_Ass \cdot e^{-\lambda_j \cdot t}$; return $\frac{WP\_Power}{1000}$ kW/WP

Power

The waste package power and linear line load at emplacement, A1, and closure, A2, calculated from array "WP_Power" and "Line_Load" are:

WP power at emplacement $WP\_Power_{A1} = 21.91$ kW Line load at Emplacement $Line\_Load_{A1} = 3.68$ kW/meter

WP power at closure $WP\_Power_{A2} = 4.36$ kW Line load at closure $Line\_Load_{A2} = 0.73$ kW/meter

Temperature Calculation

The equation for calculating the temperature due to a single finite-length decaying line source (or segment) is:

$$v(z,x,t,i,j) := \frac{e^{-\lambda_j\cdot(A1+t)}Q_j}{8\cdot\pi\cdot Krock}\cdot\int_0^t\left(erf\left(\frac{z}{2\cdot\sqrt{\kappa\cdot\theta}}\right)-erf\left(\frac{z-Seg\_L}{2\cdot\sqrt{\kappa\cdot\theta}}\right)\right)\cdot\frac{e^{\lambda_j\cdot\theta}}{\theta}\cdot e^{\frac{-x^2}{4\cdot\kappa\cdot\theta}}\,d\theta$$

The temperature contribution after ventilation shutdown is as follows, the A2 in the leading exponential re-zeros Q_{ij} for ventilation shutdown.

$$va(z,x,t,i,j) := \frac{e^{-\lambda_j\cdot(A2+t)}\cdot Q_j}{8\cdot\pi\cdot Krock}\cdot\int_0^t\left(erf\left(\frac{z}{2\cdot\sqrt{\kappa\cdot\theta}}\right)-erf\left(\frac{z-Seg\_L}{2\cdot\sqrt{\kappa\cdot\theta}}\right)\right)\cdot\frac{e^{\lambda_j\cdot\theta}}{\theta}\cdot e^{\frac{-x^2}{4\cdot\kappa\cdot\theta}}\,d\theta$$

The segment temperature contribution for the i-th segment for the three decaying components is:

```
WPtemp(z,x,t,i) :=
    tsum ← 0.0
    for j ∈ 0..2
        tsum ← tsum + (1. − Eff_i)·v(z − Seg_L·i,x,t,i,j)
        tsum ← tsum + Eff_i·va(z − Seg_L·i,x,t − Vent,i,j)  if t > Vent
    return tsum
```

The temperature contribution from all segments, "No_Seg", and neighbors, "nbors", is:

```
WPSum(z,x,t) :=
    tsum ← 0.
    for i ∈ 0..No_Seg − 1
        tsum ← tsum + WPtemp(z,x,t,i)
    for n ∈ 1..nbors
        x1Loc ← n·Drift_Space − x
        x2Loc ← n·Drift_Space + x
        for i ∈ 0..No_Seg − 1
            tsum ← tsum + WPtemp(z,x1Loc,t,i)
            tsum ← tsum + WPtemp(z,x2Loc,t,i)
    return tzero + tsum
```

The following variables define the radial, "X_Drift" and "X_Pillar", and axial, "Z-Drift" and "Z_Pillar", locations used to calculate the drift wall and mid-pillar maximum temperatures. The location of the drift wall peak temperature is at the mid-point of the drift. The location of the mid-pillar peak temperature is near the end of the drift, based on a series of sensitivity calculations the peak temperature normally occurs at approximately 80% down the length of the drift.

years after emplacement

$X\_Drift := 2.75$ $\quad X\_Pillar := \frac{Drift\_Space}{2}$ $\quad Z\_Pillar := \frac{Drift\_Length}{2}$ $\quad Z\_Drift := Drift\_Length \cdot 0.8$

Radial Distance from Drift Centerline — Axial Distance from Start of Drift

$X\_Drift = 2.75$ $\quad X\_Pillar = 40.50$ $\quad Z\_Pillar = 285.55$ $\quad Z\_Drift = 456.88$

The following loops are used to calculate the drift wall and mid-pillar maximum temperatures and time of maximum temperatures at the locations defined above.

```
Drift_Wall :=  Drift_Max_Time ← 0
               Drift_Max_Temp ← 0
               Drift_Wall ← 0
               for t ∈ Vent.. 200
                   Drift_Wall_t ← WPSum(Z_Drift, X_Drift, t)
                   Drift_Max_Time ← t if Drift_Wall_t > Drift_Max_Temp
                   Drift_Max_Temp ← Drift_Wall_t if Drift_Wall_t > Drift_Max_Temp
               return (Drift_Max_Time)
                      (Drift_Max_Temp)
```

$$\begin{pmatrix} Drift\_Max\_Time \\ Drift\_Max\_Temp \end{pmatrix} := Drift\_Wall$$

Peak Post Closure Drift Wall Temperature $\quad Drift\_Max\_Temp = 180$ °C

Time of Peak Temperature $\quad Drift\_Max\_Time = 97$ years after emplacement

```
Pillar :=  Pillar_Max_Time ← 0
           Pillar_Max_Temp ← 0
           Pillar ← 0
           for t ∈ 350.. 520
               Pillar_t ← WPSum(Z_Pillar, X_Pillar, t)
               Pillar_Max_Time ← t if Pillar_t > Pillar_Max_Temp
               Pillar_Max_Temp ← Pillar_t if Pillar_t > Pillar_Max_Temp
           return (Pillar_Max_Time)
                  (Pillar_Max_Temp)
```

$$\begin{pmatrix} Pillar\_Max\_Time \\ Pillar\_Max\_Temp \end{pmatrix} := Pillar$$

Peak Post Closure Mid-pillar Temperature $\quad Pillar\_Max\_Temp = 112$ °C

Time of Peak Temperature $\quad Pillar\_Max\_Time = 422$

Plot of Temperatures as a Function of Time

The plot below represents the temperature response as a function of time at a location on the drift wall at location "X_Drift" and "Z_Drift" (**red**) and at the mid-pillar "X_Pillar" and "Z-Pillar" (**blue**). The following variables determine the time duration of the plot, t in years, the maximum allowable drift wall temperature y1 and x1, and the maximum allowable mid-pillar temperature, y2 and x2.

$$y1 := \begin{pmatrix} 200 \\ 200 \end{pmatrix} \qquad x1 := \begin{pmatrix} 0 \\ 550 \end{pmatrix} \qquad y2 := \begin{pmatrix} 96 \\ 96 \end{pmatrix} \qquad x2 := \begin{pmatrix} 0 \\ 550 \end{pmatrix}$$

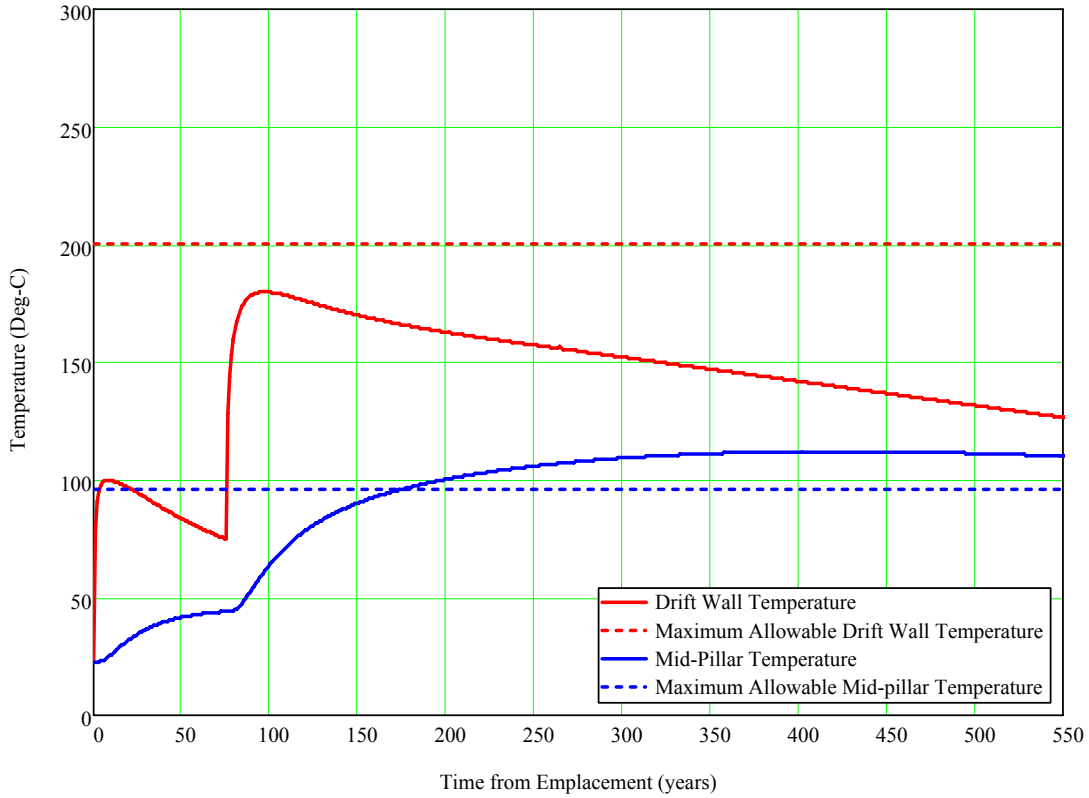

A1 = 5 $\quad$ $Line\_Load_{A1}$ = 3.68 $\quad$ Burnup = 45 $\quad$ Drift_Length = 571 $\quad$ No_WP = 96

A2 = 80 $\quad$ $Line\_Load_{A2}$ = 0.73 $\quad$ MTHM_Act = 0.4130 $\quad$ Drift_Space = 81 $\quad$ WP_Length = 5.85

Vent = 75 $\quad$ No_Seg = 8 $\quad$ WP_Spacing = 0.10

WP_Per_Seg = 12

Eff_1 = 0.90 $\quad$ Z_Drift = 456.88 $\quad$ X_Drift = 2.75

Eff_2 = 0.80 $\quad$ Z_Pillar = 285.55 $\quad$ X_Pillar = 40.50

Plot of Temperatures as a Function of Axial Drift Location

The plot below represents the temperature response as a function of axial location along the drift at drift wall location "X_Drift" at time of peak temperature "Drift_Max_Time" (**red**) and at the mid-pillar location "X_Pillar" at the times of peak temperature "Pillar_Max_Time" (**blue**). The following variables determine the axial extent of the plot, z in meters, the location where the first waste package begins, y1 and the location where the last waste package ends, y2.

$$y1 := \begin{pmatrix} 300 \\ 0 \end{pmatrix} \quad x1 := \begin{pmatrix} 0 \\ 0 \end{pmatrix} \quad y2 := \begin{pmatrix} 300 \\ 0 \end{pmatrix} \quad x2 := \begin{pmatrix} Drift\_Length \\ Drift\_Length \end{pmatrix}$$

$z := -100, -90.. 700$

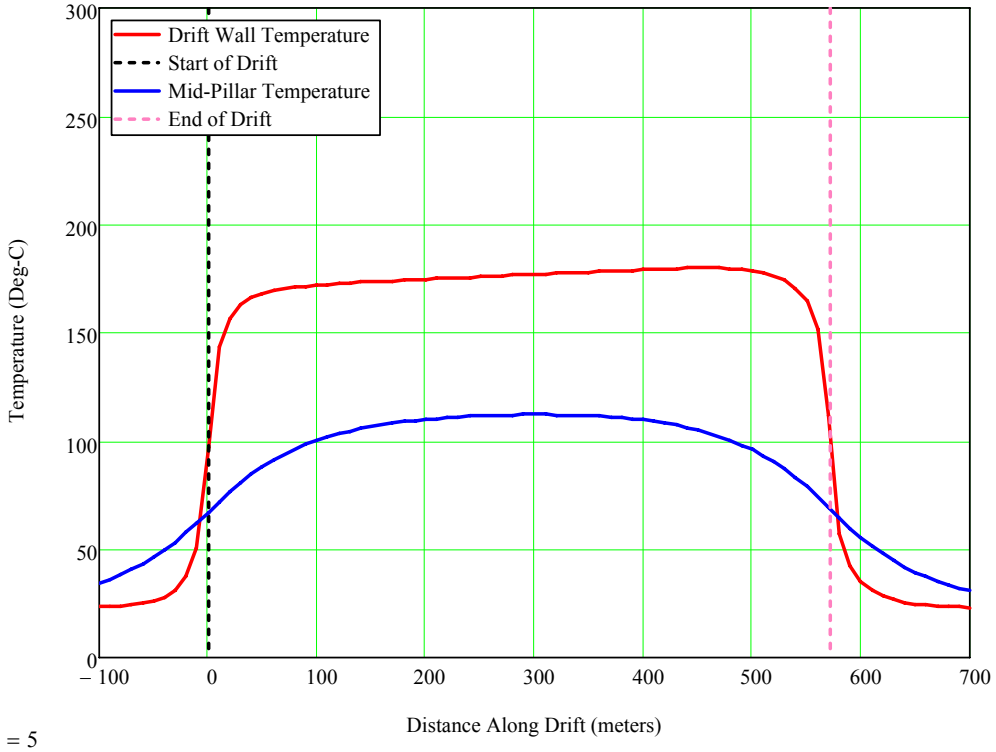

A1 = 5

A2 = 80

Vent = 75

Eff_1 = 0.90

Eff_2 = 0.80

$Line\_Load_{A1} = 3.68$

$Line\_Load_{A2} = 0.73$

Burnup = 45

MTHM_Act = 0.4130

Drift_Length = 571

Drift_Space = 81

No_Seg = 8

No_WP = 96

WP_Length = 5.85

WP_Spacing = 0.10

WP_Per_Seg = 12

Time of drift wall temperature plot (years from emplacement)

Drift_Max_Time = 97

Time of mid-pillar temperature plot (years from emplacement)

Pillar_Max_Time = 422

Appendix F
Sample Calculation Using
Finite-Length Decaying Line Source Seven-Waste-Package Segment

Finite Length Decaying Line Source, 7 package Segment

This file calculates temperatures at locations in the repository plane based on a fixed number of neighboring drifts. Each drift is similar and contains a series of identical end-to-end finite-length decaying line sources, called segments. Each segment contains 7 WPs and each WP has unique characteristics. The WP power is determined from the assembly burnup and age out of reactor and is represented by an equation with three decaying exponential terms. The total WP power of a segment is calculated as a function of time and the three decaying exponential terms associated with the total segment power are determined. During the preclosure phase, forced ventilation provides heat removal with the ventilation efficiency decreasing linearly as the flow moves down the drift.

Independent Variables

The following variables define the conditions for the calculation. The burnup should be an integer between 10 and 70 Gwd/ton.

Initial Rock Temperature tzero := 22.8 °C

Ventilation Efficiency at Start of Drift Eff_1 := 0.90 %

Ventilation Efficiency at End of Drift Eff_2 := 0.80 %

Ventilation Duration Vent := 75 Years

Est_Drift_Length := 600 meters

Drift_Space := 81 meters

WP_Spacing := .1 meters

Number of Neighboring Drifts nbors := 5 Drifts

Decay Variables Calculation

The following files contain the six constants that define the assembly power and decay as a function of burnup for BWR and PWR assemblies. The power values are calculated based on a PWR assembly with an initial loading of 0.475 MTHM/Assembly and a BWR assembly with an initial loading of 0.200 MTHM/Assembly.

BWR :=

PWR :=

The following files contain the six constants that define the canister power and decay.

DOELong :=

DOEShort :=

Age := 5 BU := 45

The following matrix defines the segment characteristics. The first column defines the type of waste package PWR, BWR, DOE Long, or DOE short. The next three columns determine the characteristics of the commercial waste packages (the DOE waste packages are assumed to have the same power and decay characteristics independent of age), The second column is the average burnup, the third column is the average age, and the forth column is the average MTHM. For DOE waste packages the value in the second column should be 10, the third column should be 0, and the forth columns should be 1.

$$Seg := \begin{pmatrix} PWR & BU & Age & .4130 \\ DOELong & 10 & 0 & 1 \\ PWR & BU & Age & .4130 \\ PWR & BU & Age & .4130 \\ DOEShort & 10 & 0 & 1 \\ PWR & BU & Age & .4130 \\ PWR & BU & Age & .4130 \end{pmatrix}$$

The six constants defining the power and decay are selected from the above files based on the type of waste package and, for the commercial waste packages, the assembly burnup defined in matrix "Seg" .

$$\lambda 0 := \text{submatrix}\left(Seg_{0,0}, Seg_{0,1} - 1, Seg_{0,1} - 1, 1, 3\right)$$
$$\lambda 1 := \text{submatrix}\left(Seg_{1,0}, Seg_{1,1} - 1, Seg_{1,1} - 1, 1, 3\right)$$
$$\lambda 2 := \text{submatrix}\left(Seg_{2,0}, Seg_{2,1} - 1, Seg_{2,1} - 1, 1, 3\right)$$
$$\lambda 3 := \text{submatrix}\left(Seg_{3,0}, Seg_{3,1} - 1, Seg_{3,1} - 1, 1, 3\right)$$
$$\lambda 4 := \text{submatrix}\left(Seg_{4,0}, Seg_{4,1} - 1, Seg_{4,1} - 1, 1, 3\right)$$
$$\lambda 5 := \text{submatrix}\left(Seg_{5,0}, Seg_{5,1} - 1, Seg_{5,1} - 1, 1, 3\right)$$
$$\lambda 6 := \text{submatrix}\left(Seg_{6,0}, Seg_{6,1} - 1, Seg_{6,1} - 1, 1, 3\right)$$

$$P0 := \text{submatrix}\left(Seg_{0,0}, Seg_{0,1} - 1, Seg_{0,1} - 1, 4, 6\right)$$
$$P1 := \text{submatrix}\left(Seg_{1,0}, Seg_{1,1} - 1, Seg_{1,1} - 1, 4, 6\right)$$
$$P2 := \text{submatrix}\left(Seg_{2,0}, Seg_{2,1} - 1, Seg_{2,1} - 1, 4, 6\right)$$
$$P3 := \text{submatrix}\left(Seg_{3,0}, Seg_{3,1} - 1, Seg_{3,1} - 1, 4, 6\right)$$
$$P4 := \text{submatrix}\left(Seg_{4,0}, Seg_{4,1} - 1, Seg_{4,1} - 1, 4, 6\right)$$
$$P5 := \text{submatrix}\left(Seg_{5,0}, Seg_{5,1} - 1, Seg_{5,1} - 1, 4, 6\right)$$
$$P6 := \text{submatrix}\left(Seg_{6,0}, Seg_{6,1} - 1, Seg_{6,1} - 1, 4, 6\right)$$

$$\lambda := \text{stack}\left(\lambda 0, \lambda 1, \lambda 2, \lambda 3, \lambda 4, \lambda 5, \lambda 6\right)$$

$$P := \text{stack}\left(P0, P1, P2, P3, P4, P5, P6\right)$$

$$\lambda = \begin{pmatrix} 0.355206 & 0.024383 & 0.002376 \\ 0.540572 & 0.023333 & 0.000000 \\ 0.355206 & 0.024383 & 0.002376 \\ 0.355206 & 0.024383 & 0.002376 \\ 0.196721 & 0.020202 & 0.000000 \\ 0.355206 & 0.024383 & 0.002376 \\ 0.355206 & 0.024383 & 0.002376 \end{pmatrix}$$

$$P = \begin{pmatrix} 2302.5 & 733.2 & 162.8 \\ 5.6 & 401.4 & 0.0 \\ 2302.5 & 733.2 & 162.8 \\ 2302.5 & 733.2 & 162.8 \\ 541.5 & 2386.2 & 0.0 \\ 2302.5 & 733.2 & 162.8 \\ 2302.5 & 733.2 & 162.8 \end{pmatrix}$$

The next loop defines the base case MTHM per assembly for commercial waste packages, the number of assemblies per commercial waste package, and the length of the waste package.

```
WP_Data := | WP_Data ← 0
           | for i ∈ 0..6
           |   WP_Data[i,0] ← 0.475 if Seg[i,0] = PWR
           |   WP_Data[i,1] ← 21 if Seg[i,0] = PWR
           |   WP_Data[i,2] ← 5.85 if Seg[i,0] = PWR
           |   WP_Data[i,0] ← 0.200 if Seg[i,0] = BWR
           |   WP_Data[i,1] ← 44 if Seg[i,0] = BWR
           |   WP_Data[i,2] ← 5.85 if Seg[i,0] = BWR
           |   WP_Data[i,0] ← 1 if Seg[i,0] = DOEShort
           |   WP_Data[i,1] ← 1 if Seg[i,0] = DOEShort
           |   WP_Data[i,2] ← 3.697 if Seg[i,0] = DOEShort
           |   WP_Data[i,0] ← 1 if Seg[i,0] = DOELong
           |   WP_Data[i,1] ← 1 if Seg[i,0] = DOELong
           |   WP_Data[i,2] ← 5.220 if Seg[i,0] = DOELong
           | return WP_Data
```

$$WP\_Data = \begin{pmatrix} 0.4750 & 21.0000 & 5.8500 \\ 1.0000 & 1.0000 & 5.2200 \\ 0.4750 & 21.0000 & 5.8500 \\ 0.4750 & 21.0000 & 5.8500 \\ 1.0000 & 1.0000 & 3.6970 \\ 0.4750 & 21.0000 & 5.8500 \\ 0.4750 & 21.0000 & 5.8500 \end{pmatrix}$$

Individual waste package power at time of emplacement, "WP_Individual" in watts/WP, is calculated in the next loop.

```
WP_Individual := | for i ∈ 0..6
                 |   WP_Individual[i] ← 0
                 |   for j ∈ 0..2
                 |     WP_Individual[i] ← WP_Individual[i] + WP_Data[i,1] P[i,j] · (Seg[i,3] / WP_Data[i,0]) · e^(−λ[i,j]·(Seg[,2]))
                 | return WP_Individual
```

$$WP\_Individual = \begin{pmatrix} 21905.4 \\ 407.0 \\ 21905.4 \\ 21905.4 \\ 2927.7 \\ 21905.4 \\ 21905.4 \end{pmatrix} \text{ watts}$$

Segment Power and Decay Constants

The total segment power, "Power" in watts, is calculated in the next loops where "t" represents the time from emplacement

$$t := 0..1000$$

$$\text{Power} := \left| \begin{array}{l} \text{for } t \in 0..500 \\ \quad \left| \begin{array}{l} \text{Power}_t \leftarrow 0 \\ \text{for } i \in 0..6 \\ \quad \text{for } j \in 0..2 \\ \quad\quad \text{Power}_t \leftarrow \text{Power}_t + \text{WP\_Data}_{i,1}\, P_{i,j} \cdot \dfrac{\text{Seg}_{i,3}}{\text{WP\_Data}_{i,0}} \cdot e^{-\lambda_{i,j} \cdot (\text{Seg}_{,2} + t)} \end{array} \right. \\ \text{return Power} \end{array} \right.$$

The loop "Power" calculates the total segment power as a function of time. The following section determines the six power and decay constants that define the total segment power. The six "Guess values" are required by MathCad to solve the six equations in six unknowns provided below. These six equations represent the segment power as the summation of three exponential terms at assembly ages of 0, 25, 50, 100, 200 and 300 years from emplacement.

Guess values: $P1 := 7000$ $P2 := 6500$ $P3 := 17000$ $\lambda 1 := .14$ $\lambda 2 := .02$ $\lambda 3 := .002$

Given

$$P1 \cdot e^{-0 \cdot \lambda 1} + P2 \cdot e^{-0 \cdot \lambda 2} + P3 \cdot e^{-0 \cdot \lambda 3} = \text{Power}_0$$

$$P1 \cdot e^{-25 \cdot \lambda 1} + P2 \cdot e^{-25 \cdot \lambda 2} + P3 \cdot e^{-25 \cdot \lambda 3} = \text{Power}_{25}$$

$$P1 \cdot e^{-50 \cdot \lambda 1} + P2 \cdot e^{-50 \cdot \lambda 2} + P3 \cdot e^{-50 \cdot \lambda 3} = \text{Power}_{50}$$

$$P1 \cdot e^{-100 \cdot \lambda 1} + P2 \cdot e^{-100 \cdot \lambda 2} + P3 \cdot e^{-100 \cdot \lambda 3} = \text{Power}_{100}$$

$$P1 \cdot e^{-200 \cdot \lambda 1} + P2 \cdot e^{-200 \cdot \lambda 2} + P3 \cdot e^{-200 \cdot \lambda 3} = \text{Power}_{200}$$

$$P1 \cdot e^{-500 \cdot \lambda 1} + P2 \cdot e^{-500 \cdot \lambda 2} + P3 \cdot e^{-500 \cdot \lambda 3} = \text{Power}_{500}$$

$$\begin{pmatrix} \text{P1\_Value} \\ \text{P2\_Value} \\ \text{P3\_Value} \\ \lambda 1\text{\_Value} \\ \lambda 2\text{\_Value} \\ \lambda 3\text{\_Value} \end{pmatrix} := \text{Find}(P1, P2, P3, \lambda 1, \lambda 2, \lambda 3)$$

MathCad calculated the following values for the six constants:

$\lambda 1\_Value = 0.2910$

$\lambda 2\_Value = 0.0242$

$\lambda 3\_Value = 0.0024$

$P1\_Value = 36217.34$

$P2\_Value = 61943.63$

$P3\_Value = 14700.5535$

$$\lambda := \begin{pmatrix} \lambda 1\_Value \\ \lambda 2\_Value \\ \lambda 3\_Value \end{pmatrix} \qquad Half\_Life := \frac{.693}{\lambda} \qquad P := \begin{pmatrix} P1\_Value \\ P2\_Value \\ P3\_Value \end{pmatrix}$$

$$Half\_Life = \begin{pmatrix} 2.4 \\ 28.7 \\ 291.4 \end{pmatrix} \qquad \lambda = \begin{pmatrix} 0.2910 \\ 0.0242 \\ 0.0024 \end{pmatrix} \qquad P = \begin{pmatrix} 36217.3449 \\ 61943.6302 \\ 14700.5535 \end{pmatrix}$$

Emplacement Drift Parameters

The following calculation determines the exact length of the drift and the number of waste packages per drift based on the assumptions provided above.

$$Seg\_L := \left| \begin{array}{l} Seg\_L \leftarrow 0 \\ \text{for } i \in 0..6 \\ \quad Seg\_L \leftarrow Seg\_L + WP\_Data_{i,2} + WP\_Spacing \end{array} \right.$$

$$No\_Seg := round\left(\frac{Est\_Drift\_Length}{Seg\_L}\right) \qquad Drift\_Length := No\_Seg \cdot Seg\_L \qquad No\_WP := No\_Seg \cdot 7$$

Actual Drift Length $Drift\_Length = 583.01$ meters Number of WP per Drift $No\_WP = 105$ WP per Drift

Number of Segments per Drift $No\_Seg = 15$ Segments Segment Length $Seg\_L = 38.87$ meters

The next expression converts the power in watts to linear power in watts/meter

$$Q := \frac{P}{Seg\_L}$$

$$Q = \begin{pmatrix} 931.8276 \\ 1593.7333 \\ 378.2271 \end{pmatrix} \text{ wats/meter}$$

Ventilation Efficiency

The following loop calculates the ventilation efficiency for each segment based on the efficiency at the start of the drift of Eff_1 and the efficiency at the end of the drift Eff_2.

$Eff\_1 = 0.9000$ $Eff\_2 = 0.8000$

$$\begin{array}{l} Eff := \left| \begin{array}{l} \text{for } n \in 0..No\_Seg - 1 \\ \quad \left| \begin{array}{l} x \leftarrow \dfrac{Seg\_L}{2} + n \cdot Seg\_L \\ Eff_n \leftarrow \dfrac{(Eff\_2 - Eff\_1)}{Drift\_Length} \cdot x + Eff\_1 \end{array} \right. \\ \text{return } Eff \end{array} \right. \end{array}$$

Power

The next loops calculates the average waste package power, "WP_Power", and linear line load, "Line_Load", as a function of time from emplacement.

$$\begin{array}{l} WP\_Power := \left| \begin{array}{l} \text{for } t \in 0..200 \\ \quad \left| \begin{array}{l} WP\_Power_t \leftarrow 0 \\ \text{for } j \in 0..2 \\ \quad WP\_Power_t \leftarrow WP\_Power_t + P_j \cdot e^{-\lambda_j \cdot t} \end{array} \right. \\ \text{return } \dfrac{WP\_Power}{7} \end{array} \right. \end{array}$$

$$\begin{array}{l} Line\_Load := \left| \begin{array}{l} \text{for } t \in 0..Vent + 100 \\ \quad \left| \begin{array}{l} Line\_Load_t \leftarrow 0 \\ \text{for } j \in 0..2 \\ \quad Line\_Load_t \leftarrow Line\_Load_t + Q_j \cdot \dfrac{e^{-\lambda_j \cdot t}}{1000} \end{array} \right. \\ \text{return } Line\_Load \end{array} \right. \end{array}$$

The Average waste package power and linear line load at emplacement, time = 0, and closure, time = vent, calculated from array "WP_Power" and "Line_Load" are:

WP power at emplacement $WP\_Power_0 = 16123.1$ Watts Line load at Emplacement $Line\_Load_0 = 2.90$ kW/meter

WP power at closure $WP\_Power_{Vent} = 3200.1$ Watts Line load at closure $Line\_Load_{Vent} = 0.58$ kW/meter

Constants

The following constants are required for the calculation.

$Krock := 1.83$ watt/meter - ^oC $\rho := 2097$ kg/meter^3 $Cp := 1119.0$ joules/kg - ^oC

$$\kappa := \frac{Krock \cdot 3600\,24 \cdot 365}{\rho \cdot Cp} \quad \text{meter}^2\text{/year}$$

Temperature Calculation

The equation for calculating the temperature due to a single finite-length decaying line source (or segment) is:

$$v(z,x,t,j) := \frac{e^{-\lambda_j \cdot t} \cdot Q_j}{8 \cdot \pi \cdot Krock} \cdot \int_0^t \left(erf\left(\frac{z}{2\cdot\sqrt{\kappa \cdot \theta}}\right) - erf\left(\frac{z - Seg\_L}{2\cdot\sqrt{\kappa \cdot \theta}}\right)\right) \cdot \frac{e^{\lambda_j \cdot \theta}}{\theta} \cdot e^{\frac{-x^2}{4\cdot\kappa\cdot\theta}} \, d\theta$$

The temperature contribution after ventilation shutdown is as follows, the A2 in the leading exponential re-zeros Q_{ij} for ventilation shutdown.

$$va(z,x,t,j) := \frac{e^{-\lambda_j \cdot (Vent+t)} \cdot Q_j}{8 \cdot \pi \cdot Krock} \cdot \int_0^t \left(erf\left(\frac{z}{2\cdot\sqrt{\kappa \cdot \theta}}\right) - erf\left(\frac{z - Seg\_L}{2\cdot\sqrt{\kappa \cdot \theta}}\right)\right) \cdot \frac{e^{\lambda_j \cdot \theta}}{\theta} \cdot e^{\frac{-x^2}{4\cdot\kappa\cdot\theta}} \, d\theta$$

The segment temperature contribution for the n-th segment for the three decaying components is:

```
WPtemp(z,x,t,n) := | tsum ← 0.0
                   | for j ∈ 0..2
                   |     tsum ← tsum + (1. − Eff_n)·v(z − Seg_L·n,x,t,j)
                   |     tsum ← tsum + Eff_n·va(z − Seg_L·n,x,t − Vent,j)  if t > Vent
                   | return tsum
```

The temperature contribution from all segments, "No_Seg", and neighbors, "nbors", is:

```
WPSum(z,x,t) := | tsum ← 0.
                | for n ∈ 0..No_Seg − 1
                |   tsum ← tsum + WPtemp(z,x,t,n)
                | for m ∈ 1..nbors
                |     x1Loc ← m·Drift_Space − x
                |     x2Loc ← m·Drift_Space + x
                |     for n ∈ 0..No_Seg − 1
                |         tsum ← tsum + WPtemp(z,x1Loc,t,n)
                |         tsum ← tsum + WPtemp(z,x2Loc,t,n)
                | return tzero + tsum
```

The following variables define the radial, "X_Drift" and "X_Pillar", and axial, "Z-Drift" and "Z_Pillar", locations used to calculate the drift wall and mid-pillar maximum temperatures. The location of the drift wall peak temperature is at the mid-point of the drift. The location of the mid-pillar peak temperature is near the end of the drift, based on a series of sensitivity calculations the peak temperature normally occurs at approximately 80% down the length of the drift.

$X\_Drift := 2.75$ $\quad X\_Pillar := \frac{Drift\_Space}{2}$ $\quad Z\_Pillar := \frac{Drift\_Length}{2}$ $\quad Z\_Drift := Drift\_Length \cdot 0.8$

Radial Distance from Drift Centerline — Axial Distance from Start of Drift

$X\_Drift = 2.75$ $\quad X\_Pillar = 40.50$ $\quad Z\_Drift = 466.40$ $\quad Z\_Pillar = 291.50$

The following loops are used to calculate the drift wall and mid-pillar maximum temperatures and time of maximum temperatures at the locations defined above.

```
Pillar := | Pillar_Max_Time ← 0
          | Pillar_Max_Temp ← 0
          | Pillar ← 0
          | for t ∈ 350..450
          |     Pillar_t ← WPSum(Z_Pillar, X_Pillar, t)
          |     Pillar_Max_Time ← t  if Pillar_t > Pillar_Max_Temp
          |     Pillar_Max_Temp ← Pillar_t  if Pillar_t > Pillar_Max_Temp
          | return (Pillar_Max_Time)
          |        (Pillar_Max_Temp)
```

$$\begin{pmatrix} Pillar\_Max\_Time \\ Pillar\_Max\_Temp \end{pmatrix} := Pillar$$

Peak Post Closure Mid-pillar Temperature $\quad Pillar\_Max\_Temp = 92$ $\quad ^oC$

Time of Peak Temperature $\quad Pillar\_Max\_Time = 420$ $\quad$ years after emplacement

```
Drift_Wall := | Drift_Max_Time ← 0
              | Drift_Max_Temp ← 0
              | Drift_Wall ← 0
              | for t ∈ Vent..225
              |     Drift_Wall_t ← WPSum(Z_Drift, X_Drift, t)
              |     Drift_Max_Time ← t  if Drift_Wall_t > Drift_Max_Temp
              |     Drift_Max_Temp ← Drift_Wall_t  if Drift_Wall_t > Drift_Max_Temp
              | return (Drift_Max_Time)
              |        (Drift_Max_Temp)
```

$$\begin{pmatrix} Drift\_Max\_Time \\ Drift\_Max\_Temp \end{pmatrix} := Drift\_Wall$$

Peak Post Closure Drift Wall Temperature $\quad Drift\_Max\_Temp = 146$ $\quad ^oC$

Time of Peak Temperature $\quad Drift\_Max\_Time = 96$ $\quad$ years after emplacement

Plot of Temperatures as a Function of Time

The plot below represents the temperature response as a function of time at a location on the drift wall at location "X_Drift" and "Z_Drift" (**red**) and at the mid-pillar "X_Pillar" and "Z-Pillar" (**blue**). The following variables determine the time duration of the plot, t in years, the maximum allowable drift wall temperature y1 and x1, and the maximum allowable mid-pillar temperature, y2 and x2.

$t := 0, 2 .. 550$ $\quad y1 := \begin{pmatrix} 200 \\ 200 \end{pmatrix}$ $\quad x1 := \begin{pmatrix} 0 \\ 550 \end{pmatrix}$ $\quad y2 := \begin{pmatrix} 96 \\ 96 \end{pmatrix}$ $\quad x2 := \begin{pmatrix} 0 \\ 550 \end{pmatrix}$

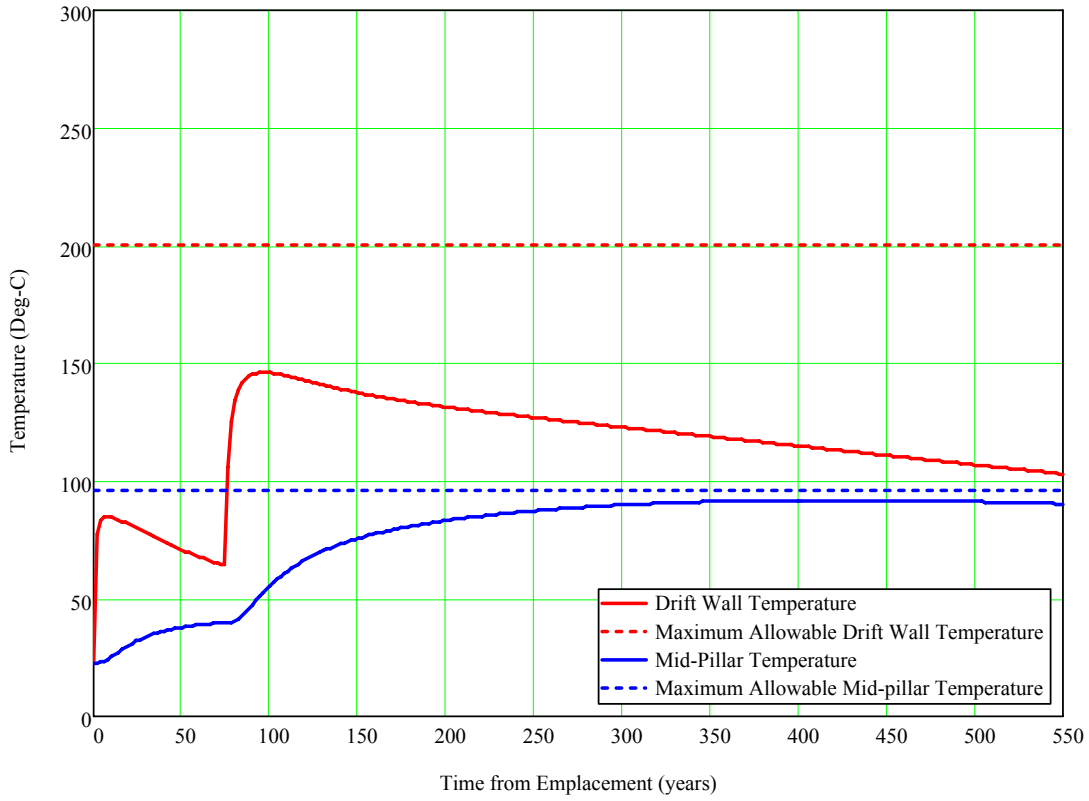

$Line\_Load_0 = 2.90$

$Line\_Load_{Vent} = 0.58$

$Vent = 75$

$Eff\_1 = 0.90$

$Eff\_2 = 0.80$

$Z\_Drift = 466.40$

$Z\_Pillar = 291.50$

$X\_Drift = 2.75$

$X\_Pillar = 40.50$

$Drift\_Length = 583$

$Drift\_Space = 81$

$WP\_Spacing = 0.10$

$No\_WP = 105$

$No\_Seg = 15$

Plot of Temperatures as a Function of Axial Drift Location

The plot below represents the temperature response as a function of axial location along the drift at drift wall location "X_Drift" at time of peak temperature "Drift_Max_Time" (**red**) and at the mid-pillar location "X_Pillar" at the times of peak temperature "Pillar_Max_Time" (**blue**). The following variables determine the axial extent of the plot, z in meters, the location where the first waste package begins, y1 and the location where the last waste package ends, y2.

$$y1 := \begin{pmatrix} 300 \\ 0 \end{pmatrix} \qquad x1 := \begin{pmatrix} 0 \\ 0 \end{pmatrix} \qquad y2 := \begin{pmatrix} 300 \\ 0 \end{pmatrix} \qquad x2 := \begin{pmatrix} Drift\_Length \\ Drift\_Length \end{pmatrix}$$

$z := -100, -90.. 700$

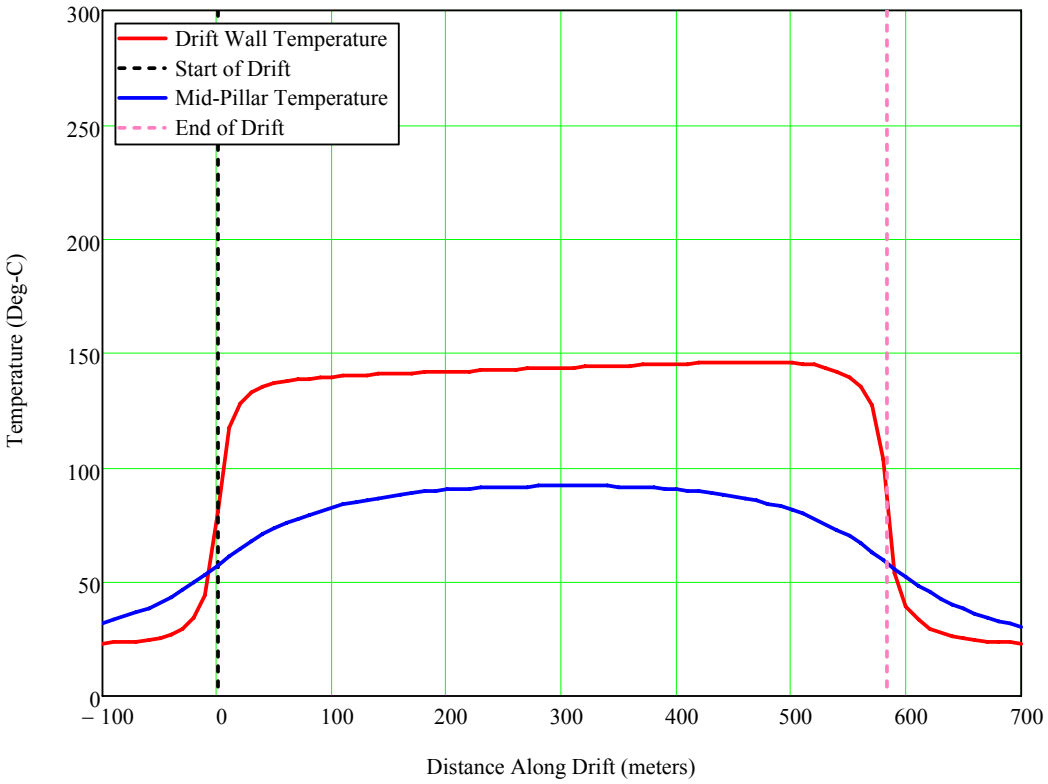

$Line\_Load_0 = 2.90$

$Line\_Load_{Vent} = 0.58$

$Vent = 75$

$Eff\_1 = 0.90$

$Eff\_2 = 0.80$

$Z\_Drift = 466.40$

$Z\_Pillar = 291.50$

$X\_Drift = 2.75$

$X\_Pillar = 40.50$

$Drift\_Length = 583$

$Drift\_Space = 81$

$WP\_Spacing = 0.10$

$No\_WP = 105$

$No\_Seg = 15$

Time of drift wall temperature plot (years from emplacement)

$Drift\_Max\_Time = 96$

Time of mid-pillar temperature plot (years from emplacement)

$Pillar\_Max\_Time = 420$

Appendix G
Sample Calculation using
Infinite Length Decaying Line Source

Infinite Length Cylinder Calculation

This file calculates the drift-wall temperature due to an average line load for time frames less than approximately 15 years. The line source strength, watts/meter, is for an infinite-length drift. Ventilation is taken into account with two ventilation efficiencies, the first one for normal operation, "Eff_F", and the second one for natural ventilation after forced ventilation failure, "Eff_N". The second ventilation efficiency can be set to 0. There are no neighboring drifts. This short-term approximation is valid because for these short time frames a neighbor will not be "felt." The mathematics are based on the temperature due to a decaying flux on the wall in the infinite region bounded internally by a cylinder.

Independent Variables

The following variables define the conditions for the calculation. The burnup should be an integer between 10 and 70 Gwd/ton.

Initial Rock Temperature tzero := 22.8 ^{o}C

Ventilation efficiency with forced ventilation Eff_F := 0.9 %

Ventilation efficiency with natural ventilation Eff_N := 0.0 %

Age at Emplacement A1 := 16 Years Out of Reactor

WP_Length := 5.85 Meters

WP_Spacing := 0.7 Meters

Drift_Rad := 2.75 Meters

Burnup := 48 GWd/ton

Constants

The following constants are required for the calculation.

Krock := 1.83 watt/meter - ^{o}C

ρ := 2097 kg/meter^3

Cp := 1119.0 joules/kg - ^{o}C

$$\kappa := \frac{Krock \cdot 3600 \cdot 24}{\rho \cdot Cp} \quad \text{meter}^2\text{/day}$$

κ = 0.0674

Decay Variables Calculation

The following files contain the six constants that define the assembly power and decay as a function of burnup for BWR and PWR assemblies. The power values are calculated based on a PWR assembly with an initial loading of 0.475 MTHM/Assembly and a BWR assembly with an initial loading of 0.200 MTHM/Assembly.

BWR :=

PWR :=

The six constants are selected from the above files based on the burnup defined above and whether BWR or PWR assemblies are loaded into the waste package. To select the type of assembly, change the first term inside the () below to either "BWR" or "PWR" and define the number of assemblies contained in the WP, normally 44 for BWR WPs and 21 for PWR WP's in the "No_Ass" variable. In addition, a correction for the initial assembly MTHM contained in each assembly needs to be performed by defining the base loading, 0.475 for PWR assemblies and 0.200 for BWR assemblies in the "MTHM_Base" variable, and the actual assembly MTHM in the "MTHM_Actual" variable.

MTHM_Base := 0.475 MTHM_Act := 0.413 No_Ass := 21

Decay := submatrix(PWR, Burnup − 1, Burnup − 1, 1, 3) Power_Base := submatrix(PWR, Burnup − 1, Burnup − 1, 4, 6)

Decay = (0.351243 0.024561 0.002473) $Years^{-1}$ Power_Base = (2431.86 791.50 177.66) watts

$$Half\_Life := \frac{.693}{Decay}$$

$$Power\_Correction := \frac{MTHM\_Act}{MTHM\_Base}$$

$$Power := Power\_Correction \cdot Power\_Base$$

Half_Life = (2.0 28.2 280.2) Years Power = (2114.44 688.19 154.47) watts

Arrays

The following arrays are necessary in order to perform the linear line load and temperature calculations.

T_Max := 500(

t := 0.. T_Max

$$\lambda := \left| \begin{array}{l} \text{for } j \in 0..2 \\ \quad \lambda_j \leftarrow Decay_{0,j} \\ \text{return } \lambda \end{array} \right.$$

$$Q := \left| \begin{array}{l} \text{for } j \in 0..2 \\ \quad Q_j \leftarrow Power_{0,j} \cdot \frac{No\_Ass \cdot e^{-\lambda_j \cdot A1}}{WP\_Length + WP\_Spacing} \\ \text{return } Q \end{array} \right.$$

$$Line\_Load\_Emplace := \left| \begin{array}{l} Line\_Load\_Emplace \leftarrow 0. \\ \text{for } j \in 0..2 \\ \quad Line\_Load\_Emplace \leftarrow Line\_Load\_Emplace + Q_j \\ \text{return } \frac{Line\_Load\_Emplace}{1000} \end{array} \right.$$

Line load at Emplacement Line_Load_Emplace = 1.99 kW/meter

Q and λ need to be corrected for unit consistency.

$$Q := \frac{3600 \cdot 24 \cdot Q}{2 \cdot \pi \cdot Drift\_Rad}$$

$$\lambda := \frac{\lambda}{365}$$

$$\lambda = \begin{pmatrix} 0.00096231 \\ 0.00006729 \\ 0.000006775 \end{pmatrix} \quad Days^{-1}$$

$$Q = \begin{pmatrix} 122881.88 \\ 7447649.47 \\ 2380351.6 \end{pmatrix} \quad joules/meter^2\text{-}day$$

^{o}C

The temperature for the infinite region bounded internally by a cylinder of radius "Drift_Rad" with a decaying wall flux is:

$$v(r,t,j) := \frac{2\cdot Q_j}{\pi\cdot\rho\cdot Cp}\cdot\int_0^{\infty}\frac{e^{-\lambda_j\cdot t}-e^{-\kappa\cdot u^2\cdot t}}{\lambda_j-\kappa\cdot u^2}\cdot\left(\frac{J0(u\cdot r)\,Yl(u\cdot Drift\_Rad)-Y0(u\cdot r)\cdot J1(u\cdot Drift\_Rad)}{J1(u\cdot Drift\_Rad)^2+Yl(u\cdot Drift\_Rad)^2}\right)du$$

Units in front of the integral are Joules/(meter^2-day) divided by (kg/m^3)*(Joules/kg-^{o}C) which yields (meter ^{o}C)/day. The units for the integral are day/m from the in the denominator and du. Therefore, the units are degrees C. The "time" of this equation is determined by the units of, which in this case is days. Calculate the temperature as a function of time, t, with a forced ventilation efficiency "Eff_F" as follows.

```
Wall_Temp := | for t ∈ 0.. T_Max
             |   Wall_Temp_t ← tzero
             |   for j ∈ 0.. 2
             |     Wall_Temp_t ← Wall_Temp_t + (1 − Eff_F)·v(Drift_Rad, t, j)
             | return Wall_Temp
```

```
Wall(t) := | Wall_Temp ← tzero
           | for j ∈ 0.. 2
           |   Wall_Temp ← Wall_Temp + (1 − Eff_F)·v(Drift_Rad, t, j)
           | return Wall_Temp
```

```
Max_Wall := | Wall_Max_Time ← 0
            | Wall_Max_Temp ← 0
            | for t ∈ 0.. T_Max
            |   Wall_Max_Time ← t if Wall_Temp_t > Wall_Max_Temp
            |   Wall_Max_Temp ← Wall_Temp_t if Wall_Temp_t > Wall_Max_Temp
            | return (Wall_Max_Time, Wall_Max_Temp)
```

$$\begin{pmatrix}Wall\_Max\_Time\\Wall\_Max\_Temp\end{pmatrix} := Max\_Wall$$

$$Wall\_Max\_Years := \frac{Wall\_Max\_Time}{365}$$

Wall_Max_Time = 4996 Days from Emplacement

Wall_Max_Years = 13.69 Years from Emplacement

Wall_Max_Temp = 55.33

Below is a plot of drift wall temperature as a function of time for the normal case.

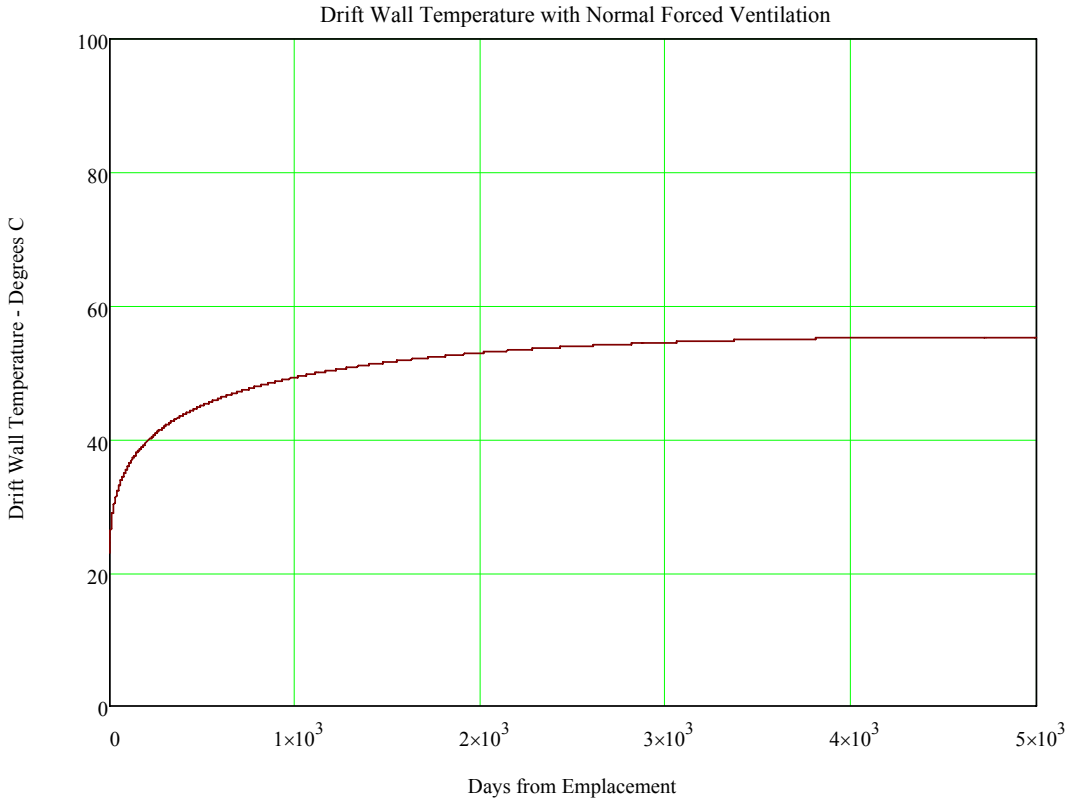

Age at emplacement (years) A1 = 16

Line load at emplacement (Kw/meter) Line_Load_Emplace = 1.99

Forced ventilation efficiency Eff_F = 0.9

WP_Spacing = 0.7

WP_Length = 5.85

Drift_Rad = 2.75

Burnup = 48

The temperature after ventilation is lost has the leading Q rezeroed according to the ventilation duration, "vt",:

$$va(r,vt,t,j) := \frac{2\cdot Q_j\cdot e^{-\lambda_j\cdot vt}}{\pi\cdot\rho\cdot Cp}\cdot\int_0^{\infty}\frac{e^{-\lambda_j\cdot t}-e^{-\kappa\cdot u^2\cdot t}}{\lambda_j-\kappa\cdot u^2}\cdot\left(\frac{J0(u\cdot r)\,Y1(u\cdot Drift\_Rad)-Y0(u\cdot r)\cdot J1(u\cdot Drift\_Rad)}{J1(u\cdot Drift\_Rad)^2+Y1(u\cdot Drift\_Rad)^2}\right)du$$

The calculation of temperature as a function of time for a loss of ventilation event at rock location "Drift_Rad", with a specified preclosure forced ventilation duration," vt", forced ventilation efficiency "Eff_F", natural ventilation efficiency, "Eff_N",is as follows.

```
Twall(Drift_Rad, vt, effcy, t) := | sum ← 0.
                                  | for j ∈ 0..2
                                  |     sum ← sum + (1 − Eff_F)·v(Drift_Rad, t, j)
                                  |     sum ← sum + (Eff_F − Eff_N)·va(Drift_Rad, vt, t − vt, j)  if t > vt
                                  | return sum + tzero
```

Drift wall temperature 30 days after loss of ventilation $Twall(Drift\_Rad, 30, Eff\_F, 60) = 108.11$ °C

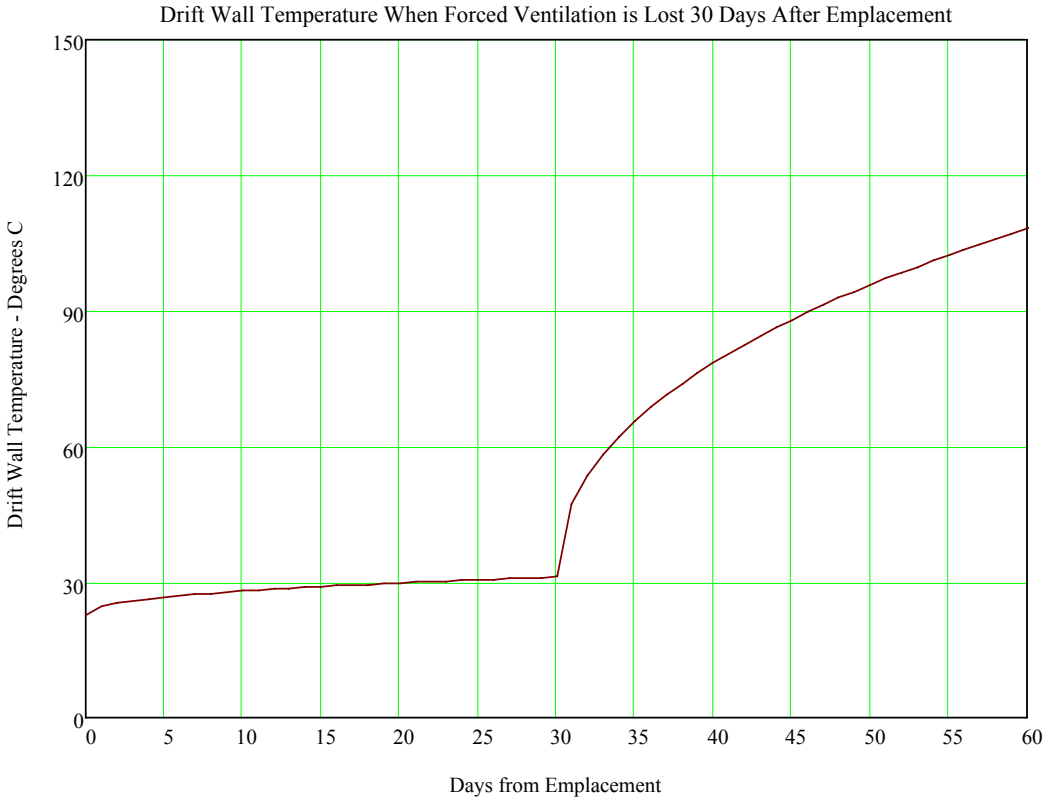

The following function calculates the number of years required to reach 200 ^{o}C drift wall temperature for several times times of ventilation loss. The matrix "Max_Time" provides the results of this calculation. The first column is the case number, the second column is the number of days from emplacement that the forced ventilation is lost, and the third column is the number of days required to reach 200 ^{o}C.

```
Time_to_200 := | Max_Time ← 0.
               | Drift_Max_Temp ← 200
               | Drift_Wall ← 0
               | Number ← 0
               | for vt ∈ 100, 200.. 1400
               |   for t ∈ 0.. T_Max
               |     Drift_Wall ← Twall(Drift_Rad, vt, Eff_N, t)
               |     Time_to_200[Number, 0] ← Number
               |     Time_to_200[Number, 1] ← vt   if Drift_Wall > Drift_Max_Temp
               |     Time_to_200[Number, 2] ← t − vt   if Drift_Wall > Drift_Max_Temp
               |     Number ← Number + 1   if Drift_Wall > Drift_Max_Temp
               |     break   if Drift_Wall > Drift_Max_Temp
               | return Time_to_200
```

$$\text{Time\_to\_200} = \begin{pmatrix} 0 & 100 & 229 \\ 1 & 200 & 226 \\ 2 & 300 & 225 \\ 3 & 400 & 224 \\ 4 & 500 & 224 \\ 5 & 600 & 224 \\ 6 & 700 & 225 \\ 7 & 800 & 226 \\ 8 & 900 & 228 \\ 9 & 1000 & 229 \\ 10 & 1100 & 231 \\ 11 & 1200 & 233 \\ 12 & 1300 & 235 \\ 13 & 1400 & 238 \end{pmatrix}$$

From the "Time_to_200" matrix it can be seen that the most limiting case (i.e. the shortest time to reach 200 ^{o}C) is between 300 and 400 days from emplacement.

The graph below shows the drift wall temperature as a function of time for the above scenarios.

$$x1 := \begin{pmatrix} 0 \\ 5000 \end{pmatrix} \qquad y1 := \begin{pmatrix} 200 \\ 200 \end{pmatrix}$$

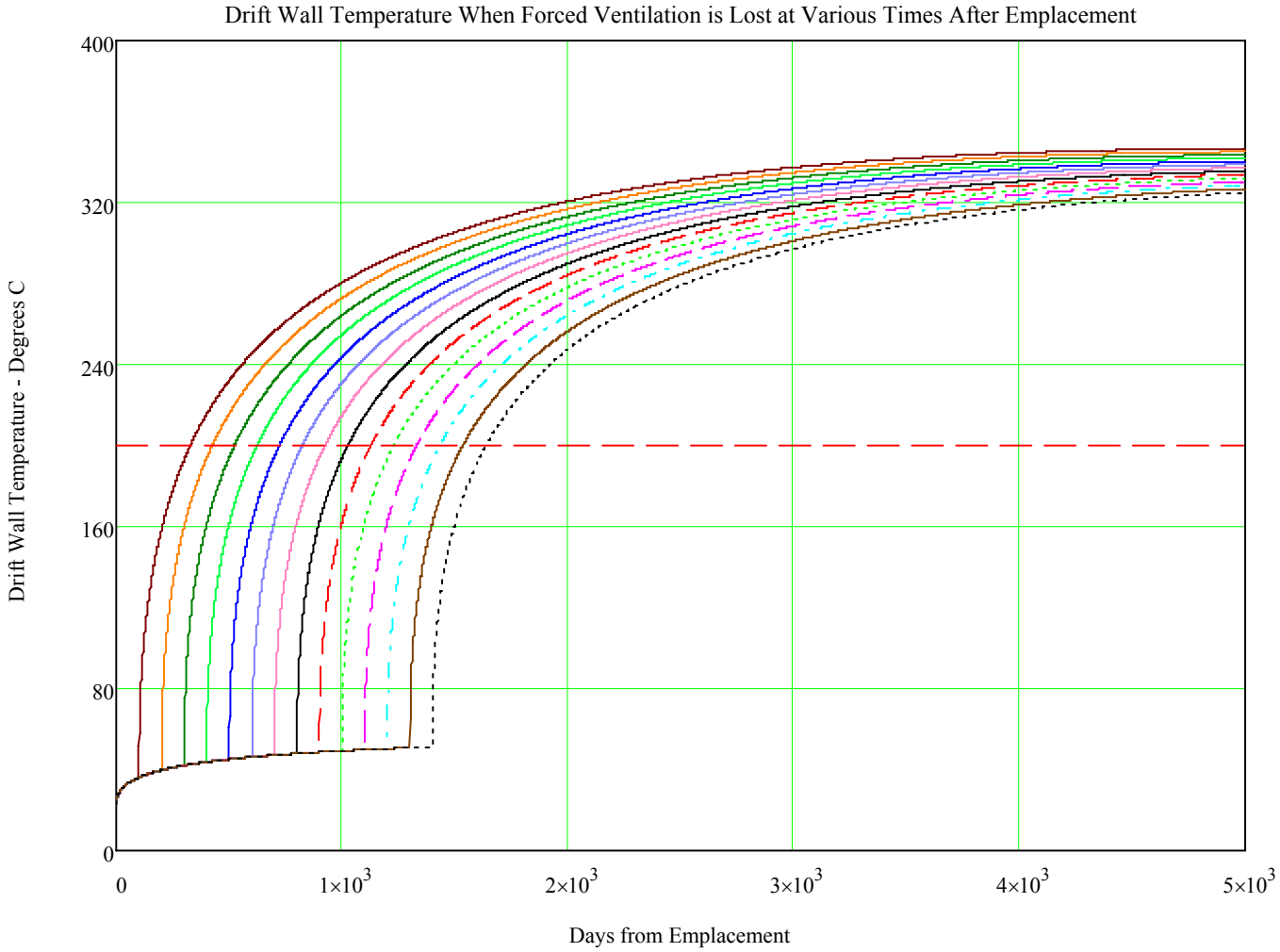

Appendix H
Sample Calculation Using
Radiant-Heat Transfer Between Two Concentric Cylinders

Finite Length Decaying Line Source, 7 package Segment

This file calculates temperatures at locations in the repository plane based on a fixed number of neighboring drifts. Each drift is similar and contains a series of identical end-to-end finite-length decaying line sources, called segments. Each segment contains 7 WPs and each WP has unique characteristics. The WP power is determined from the assembly burnup and age out of reactor and is represented by an equation with three decaying exponential terms. The total WP power of a segment is calculated as a function of time and the three decaying exponential terms associated with the total segment power are determined. During the preclosure phase, forced ventilation provides heat removal with the ventilation efficiency decreasing linearly as the flow moves down the drift.

Independent Variables

The following variables define the conditions for the calculation. The burnup should be an integer between 10 and 70 Gwd/ton.

Initial Rock Temperature tzero := 22.8 °C

Ventilation Efficiency at Start of Drift Eff_1 := 0.90 %

Ventilation Efficiency at End of Drift Eff_2 := 0.80 %

Ventilation Duration Vent := 25 Years

Est_Drift_Length := 600 meters

Drift_Space := 81 meters

WP_Spacing := .1 meters

WP_Dia := 1.882 meters

Number of Neighboring Drifts nbors := 5 Drifts

Decay Variables Calculation

The following files contain the six constants that define the assembly power and decay as a function of burnup for BWR and PWR assemblies. The power values are calculated based on a PWR assembly with an initial loading of 0.475 MTHM/Assembly and a BWR assembly with an initial loading of 0.200 MTHM/Assembly.

BWR :=

PWR :=

The following files contain the six constants that define the canister power and decay.

DOELong :=

DOEShort :=

Age := 27 BU := 50

The following matrix defines the segment characteristics. The first column defines the type of waste package PWR, BWR, DOE Long, or DOE short. The next three columns determine the characteristics of the commercial waste packages (the DOE waste packages are assumed to have the same power and decay characteristics independent of age), The second column is the average burnup, the third column is the average age, and the forth column is the average MTHM. For DOE waste packages the value in the second column should be 10, the third column should be 0, and the forth columns should be 1.

$$Seg := \begin{pmatrix} PWR & BU & Age & .4130 \\ DOELong & 10 & 0 & 1 \\ PWR & BU & Age & .4130 \\ PWR & BU & Age & .4130 \\ DOEShort & 10 & 0 & 1 \\ PWR & BU & Age & .4130 \\ PWR & BU & Age & .4130 \end{pmatrix}$$

The six constants defining the power and decay are selected from the above files based on the type of waste package and, for the commercial waste packages, the assembly burnup defined in matrix "Seg" .

$$\lambda 0 := submatrix(Seg_{0,0}, Seg_{0,1} - 1, Seg_{0,1} - 1, 1, 3)$$
$$\lambda 1 := submatrix(Seg_{1,0}, Seg_{1,1} - 1, Seg_{1,1} - 1, 1, 3)$$
$$\lambda 2 := submatrix(Seg_{2,0}, Seg_{2,1} - 1, Seg_{2,1} - 1, 1, 3)$$
$$\lambda 3 := submatrix(Seg_{3,0}, Seg_{3,1} - 1, Seg_{3,1} - 1, 1, 3)$$
$$\lambda 4 := submatrix(Seg_{4,0}, Seg_{4,1} - 1, Seg_{4,1} - 1, 1, 3)$$
$$\lambda 5 := submatrix(Seg_{5,0}, Seg_{5,1} - 1, Seg_{5,1} - 1, 1, 3)$$
$$\lambda 6 := submatrix(Seg_{6,0}, Seg_{6,1} - 1, Seg_{6,1} - 1, 1, 3)$$

$$P0 := submatrix(Seg_{0,0}, Seg_{0,1} - 1, Seg_{0,1} - 1, 4, 6)$$
$$P1 := submatrix(Seg_{1,0}, Seg_{1,1} - 1, Seg_{1,1} - 1, 4, 6)$$
$$P2 := submatrix(Seg_{2,0}, Seg_{2,1} - 1, Seg_{2,1} - 1, 4, 6)$$
$$P3 := submatrix(Seg_{3,0}, Seg_{3,1} - 1, Seg_{3,1} - 1, 4, 6)$$
$$P4 := submatrix(Seg_{4,0}, Seg_{4,1} - 1, Seg_{4,1} - 1, 4, 6)$$
$$P5 := submatrix(Seg_{5,0}, Seg_{5,1} - 1, Seg_{5,1} - 1, 4, 6)$$
$$P6 := submatrix(Seg_{6,0}, Seg_{6,1} - 1, Seg_{6,1} - 1, 4, 6)$$

$$\lambda := stack(\lambda 0, \lambda 1, \lambda 2, \lambda 3, \lambda 4, \lambda 5, \lambda 6)$$

$$P := stack(P0, P1, P2, P3, P4, P5, P6)$$

$$\lambda = \begin{pmatrix} 0.348941 & 0.024667 & 0.002531 \\ 0.540572 & 0.023333 & 0.000000 \\ 0.348941 & 0.024667 & 0.002531 \\ 0.348941 & 0.024667 & 0.002531 \\ 0.196721 & 0.020202 & 0.000000 \\ 0.348941 & 0.024667 & 0.002531 \\ 0.348941 & 0.024667 & 0.002531 \end{pmatrix}$$

$$P = \begin{pmatrix} 2519.1 & 830.4 & 187.6 \\ 5.6 & 401.4 & 0.0 \\ 2519.1 & 830.4 & 187.6 \\ 2519.1 & 830.4 & 187.6 \\ 541.5 & 2386.2 & 0.0 \\ 2519.1 & 830.4 & 187.6 \\ 2519.1 & 830.4 & 187.6 \end{pmatrix}$$

The next loop defines the base case MTHM per assembly for commercial waste packages, the number of assemblies per commercial waste package, and the length of the waste package.

```
WP_Data := | WP_Data ← 0
           | for i ∈ 0..6
           |   WP_Data[i,0] ← 0.475 if Seg[i,0] = PWR
           |   WP_Data[i,1] ← 21 if Seg[i,0] = PWR
           |   WP_Data[i,2] ← 5.85 if Seg[i,0] = PWR
           |   WP_Data[i,0] ← 0.200 if Seg[i,0] = BWR
           |   WP_Data[i,1] ← 44 if Seg[i,0] = BWR
           |   WP_Data[i,2] ← 5.85 if Seg[i,0] = BWR
           |   WP_Data[i,0] ← 1 if Seg[i,0] = DOEShort
           |   WP_Data[i,1] ← 1 if Seg[i,0] = DOEShort
           |   WP_Data[i,2] ← 3.697 if Seg[i,0] = DOEShort
           |   WP_Data[i,0] ← 1 if Seg[i,0] = DOELong
           |   WP_Data[i,1] ← 1 if Seg[i,0] = DOELong
           |   WP_Data[i,2] ← 5.220 if Seg[i,0] = DOELong
           | return WP_Data
```

$$WP\_Data = \begin{pmatrix} 0.4750 & 21.0000 & 5.8500 \\ 1.0000 & 1.0000 & 5.2200 \\ 0.4750 & 21.0000 & 5.8500 \\ 0.4750 & 21.0000 & 5.8500 \\ 1.0000 & 1.0000 & 3.6970 \\ 0.4750 & 21.0000 & 5.8500 \\ 0.4750 & 21.0000 & 5.8500 \end{pmatrix}$$

Individual waste package power at time of emplacement, "WP_Individual" in watts/WP, is calculated in the next loop.

```
WP_Individual := | for i ∈ 0..6
                 |   WP_Individual[i] ← 0
                 |   for j ∈ 0..2
                 |     WP_Individual[i] ← WP_Individual[i] + WP_Data[i,1] P[i,j] · (Seg[i,3] / WP_Data[i,0]) · e^(−λ[i,j]·(Seg[i,2]))
                 | return WP_Individual
```

$$WP\_Individual = \begin{pmatrix} 10992.2 \\ 407.0 \\ 10992.2 \\ 10992.2 \\ 2927.7 \\ 10992.2 \\ 10992.2 \end{pmatrix} \text{ watts}$$

Segment Power and Decay Constants

The total segment power, "Power" in watts, is calculated in the next loops where "t" represents the time from emplacement

$$t := \left| \begin{array}{l} \text{for } k \in 0..1000 \\ \quad t_k \leftarrow k \\ \text{return } t \end{array} \right.$$

$$\text{Power} := \left| \begin{array}{l} \text{for } t \in 0..500 \\ \quad \text{Power}_t \leftarrow 0 \\ \quad \text{for } i \in 0..6 \\ \quad\quad \text{for } j \in 0..2 \\ \quad\quad\quad \text{Power}_t \leftarrow \text{Power}_t + \text{WP\_Data}_{i,1} \cdot P_{i,j} \cdot \frac{\text{Seg}_{i,3}}{\text{WP\_Data}_{i,0}} \cdot e^{-\lambda_{i,j} \cdot (\text{Seg}_{,2} + t)} \\ \text{return Power} \end{array} \right.$$

The loop "Power" calculates the total segment power as a function of time. The following section determines the six power and decay constants that define the total segment power. The six "Guess values" are required by MathCad to solve the six equations in six unknowns provided below. These six equations represent the segment power as the summation of three exponential terms at assembly ages of 0, 25, 50, 100, 200 and 300 years from emplacement.

Guess values: $P1 := 7000$ $P2 := 6500$ $P3 := 1700$ $\lambda 1 := .14$ $\lambda 2 := .02$ $\lambda 3 := .002$

Given

$$P1 \cdot e^{-0 \cdot \lambda 1} + P2 \cdot e^{-0 \cdot \lambda 2} + P3 \cdot e^{-0 \cdot \lambda 3} = \text{Power}_0$$

$$P1 \cdot e^{-25 \cdot \lambda 1} + P2 \cdot e^{-25 \cdot \lambda 2} + P3 \cdot e^{-25 \cdot \lambda 3} = \text{Power}_{25}$$

$$P1 \cdot e^{-50 \cdot \lambda 1} + P2 \cdot e^{-50 \cdot \lambda 2} + P3 \cdot e^{-50 \cdot \lambda 3} = \text{Power}_{50}$$

$$P1 \cdot e^{-100 \cdot \lambda 1} + P2 \cdot e^{-100 \cdot \lambda 2} + P3 \cdot e^{-100 \cdot \lambda 3} = \text{Power}_{100}$$

$$P1 \cdot e^{-200 \cdot \lambda 1} + P2 \cdot e^{-200 \cdot \lambda 2} + P3 \cdot e^{-200 \cdot \lambda 3} = \text{Power}_{200}$$

$$P1 \cdot e^{-500 \cdot \lambda 1} + P2 \cdot e^{-500 \cdot \lambda 2} + P3 \cdot e^{-500 \cdot \lambda 3} = \text{Power}_{500}$$

$$\begin{pmatrix} \text{P1\_Value} \\ \text{P2\_Value} \\ \text{P3\_Value} \\ \lambda 1\text{\_Value} \\ \lambda 2\text{\_Value} \\ \lambda 3\text{\_Value} \end{pmatrix} := \text{Find}(P1, P2, P3, \lambda 1, \lambda 2, \lambda 3)$$

MathCad calculated the following values for the six constants:

$\lambda 1\_Value = 0.1318$

$\lambda 2\_Value = 0.0243$

$\lambda 3\_Value = 0.0025$

$P1\_Value = 663.03$

$P2\_Value = 41620.43$

$P3\_Value = 16012.3844$

$$\lambda := \begin{pmatrix} \lambda 1\_Value \\ \lambda 2\_Value \\ \lambda 3\_Value \end{pmatrix} \qquad Half\_Life := \frac{.693}{\lambda} \qquad P := \begin{pmatrix} P1\_Value \\ P2\_Value \\ P3\_Value \end{pmatrix}$$

$$Half\_Life = \begin{pmatrix} 5.3 \\ 28.5 \\ 273.6 \end{pmatrix} \qquad \lambda = \begin{pmatrix} 0.1318 \\ 0.0243 \\ 0.0025 \end{pmatrix} \qquad P = \begin{pmatrix} 663.0348 \\ 41620.4314 \\ 16012.3844 \end{pmatrix}$$

Emplacement Drift Parameters

The following calculation determines the exact length of the drift and the number of waste packages per drift based on the assumptions provided above.

$$Seg\_L := \left| \begin{array}{l} Seg\_L \leftarrow 0 \\ \text{for } i \in 0..6 \\ \quad Seg\_L \leftarrow Seg\_L + WP\_Data_{i,2} + WP\_Spacing \end{array} \right.$$

$$No\_Seg := \text{round}\left(\frac{Est\_Drift\_Length}{Seg\_L}\right) \qquad Drift\_Length := No\_Seg \cdot Seg\_L \qquad No\_WP := No\_Seg \cdot 7$$

Actual Drift Length $Drift\_Length = 583.01$ meters Number of WP per Drift $No\_WP = 105$ WP per Drift

Number of Segments per Drift $No\_Seg = 15$ Segments Segment Length $Seg\_L = 38.87$ meters

The next expression converts the power in watts to linear power in watts/meter

$$Q := \frac{P}{Seg\_L}$$

$$Q = \begin{pmatrix} 17.0591 \\ 1070.8424 \\ 411.9789 \end{pmatrix} \text{ watts/meter}$$

Ventilation Efficiency

The following loop calculates the ventilation efficiency for each segment based on the efficiency at the start of the drift of Eff_1 and the efficiency at the end of the drift Eff_2.

$Eff\_1 = 0.9000$ $Eff\_2 = 0.8000$

$$\begin{array}{l} Eff := \left| \begin{array}{l} \text{for } n \in 0..No\_Seg - 1 \\ \quad \left| \begin{array}{l} x \leftarrow \dfrac{Seg\_L}{2} + n \cdot Seg\_L \\ Eff_n \leftarrow \dfrac{(Eff\_2 - Eff\_1)}{Drift\_Length} \cdot x + Eff\_1 \end{array} \right. \\ \text{return } Eff \end{array} \right. \end{array}$$

Power

The next loops calculate the average waste package power, "WP_Power", and linear line load, "Line_Load", as a function of time from emplacement.

$$\begin{array}{l} WP\_Power := \left| \begin{array}{l} \text{for } t \in 0..200 \\ \quad \left| \begin{array}{l} WP\_Power_t \leftarrow 0 \\ \text{for } j \in 0..2 \\ \quad WP\_Power_t \leftarrow WP\_Power_t + P_j \cdot e^{-\lambda_j \cdot t} \end{array} \right. \\ \text{return } \dfrac{WP\_Power}{7} \end{array} \right. \end{array}$$

$$\begin{array}{l} Line\_Load := \left| \begin{array}{l} \text{for } t \in 0..Vent + 100 \\ \quad \left| \begin{array}{l} Line\_Load_t \leftarrow 0 \\ \text{for } j \in 0..2 \\ \quad Line\_Load_t \leftarrow Line\_Load_t + Q_j \cdot \dfrac{e^{-\lambda_j \cdot t}}{1000} \end{array} \right. \\ \text{return } Line\_Load \end{array} \right. \end{array}$$

The Average waste package power and linear line load at emplacement, time = 0, and closure, time = vent, calculated from array "WP_Power" and "Line_Load" are:

WP power at emplacement $WP\_Power_0 = 8328.0$ Watts Line load at Emplacement $Line\_Load_0 = 1.50$ kW/meter

WP power at closure $WP\_Power_{Vent} = 5386.3$ Watts Line load at closure $Line\_Load_{Vent} = 0.97$ kW/meter

Constants

The following constants are required for the calculation.

$Krock := 1.83$ watt/meter - ^oC $\rho := 2097$ kg/meter^3 $Cp := 1119.0$ joules/kg - ^oC

Emissivities are:

$$\kappa := \frac{Krock \cdot 3600 \cdot 24 \cdot 365}{\rho \cdot Cp} \text{ meter}^2\text{/year}$$

$e\_Drift := 0.9$ $e\_Drip := 0.9$ $e\_WP := 0.9$ $\sigma := 5.67 \cdot 10^{-8}$ watts/meter^2-$^oC^4$

Temperature Calculation

The equation for calculating the temperature due to a single finite-length decaying line source (or segment) is:

$$v(z,x,t,j) := \frac{e^{-\lambda_j \cdot t} \cdot Q_j}{8 \cdot \pi \cdot Krock} \cdot \int_0^t \left(erf\left(\frac{z}{2\cdot\sqrt{\kappa \cdot \theta}}\right) - erf\left(\frac{z - Seg\_L}{2\cdot\sqrt{\kappa \cdot \theta}}\right)\right) \cdot \frac{e^{\lambda_j \cdot \theta}}{\theta} \cdot e^{\frac{-x^2}{4\cdot\kappa\cdot\theta}}\, d\theta$$

The temperature contribution after ventilation shutdown is as follows, the A2 in the leading exponential re-zeros Q_{ij} for ventilation shutdown.

$$va(z,x,t,j) := \frac{e^{-\lambda_j \cdot (Vent+t)} \cdot Q_j}{8 \cdot \pi \cdot Krock} \cdot \int_0^t \left(erf\left(\frac{z}{2\cdot\sqrt{\kappa \cdot \theta}}\right) - erf\left(\frac{z - Seg\_L}{2\cdot\sqrt{\kappa \cdot \theta}}\right)\right) \cdot \frac{e^{\lambda_j \cdot \theta}}{\theta} \cdot e^{\frac{-x^2}{4\cdot\kappa\cdot\theta}}\, d\theta$$

The segment temperature contribution for the n-th segment for the three decaying components is:

```
WPtemp(z,x,t,n) :=
    tsum ← 0.0
    for j ∈ 0..2
        tsum ← tsum + (1. − Eff_n)·v(z − Seg_L·n, x, t, j)
        tsum ← tsum + Eff_n·va(z − Seg_L·n, x, t − Vent, j)  if t > Vent
    return tsum
```

The temperature contribution from all segments, "No_Seg", and neighbors, "nbors", is:

```
WPSum(z,x,t) :=
    tsum ← 0.
    for n ∈ 0.. No_Seg − 1
        tsum ← tsum + WPtemp(z,x,t,n)
    for m ∈ 1.. nbors
        x1Loc ← m·Drift_Space − x
        x2Loc ← m·Drift_Space + x
        for n ∈ 0.. No_Seg − 1
            tsum ← tsum + WPtemp(z,x1Loc,t,n)
            tsum ← tsum + WPtemp(z,x2Loc,t,n)
    return tzero + tsum
```

The following variables define the radial, "X_Drift", "X_Drip", and "X_WP" and axial, "Z_Drift" locations used to calculate the maximum temperature. The location of the Drift Wall peak temperature is near the end of the drift, based on a series of sensitivity calculations the peak temperature normally occurs at approximately 80% down the length of the drift.

$X\_Drift := 2.75 \qquad X\_Drip := 1.3 \qquad X\_WP := \frac{WP\_Dia}{2} \qquad Z\_Drift := Drift\_Length \cdot 0.8$

The following loop are used to calculate the drift wall maximum temperature and time of maximum temperature at the locations defined above.

```
Drift_Wall := | Drift_Max_Time ← 0
              | Drift_Max_Temp ← 0
              | Drift_Wall ← 0
              | for t ∈ Vent.. 225
              |   Drift_Wall_t ← WPSum(Z_Drift, X_Drift, t)
              |   Drift_Max_Time ← t if Drift_Wall_t > Drift_Max_Temp
              |   Drift_Max_Temp ← Drift_Wall_t if Drift_Wall_t > Drift_Max_Temp
              | return (Drift_Max_Time)
              |        (Drift_Max_Temp)
```

$$\begin{pmatrix} Drift\_Max\_Time \\ Drift\_Max\_Temp \end{pmatrix} := Drift\_Wall$$

Peak Post Closure Drift Wall Temperature $Drift\_Max\_Temp = 200$ °C

Time of Peak Temperature $Drift\_Max\_Time = 42$ years after emplacement

The invert is assumed to be an insulator so the surface areas "A_Drift", "A_Drip", and "A_WP" used to calculate the drip shield and waste package surface temperatures are reduced to 75% of their actual area.

$A\_Drift := (2 \cdot \pi \cdot X\_Drift) \cdot 0.75 \qquad A\_Drip := (2 \cdot \pi \cdot X\_Drip) \cdot 0.75 \qquad A\_WP := (2\pi \cdot X\_WP) \cdot 0.75$

The energy transported between two surfaces, "Q1",can be calculated as follows:

```
Q1 := | for t ∈ 0.. 300
      |   Q1_t ← 0
      |   for j ∈ 0.. 2
      |     Q1_t ← Q1_t + Q_j e^(−λ_j · t)
      | return Q1
```

$Q1_{Drift\_Max\_Time} = 755.76$ joules/meter-sec

The following expressions are used to calculate the drip shield and waste package temperatures using the radiant heat transfer between two concentric cylinders at the time of maximum drift wall temperature.

Drip shield temperature

$$Drip\_Max\_Temp := \left[\frac{Q1_{Drift\_Max\_Time}}{\sigma}\cdot\left[\frac{1.}{A\_Drip\cdot e\_Drip} + \frac{1}{A\_Drift}\left(\frac{1}{e\_Drift} - 1\right)\right] + (273 + Drift\_Max\_Temp)^4\right]^{0.25} - 273$$

Maximum drip shield temperature $Drip\_Max\_Temp = 206$ °C

Waste package surface temperature

$$WP\_Max\_Temp := \left[\frac{Q1_{Drift\_Max\_Time}}{\sigma}\cdot\left[\frac{1.}{A\_WP\cdot e\_WP} + \frac{1}{A\_Drip}\left(\frac{1}{e\_Drip} - 1\right)\right] + (273 + Drip\_Max\_Temp)^4\right]^{0.25} - 273$$

Maximum waste package temperature $WP\_Max\_Temp = 214$ °C

The temperature profile of the waste package, drip shield, and drift wall as a function of time are calculated from the three loops below.

$$\begin{aligned} Drift := \;& Drift \leftarrow 0 \\ & \text{for } t \in 0..300 \\ & \quad Drift_t \leftarrow WPSum(Z\_Drift, X\_Drift, t) \\ & \text{return } Drift \end{aligned}$$

$$\begin{aligned} Drip := \;& \text{for } t \in 0..300 \\ & \quad Drip_t \leftarrow \left[\frac{Q1_t}{\sigma}\cdot\left[\frac{1.}{A\_Drip\cdot e\_Drip} + \frac{1}{A\_Drift}\left(\frac{1}{e\_Drift} - 1\right)\right] + \left(273 + Drift_t\right)^4\right]^{0.25} - 273 \\ & \text{return } Drip \end{aligned}$$

$$\begin{aligned} WP := \;& \text{for } t \in 0..300 \\ & \quad WP_t \leftarrow \left[\frac{Q1_t}{\sigma}\cdot\left[\frac{1.}{A\_WP\cdot e\_WP} + \frac{1}{A\_Drip}\left(\frac{1}{e\_Drip} - 1\right)\right] + \left(273 + Drip_t\right)^4\right]^{0.25} - 273 \\ & \text{return } WP \end{aligned}$$

The graph of waste package, drip shield, and drift wall temperature as a function of time is provided below.

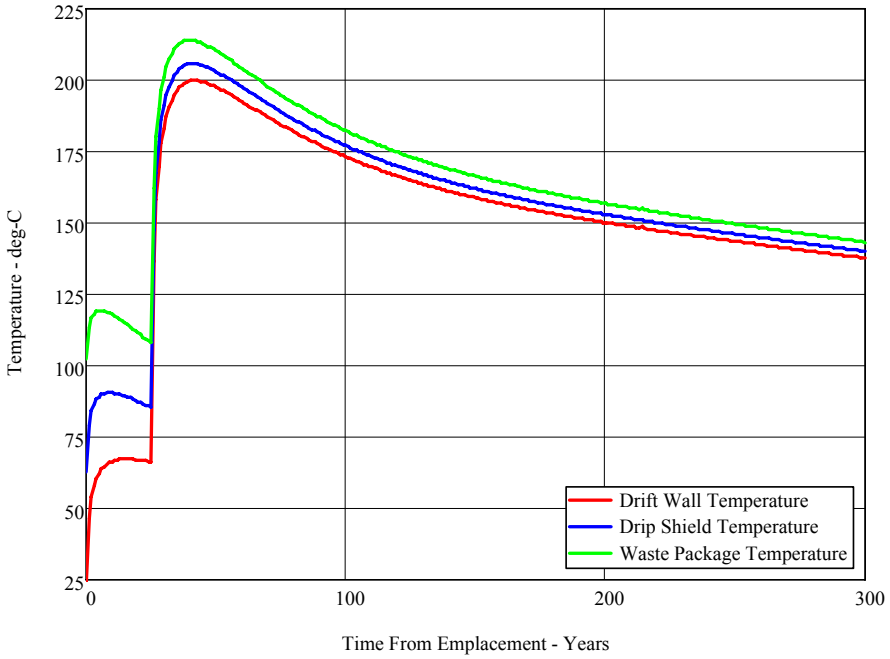

Drift_Max_Temp = 200 °C Drip_Max_Temp = 206 °C WP_Max_Temp = 214 °C

Age := 27 BU := 60

$$Seg := \begin{pmatrix} PWR & BU & Age & .4130 \\ DOELong & 10 & 0 & 1 \\ PWR & BU & Age & .4130 \\ PWR & BU & Age & .4130 \\ DOEShort & 10 & 0 & 1 \\ PWR & BU & Age & .4130 \\ PWR & BU & Age & .4130 \end{pmatrix}$$

Ventilation Efficiency at Start of Drift Eff_1 = 0.90 %

Ventilation Efficiency at End of Drift Eff_2 = 0.80 %

Ventilation Duration Vent = 25 Years

Line load at Emplacement $Line\_Load_0 = 1.50$ watts/meter

Line load at closure $Line\_Load_{Vent} = 0.97$ watts/meter